Gaze stabilization reflexes in the mouse: New tools to study vision and sensorimotor integration

Bart van Alphen

Gaze stabilization reflexes in the mouse: New tools to study vision and sensorimotor integration

ISBN: 978-90-9025822-5

Printed by Ipskamp Drukkers

Gaze stabilization reflexes in the mouse: New tools to study vision and sensorimotor integration

Blik stabilisatie reflexen in de muis: Nieuwe gereedschappen om gezichtsvermogen en sensorimotor integratie te bestuderen

Proefschrift

ter verkrijging van de graad van doctor aan de
Erasmus Universiteit Rotterdam
op gezag van de
rector magnificus

Prof. dr. H.G. Schmidt

En volgens besluit van het College voor Promoties

De openbare verdediging zal plaatsvinden op
dinsdag 14 december 2010 om 11.30 uur

door

Bart van Alphen
geboren te Breda

Promotiecommissie

Promotor:	Prof. dr. M.A. Frens
Overige leden:	Prof dr. C.I. de Zeeuw Prof. dr. A.J. van Opstal Prof. dr. J.R. Vingerling

Voor mijn ouders

Table of Contents

Scope of this thesis

Gaze stabilization reflexes are a popular model system in neuroscience for connecting neurophysiology and behavior as well as studying the neural correlates of behavioral plasticity. These compensatory eye movements are one of the simplest motor behaviors, consisting of a more or less spherical object that rotates with three degrees of freedom, without significantly changing the load during a movement trajectory. Additionally, it is a model system where the sensory input, consisting of visual and/or vestibular stimulation, can be fully controlled. The output, reflexive compensatory eye movements and electrophysiological activity, can be recorded and correlated with the sensory input. By manipulating those reflexive eye movements by using different combinations of sensory input, motor learning can be studied in a well-controlled environment.

In this thesis, we describe several innovative approaches that can be added to the neuroscientific arsenal. We are the first lab to describe how to record three dimensional eye movements in mice using video-oculography. Additionally, we describe how compensatory eye movements can be used to quantify contrast sensitivity; the ability to detect small increments in shades of gray on a uniform background, which is one of the main limiting factors in a wide variety of visual tasks. This new and sensitive method is useful in characterizing mouse models where vision is affected as a result of mutations, aging, retinal degeneration or neurological impairment of the visual system.

Chapter 1

General Introduction

Introduction

Motor learning is the process of improving the smoothness and accuracy of movements, both of reflexes like gaze stabilization reflexes and of more complex movements such as playing tennis or driving a bicycle. This is a never-ending process as the body changes over time, requiring movements to be continuously fine-tuned. The cerebellum (Latin for little brain) is the region of the brain that plays a critical role in this fine tuning. It is a highly structured part of the brain that is well conserved among vertebrates (Bolk, 1906), illustrating the universal need for properly calibrated movement. In order to coordinate motor control the cerebellum integrates sensory information from different internal and external sources and functions as an online control system that evaluates discrepancies between intention and action and adjusts movements to minimize these discrepancies.

The cerebellum

The cerebellum was mapped out anatomically during the 18th century (see Glickstein et al 2009 for a review). From the 19th century on, focus shifted to the function of the cerebellum. When the cerebellum is damaged by injuries or lesions this results in distinctive motor symptoms like ataxia (lack of coordination), decreased muscle tone and intention tremor (Rolando, 1809; Babinski, 1902; Holmes, 1917). However, even complete ablation of the cerebellum does not result in paralysis or involuntary movements, which indicates that the cerebellum calibrates rather than initiates movements (Flourens, 1824).

In their classic work, Eccles, Ito and Szentágothai (Eccles et al., 1967) described a complete picture of the cerebellar architecture, where mossy fibres and climbing fibres form the input and the axons of Purkinje cells form the sole output. Throughout the cerebellar cortex, neurons are arranged in a highly regular manner as repeating units that consist of five types of neurons: inhibitory stellate, basket, Purkinje and Golgi cells and excitatory granule cells each appearing in one of the three layers of the cerebellar cortex.

Cerebellar anatomy

The cerebellar cortex consists of three layers; from inner to outer layer these are the granular, Purkinje and molecular layer.

The human granular layer contains 6-8 * 10^{11} tiny granule cells, making up approximately 70% of the total amount of cells in the brain and spinal cord combined while taking up only ten percent of the volume of the brain (Herculano-Houzel, 2005). Granule cells receive inhibitory feedback from Golgi cells and send their axons up into the molecular layer, where they bifurcate into a T shape where each horizontal part of the T makes weak excitatory (glutamatergic) synapses with approximately 300 Purkinje cells.

The Purkinje layer contains the cell bodies of the sole output source of the cerebellum: Purkinje cells. These cells, first described in 1837 by Czech physiologist Jan Evangelista Purkyně, are among the largest cells in the human brain and have a characteristic morphology with an elaborate dendritic tree that expands in two dimensions. Purkinje cells are stacked like cards in the cerebellar cortex, with their dendritic trees parallel to each other in the molecular layer (FIG). Perpendicular to the dendritic trees run the parallel fibres. Each Purkinje cell is innvervated by ~ 150000 parallel fibres, where each fibre has one or two connections with a single Purkinje cell. In the molecular layer billions of parallel fibres form synapses with the dendritic arbors of Purkinje cells. Among these crossing axon pathways there are two types of GABAergic (inhibitory) interneurons: Basket cells and stellate cells. Besides the thousands of Purkinje cell-parallel fibre synpses, each Purkinje cell is innvervated by a single climbing fibre. This climbing fibre originates in the inferior olive and wraps itself about the Purkinje cell soma, creating a connection that is so strong that a presynaptic spike in the climbing fibre always triggers a postsynaptic spike in the Purkinje cell.

Based on both functional and phylogenetic criteria, the cerebellum can be diveded into three parts: The vestibulocerebellum (archicerebellum) is the oldest part of the cerebellum and consists of the floccular node and the adjacent part of the vermis. Here, vestibular information from the semicircular canals and vestibular nuclei is combined with visual input from

the visual cortex and superior colliculus to regulate balance and eye movements. Of intermediate age is the spinocerebellum (Paleaocerebellum) which consists of the vermis and paravermis and regulates body and limb movements by integrating input from the spinal cord, the visual and the auditory system. The youngest part of the cerebellum is the Cerebrocerebellum (Neocerebellum) is located in the lateral parts of the cerebellar hemispheres. It is involved in evaluating sensory information and utilizing this to plan imminent motion. The Cerebrocerebellum receives input from the cerebral cortex, through the pontine nuclei and projects information back to the Inferior Olive and to the motor areas of the cortex through the thalamus. It is also thought to be involved in purely cognitive processes.

Cerebellar learning

Donald Hebb (1949) proposed that information can be stored in an assembly of neurons by modifying the strength of synaptic connections, based on activities experienced. Based on Hebb's learning rule, Rosenblatt (1962) constructed the Simple Perceptron, an array of neurons consisting of three layers that are connected in one direction. The first layer is a sensory layer that is connected with fixed input to the second layer; the association layer. This association layer is connected to the third layer, the response layer, by connections that can be modified by an outside teacher.

The concept of Hebbian learning in a Simple Perceptron was first applied to the cerebellum by Marr (1969) and Albus (1971). Mossy fibres were assigned to the input layer, granule cells and their parallel fibres to the association layer and Purkinje cells to the output layer, with the climbing fibre, originating in the Inferior Olive, acting as teacher signal. The teacher signal can either strengthen or weaken connections and Marr and Albus had different ideas about its function. Marr assumed that that climbing fibre signals strengthen the parallel fibre-Purkinje cell synapse, reinforcing it when the Purkinje cell output was correct while Albus assumed that the climbing fibre signal was an error signal, weakening the parallel fibre-Purkinje cell synapse when the output was incorrect. Later, Ito et al (1982) demonstrated that electrical stimulation of the climbing fibre resulted in a

persistent decrease in synaptic strength at the parallel fibre-Purkinje cell synapse of parallel fibres that were activated simultaneously. This persistent decrease was labelled cerebellar Long Term Depression (LTD) and has been a key candidate for the plasticity mechanism that governs motor learning, leading to multiple theories of cerebellar functioning (Reviewed by Ito, 2002; Boyden et al, 2004). Recently however, the role of LTD in motor learning as described by Marr, Albus and Ito was questioned (Schonewille, 2008).

The uniformity of the cerebellar architecture suggests that signals are processed in a similar way across different modules, even though different parts of the cerebellum receive different kinds of input and project to different targets. From this it can be inferred that by studying one kind of cerebellar motor learning general principles can be uncovered that characterize cerebellar function in general. Compensatory eye movements have become a popular model system for characterizing cerebellar function and studying the neural correlates of behavioral plasticity (de Zeeuw et al, 1998; Picciotto, 1998; Stahl, 2004).

Compensatory eye movements

In order to see the world clearly, a stable image needs to be projected on the retina. As an organism moves through the world, its self-generated motion would result in image slip over the retina, already blurring the image and reducing visual acuity when velocity is more than a few degrees per second (Burr and Ross, 1982; Westheimer and Mckee, 1975). In order to preserve acute vision, image slip over the retina needs to be minimized. Vertebrates have evolved two mechanisms to achieve this. One is the Vestibulo-Ocular Reflex, which detects head motion through the vestibular system and translates this information into motor commands, thus rotating the eye in the opposite direction of the head movement. The other reflex mechanism is the Optokinetic Reflex (OKR), a feedback mechanism that generates compensatory eye movements directly based on retinal slip. Together, these two reflexes help stabilize the retinal image over a large range of motions. When you move your head to the right while reading this text, your eyes will move reflexively to the left, keeping the text on the fovea and allowing you to keep reading.

The Vestibulo-Ocular reflex

Head movements are detected by the vestibular system. Changes in linear acceleration are detected by otolith organs while angular accelerations of the head are detected three semi-circular canals of the inner ear that are perpendicular to each other, forming a three-dimensional detection system. Each semi-circular canal is filled with endolymph. Head rotations lead to endolymph flow in one or more semi-circular canals which causes a deviation of the cupula, a flexible membrane that contains hair cells that transform the mechanical movement to electrical signals. Movement in one direction excites these cells while movement in the opposite direction inhibits them. Due to the mechanical properties of the cupula and hair cells and the viscosity of the endolymph, head acceleration is mechanically integrated to a velocity signal; the vestibular system functions as a high pass filter with respect to angular velocity (Steinhausen, 1933).

The main VOR circuit is a three neuron arc that functions as an open loop system: the head velocity signal is sent to the vestibular nuclei in the brainstem by the vestibular nerve (cranial nerve VIII), from where it projects to oculomotor nuclei, which contain motor neurons that drive eye muscle activity (Figure 1). This circuit is capable of detecting head movements much sooner than the visual system would using retinal motion. Thus, VOR evoked eye movements occur at very short latencies of less than 16 ms (Leigh and Zee, 1997). An inhibitory side loop is goes through the flocculus and the ventral paraflocculus in the cerebellum. In this loop, vestibular information is transmitted by mossy fibres to Purkinje cells, which in turn inhibit VOR interneurons in the vestibular nuclei.

The fast acting VOR works best at high frequency head movements (Collewijn, 1969). You can try this yourself by quickly moving your head back and forth from left to right while reading this page. You'll find that this won't impair your reading abilities.

The Optokinetic Reflex

However, the VOR cannot compensate for retinal slip generated by low velocity movements (or constant velocity movements, even though these rarely occur in nature). Thus, another mechanism is required to deal with low velocity retinal slip: the optokinetic reflex (OKR).

Low velocity image motion over the retina is detected as retinal slip by 'on type' direction selective retinal ganglion cells and processed through the accessory optic system (AOS) and converted in an estimate of how the world rotates about the subject (Simpson, 1984) that is then used to program compensatory eye movements that follow motion in the outside world, thus reducing retinal slip. This functions as a closed loop negative feedback system where the output (compensatory eye movements) minimizes the error signal that forms its input (retinal slip). The OKR is velocity dependent: at low stimulus velocity, the OKR perfectly compensates for retinal slip while this compensation decreases as stimulus velocity increases. Retinal ganglion cells are optimally sensitive to low (< 2 º/s) velocities, which is thought to underlie the velocity dependent nature of the OKR (Collewijn, 1972).

Again you can test this, by moving this thesis from left to right and back again in front of your eyes while keeping your head still. At low velocities, you'll be able to read. If you move faster, reading becomes impossible. Due to this velocity dependence, the OKR functions as a complementary system to the fast-acting VOR, particularly under natural conditions where the VOR produces near-perfect compensation. The resulting residual slip has a low velocity, which is easily compensated for by the OKR.

Combined effect of VOR and OKR: VVOR

Thus, retinal slip is minimized by two complementary reflexes. The VOR works as a high pass filter, which means that it functions best at high frequency head movements while the OKR, with its low pass characteristics, operates best at low or constant angular velocities of the head. The combined, synergistic action of these two reflexes synergy is called the visually enhanced VOR (VVOR) and results in a good ocular stability over

the entire frequency range of natural head rotations (Baarsma and Collewijn, 1974; Batini et al., 1979).

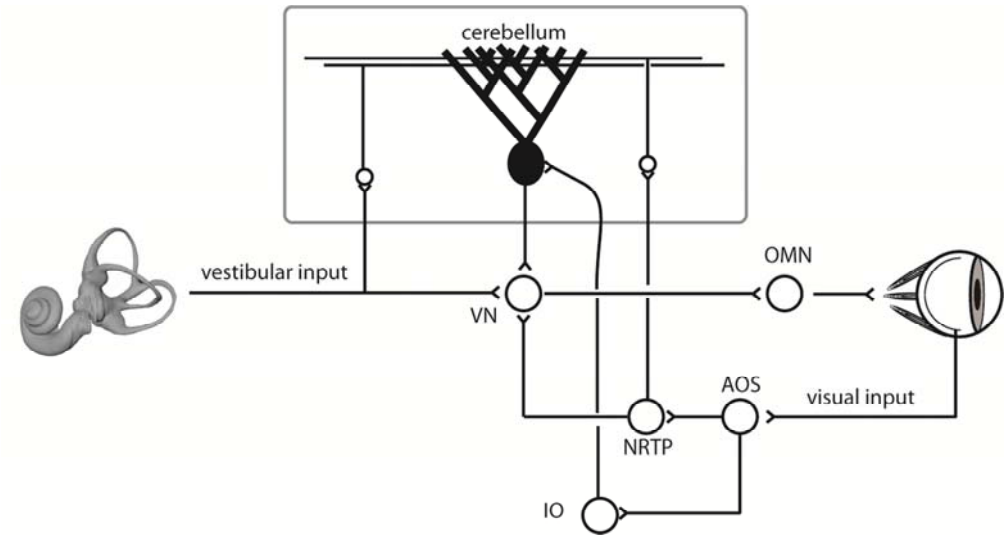

Figure 1: Schematic representation of compensatory eye movement pathways. *Vestibular input from the semicircular canals is projected to the vestibular nuclei (VN) and from there on the oculomotor nuclei (OMN) that control the six extra ocular muscles that drive eye movements. A side loop through the cerebellar flocculus forms a feedback loop that also projects back on the vestibular nuclei. Visual input (retinal slip) is processed by the accessory optic system (AOS) which is, despite its name, a primary visual centre. The AOS projects to the nucleus reticularis tegmentum pontis (NRTP), which innervates the vestibular nuclei directly and indirectly through the cerebellar side loop. AOS also projects to the inferior olive (IO), which has been proposed to function as an error detector, innervating cerebellar Purkinje cells through climbing fibres. As seen from this figure, the VOR is a feed forward reflex driving eye movements. The OKR is a feedback reflex where performance error, signalled by retinal slip, is fed back into nuclei innervating the oculomotor nuclei. Motor learning is proposed to take place in the cerebellar flocculus, where vestibular and visual inputs are integrated.*

The almost machine-like properties of the VOR and OKR make the oculomotor system an interesting model system to study the neural control

of movement. It is a system where sensory input (visual and vestibular stimulation) can be controlled perfectly and the behavioral output (eye movements) can be recorded. Furthermore, the VOR and OKR have to be recalibrated during life, as an animal grows and the size and proportions of its body changes. This learning process can also be induced artificially in the lab, by artificially uncoupling the relationship between head motion and retinal slip. In these experiments, an animal is rotated while its visual surround rotates at a different velocity. For example, when head motion to the right is combined with image motion to the right, the resulting retinal slip is lower than would be predicted from the vestibular signal, and the magnitude of the VOR would decrease. Thus, dynamic changes in amplitude and timing of both reflexes can be used as a model system to study motor learning (Collewijn and Grootendorst, 1979; Nagao, 1983; Iwashita et al, 2001; van Alphen and de Zeeuw, 2002; Boyden et al, 2004; Stahl, 2004)

Vision in mice and men

Vision starts in the retina. There are substantial differences between the eyes of mice and men. In man, vision is mainly governed by a small and highly specialized area, called the fovea, where photoreceptors are densely packed. Man has about 150 million photoreceptors; seven million cones that are active during the daytime and 140 million rods that work in low light conditions. These photoreceptors are not distributed homogenously over the retina. Cones have a low density throughout most of the retina of ~10000/ mm^2 but this density peaks sharply in the fovea to over 180,000/mm^2 (Wikler and Rakic, 1990). Rod density gradually increases as eccentricity decreases and peaks to 35,000/ mm^2 to 180,000/ mm^2 at 20 degrees from the fovea.

In order to observe the world, the fovea has to be aimed at areas of interest. In primates, there are three different movement systems that aim the fovea at a target while the VOR and OKR keep it there (Leigh and Zee, 1994). The fovea is shifted to a target by a saccade, a fast, ballistic eye movement. Vergence movements rotate the eyes in opposite direction in order to aim both foveas at a single target and to focus on objects at different distances.

Finally, smooth pursuit movements keep the fovea locked on a moving target.

On average, the mouse has ~6.5 million photoreceptors, where cones are 2.8% and rods are 97.2% of the total number (Jeon et al, 1998; Carter-Dawson and LaVail, 1979). These are distributed much more evenly over the retina. The average cone density is 12,400 cells/ mm^2, which hardly varies. The average density of rods is about 437,000 cells/ mm^2 (Jeon et al 1998), more than twice as many cells as are found in the primate fovea. Despite these large numbers, mice do not see twice as well as men. Both species project the same image of the outside world on a retina that differs greatly in size.

In primates, foveal visual acuity is limited by the density of cones, as they have a one-to-one correspondence between cones and ganglion cells in the highest-density region of the retina (Perry and Cowey, 1985). In lower mammals, there is a significant degree of convergence of cones onto ganglion cells so the upper limit is imposed by the peak density of the retinal ganglion cell mosaic. In mice there are about 3300 retinal ganglion cells/ mm^2 (Jeon et al 1998), that are distributed evenly over the retina and do not show a substantial variation from the periphery to the centre (Drager and Olsen, 1981). So, in mice there are about 140 times as many photoreceptors as retinal ganglion cells so visual acuity is not limited by cone density but by retinal ganglion cell density. When such a degree of convergence exists, visual acuity can be estimated from the peak density of retinal ganglion cells (Pettigrew et al, 1988), correcting for retinal magnification factor i.e. the distance on the retina subtending 1° of visual angle, usually expressed in μm/° (Holden and Fitzke, 1988).

Unlike man but similar to many other mammals, the mouse only has two types of cone photo pigments, a middle wavelength sensitive pigment and a short wavelength sensitive pigment (Jacobs, Neitz, & Deegan, 1991). These findings suggest that mice have at least dichromatic vision; they can see green and blue but not red (Jacobs, Williams, & Fenwick, 2004).

Species	Behavioral acuity (cpd)	References
Bat *(Rhinolophus rouxi)*	0.2	Pettigrew et al. (1988)
Mouse	0.4-0.6	See table 2
Rat	1	Birch & Jacobs 1979; Wiesenfeld & Branchek 1976; Prusky et al, 2000
Dolphin	2.4	Herman et al (1975)
Rabbit	3.4	Van Hof (1975)
Cat	6	Blake et al. (1974); Fiorentini et al. (1995);
Dog (Beagle)	6.3	Miller & Murphy (1995)
Horse	22.25	Timney & Keil (1992)
Man	60	Campbell 1965

Table 1. *Maximal behavioral acuity in mice and other mammals. Visual acuity in mice is much lower than in other mammals partly because of the convergence of lots of photoreceptors on a rather limited number of retinal ganglion cells and partly because the small size of the retina.*

Recording eye movements and vision in mice

Because the mouse retina lacks a fovea, mice don't look around to observe the world. They don't make goal directed eye movements like saccades or smooth pursuit to aim a patch of high density photoreceptors at a target.. Instead, mice only move their eyes reflexively, to stabilize vision. Where man uses five systems to guide vision, mice only use two: the VOR and OKR. This complete lack of voluntary, exploratory eye movements makes mice highly suitable to study motor control of gaze stabilization reflexes as they will only move their eyes in response to visual and vestibular stimulation to compensate for blurring, without any top down control of eye movements.

Mouse mutants

A good way to study how the brain works is to tinker with it: introduce small variations that slightly alter the way the brain works and study how

the behavior of this altered organism is changed. Mice have become the most prominent mammalian model for this approach, due to their fast generation times and the availability of many good methods to record low level behavior (i.e. eye movements).

Over the last decade, a wide range of techniques have become available that allows direct manipulation of the mouse genome by altering the genetic make-up of cultured embryonic stem cells and implanting these into developing blastocytes, which leads to expression of the altered genome in the adult organism. A mutant mouse is created from a normal, wild type mouse embryo. This is done by creating a gene-targeting vector with the desired mutation that is inserted into cultured embryonic stem cells. This procedure changes the DNA-sequence of the stem cells into a mutant version that alters or lacks the gene of interest. The stem cells carrying the desired mutation are introduced into a blastocyst stage embryo to produce chimeras consisting of a wild type mouse and mutated embryonic stem cells. These chimeras are raised to adulthood and are then mated with wild type mice to produce heterozygous offspring carrying the mutation. When these heterozygotes are mated with their siblings a F2 population is created which will contain wild type mice (no mutant alleles), heterozygotes (one mutant allele, one wild type allele) and homozygote mutants (two mutant alleles) (Gerlai et al, 1996). Technically, this technique can be applied to any animal but in practice its application in mammals is largely limited to mice because of their short gestation time and the availability of genetically well characterized inbred strains, like the C57BL6 ('Black six') .

The genome can be manipulated in a specific way; a single gene can be deactivated *in vivo* and the resulting 'null' or 'knock out' mutant will completely lack the gene product. Other, more indirect manipulations are also possible, for example by inserting extra bit of code into the DNA that will bring specific inhibitors to expression (for example, the L7PKCi mutant; see Chapter 2).

Mouse mutants have become a prominent model animal in the neurosciences during the last few years and are used to study the role of specific proteins in the brain. The theory behind this is simple: to determine

the role of a protein, one creates a knockout mutant where the gene coding for the protein of interest is not expressed. The behavior of the mutant animal is compared with an unmutated relative, the wild type. All phenotypic and behavioral differences from the wild type must be due to the lack of that specific protein, which gives more insight in its function. Similarly, this technique can be applied to introduce lethal mutations into a particular cell type, creating an animal lacking a particular cell type.

Reality however, is far more complicated because there are a number of factors involved that make the interpretation of phenotypic changes problematic at best. A single functioning gene is not an autonomous entity; instead it is a part of an intricate pattern of interlacing functions that involves many genes and processes. Altering a single strand from this pattern might result in an avalanche of disturbed processes and compensatory measures trying to make up for the defect that can lead to a wide range of secondary phenotypic changes, either in the adult organism or during its development. Distinguishing the function of a gene from the dysfunction caused by its absence is much more complex than it seems at first because of these interlaced functions.

Recording eye movements

Fast and accurate recording of eye movements is essential when studying relations between visual or vestibular stimuli and oculomotor behavior. So far, most eye movement studies focussed on one or two dimensions of the movement. This is mostly due to practical considerations. However, eye movements occur in three dimensions. As the eye rotates in the orbit it is driven by six extraocular muscles that form three complementary pairs. Four rectus muscles originate at the apex of the orbit where they connect the sclera and move the eye. The lateral and medial recti move the eye from left to right and are the only pair with a single, complementary function. The superior and inferior recti primarily move the eye up and down. This however, is accompanied by rotational movement about the line of sight: torsion. Similarly, the superior and inferior obliques primarily induce torsion but also induce vertical motion of the eye. In order to study eye movement control properly, one should record all three components.

Over the last two decades, several techniques have been developed to record eye movements as accurately as possible. The scleral search coil technique, developed by Robinson (Robinson, 1963) and modified by Collewijn et al (1969), is still considered to be the gold standard with its precision, high sampling rate and high signal to noise ratio. However, there are also several drawbacks associated with the use of coils:

Implanted search coils can affect eye movements in several ways. Physically they obstruct free eye rotation, a problem that becomes more apparent in smaller animals (Stahl et al, 2000). The implantation procedure can damage the extraocular muscle and pulley system (Demer 1995). Temporary search coils change the dynamics and accuracy of saccades, with saccades becoming longer and slower (Frens & van der Geest, 2002). This is not directly due to mechanics, as a monocular coil affects the movements of both eyes.

More recently, video based systems became an increasingly popular alternative (Stahl, 2000). Most of these systems track the pupil and use a centre of mass or an ellipse fitting algorithm to record the eye position. These systems work well when recording horizontal and vertical (two-dimensional) eye movements. However, recording the third component, torsion, is more complicated, especially in small rodents like mice. Most systems either track two or more landmarks on the eye or they track striations of the iris. These approaches work well in humans but are less applicable in animals without obvious ocular landmarks or a well-defined iris, such as rabbits and mice, limiting the options for three-dimensional video oculography in those animals. The use of infrared video-oculography to track eye movements abolishes the need to use implanted search coils, provided eye movements can be tracked in three dimensions.

Migliaccio et al (2005) describe a system that uses a fluorescent array of three 1 mm2 markers glued to the eye to accurately measure three-dimensional eye rotation in chinchillas. This system works very well for VOR studies in the dark, where eye movements are evoked by vestibular stimulation. However, since the marker array is glued on the cornea using cyanoacrylate and covers the whole pupil it is not suitable to record oculomotor behavior

in response to visual stimulation. Also, the thickness of the array might make it less suitable for measuring eye movements in smaller animals. This is analogous to the physical obstruction caused by implanted search coils. In chapter 5 we recorded three dimensional optokinetic eye movements in mice by tracking artificial temporary markers.

Mouse mutants and vision

To quantify the way a mutation affects brain function and a whole range of behavior a large battery of tests has been developed such as the rotorod, fear conditioning, watermaze (Morris, 1981) and oculomotor tests (Stahl, 2004). The role of the mutated part of the brain can be investigated by comparing the differences in learning or motor behavior between a mutant and its wildtype. Good vision is important for many of these tests. For example, a mouse that needs to find a hidden platform in a basin of milky water needs to navigate using both its memory and visual cues to triangulate its position. Also, a mouse whose oculomotor system is tested by looking at the magnitude of its compensatory eye movements has to be able to see the visual stimulus. Should a mouse with a low visual acuity participate in these tests, they won't perform well. This sub-optimal behavior can be misinterpreted as, for instance, a learning- or motor-problem. A good test of the visual acuity is required to rule out that acuity plays a role in the behavioral test.

Contrast sensitivity

In man, visual acuity is measured with the Snellen chart, which is named after the Dutch ophthalmologist Herman Snellen who developed the test in 1892. In this test, a subject has to read increasingly smaller letters on a chart. A person with normal acuity (20/20 vision) can see standardized symbols on the chart at a distance of 20 feet (~6m). A person with 20/30 vision can see symbols on the chart from 20 feet that a person with normal vision could see from 30 feet. Other similar tests use the E-Chart or the Landolt C test; subjects are asked to report the orientation of a capital E or C. All these tests are limited, in that they only measure the ability to see objects (or letters) of different sizes at very high contrast.

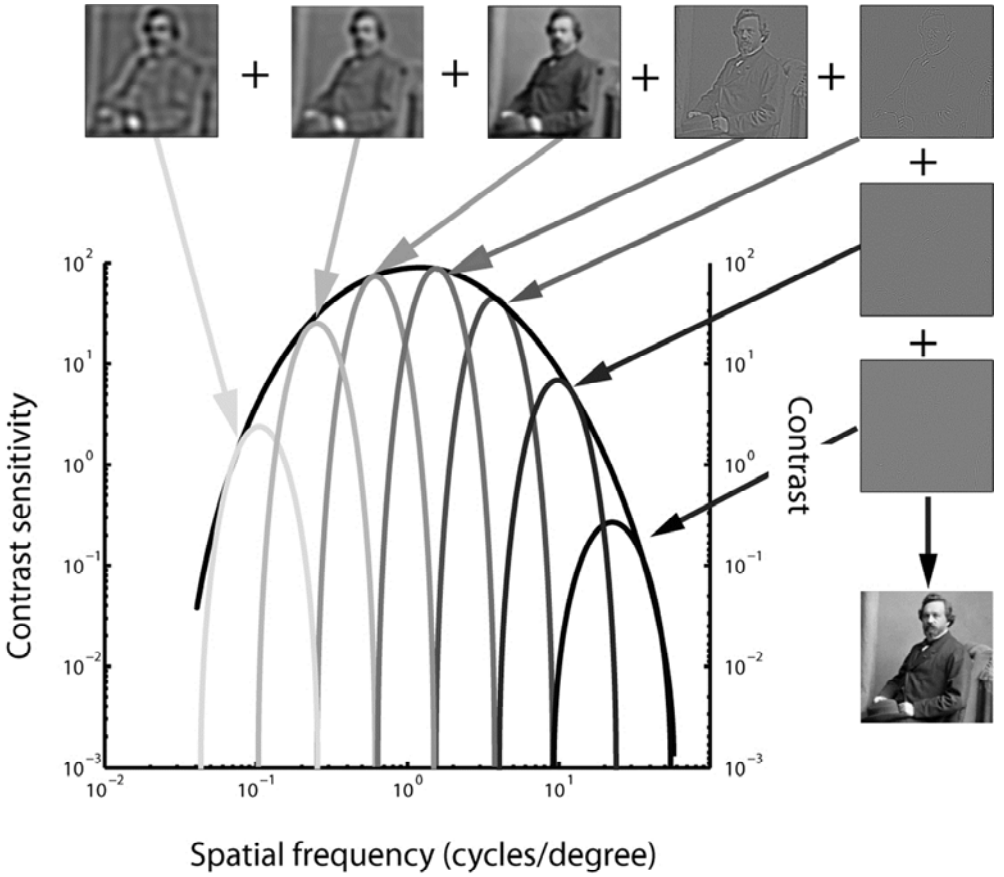

Figure 2: *The early stages of visual processing consist of channels that are sensitive to a particular range of spatial frequencies. Here an image of Franciscus Cornelis Donders, one of the founders of the science of ophthalmology, is broken down into different frequency components, ranging from low spatial frequency channels (light grey curves) that contain information about large shapes but no details to high spatial frequency channels containing information about details of the pictures but lacking information about large shapes (dark curves). Once the channels are superimposed, F.C. Donders is revealed in all his splendour. This image is modified from Ginsburg (2003).*

However, visual spatial processing is organized as a series of parallel, but independent, channels in the nervous system; each tuned to targets of a different size (Campbell and Robson, 1969; Figure 2). As a result of this parallel organization, visual acuity measurements no longer appear to adequately describe the spatial visual abilities of a given individual. The capacity to detect and identify spatial form varies widely as a function of target size, contrast, and spatial orientation (Braddick, Campbell & Atkinson, 1978; Olzak & Thomas, 1981).

A more thorough way to look at vision is to measure contrast sensitivity, the ability to detect small increments in shades of gray on a uniform background. A contrast sensitivity test measures two variables, size and contrast. Contrast sensitivity is measured by presenting an observer with sine-wave gratings as targets instead of the letters or symbols. Sine-wave gratings possess useful mathematical properties and early stages of visual processing are optimally "tuned" to such targets (Maffei, 1973; Watson, et al., 1981). Each sine-wave grating consists of a given spatial frequency, the number of sinusoidal luminance cycles per degree of visual angle (Figure 3). The contrast of the target grating is then varied while the observer's contrast detection threshold is determined.

A quick way to determine an observer's contrast sensitivity function is by using a Campbell-Robson contrast sensitivity chart (Figure 4A). This chart consists of vertical sine gratings that become increasingly narrower (horizontally) and have increasingly lower contrast (vertically). By drawing a line, right there where you can just distinguish each grating from the grey background, you can determine your contrast sensitivity curve (Figure 4B). This curve is different for each individual and depends on the viewing distance. It (generally) has an optimum somewhere left of the middle and decreases farther to the left and right. The grey areas in the upper left and right corners represent combinations of spatial frequency and contrast that are outside your normal range of perception. Or, as Campbell (1983) describes it poetically: "[these areas] represent the region where the eye cannot perceive anything, and it is in this region that ectoplasm, fairies and ghosts could exist in privacy. Thus we have to perceive the world through the clear area of Figure 4. To extend its use, man has to bring objects into this

window by means of microscopes or telescopes, or by taking his eyeballs to the surface of the moon."

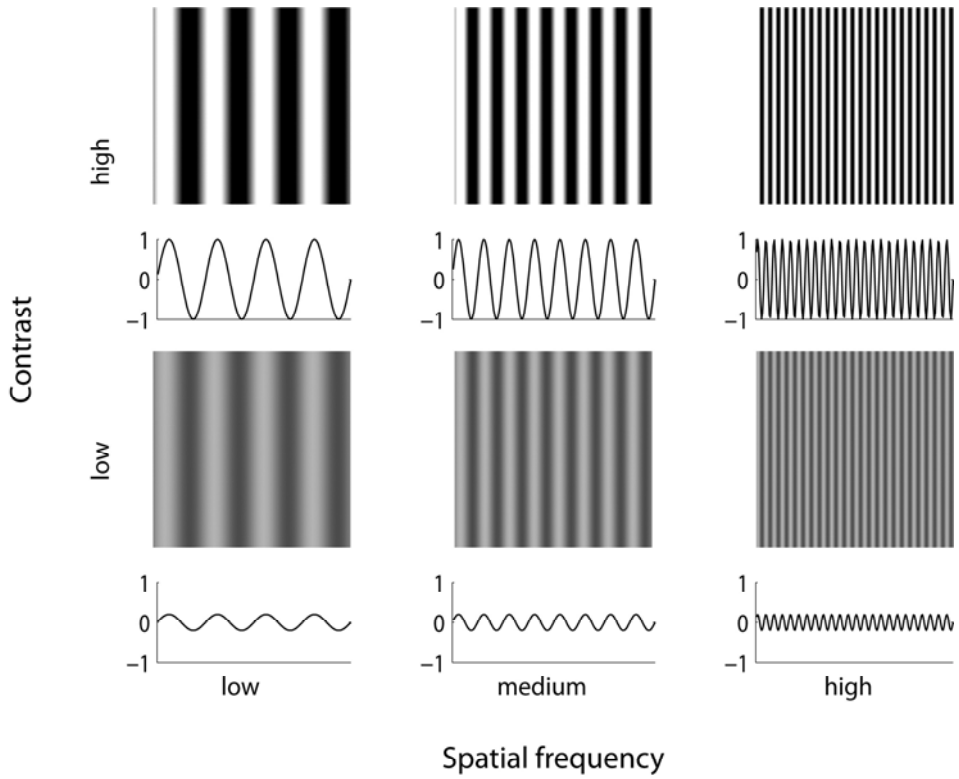

Figure 3. *Sine gratings are described by their spatial frequency, expressed in cycles/degree, and by their contrast, which is a ratio between the brightest and the darkest value.*

Why use sine gratings?

We are used to signals that vary over time, for example the audio signal that your MP3 player sends out as it plays your favourite music. This temporal signal can be broken down into its different frequency components using a Fourier transform. In the field of hearing, any sound can be synthesised by combining a number of pure tones (individual frequencies, i.e. sinusoidal sound waves) in the correct proportion.

Likewise, it is theoretically possible to construct a spatial signal (i.e. any visual image) by combining sinusoidal patterns. For example, a square wave can be generated by taking a sine wave and adding harmonics (3rd, 5th etc) with increasingly lower amplitudes, i.e. the 3rd harmonic has an amplitude of 1/3rd the fundamental, the 5th harmonic an amplitude of 1/5th of the fundamental (Figure 5). Thus, any light distribution on the retina can be expressed as the sum of its sinusoidal components.

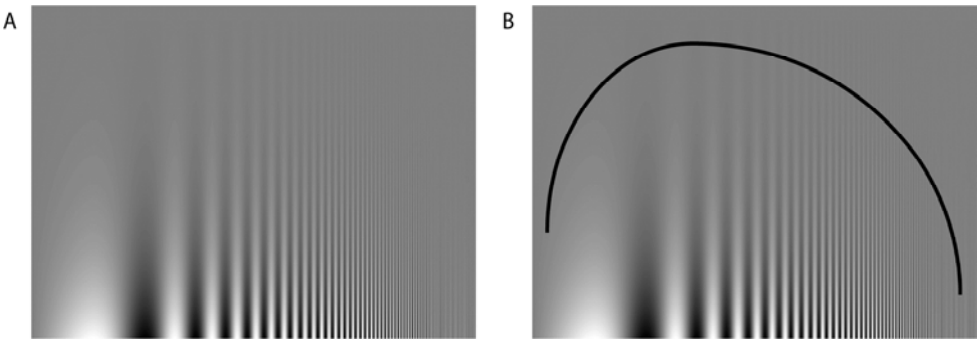

Figure 4 A. *The Campbell-Robson Contrast sensitivity chart demonstrates that the minimal observable contrast depends on the spatial frequency of the image (the size of the bars).* ***B.*** *Generally, you will see an optimum curve that looks like an inverted V or U. The height of this curve depends on your viewing distance. In this image, the spatial frequency increases logarithmically along the x axis and contrast decreases logarithmically along the y axis, from 100% to 0.5%. Luminance is constant throughout the image. In the lower right corner, there are some aliasing effects (Moire artefacts) caused by sub sampling the image in print. Image A by Izumi Ohzawa* http://ohzawa-lab.bpe.es.osaka-u.ac.jp/

The early stages of visual processing consists of filter mechanisms that are selective for specific information channels (image properties) such as spatial frequency and orientation (reviewed in Graham, 1989). The primate retina contains at least 17 distinct ganglion cell types, 13 of which project in parallel to the lateral geniculate nucleus of the thalamus and from there on to the visual cortex (reviewed in Nassi and Callaway, 2009). These cells have receptive fields of different sizes, varying as a function of retinal eccentricity

(in primates). Each type is thought to tile the retina, providing a complete representation across the entire visual field of the primary sensory cues it conveys to the brain, like different spatial or temporal frequencies, luminance and colour contrasts (Field and Chichilnisky, 2007). Maffei and Fiorentini (1972) described how retinal ganglion cells in the cat are sensitive to sine gratings with different ranges of spatial frequency, and how these channels progress through LGN and to the visual cortex. Figure 2 and 6 illustrate how the visual system uses these different channels to form an image of the outside world.

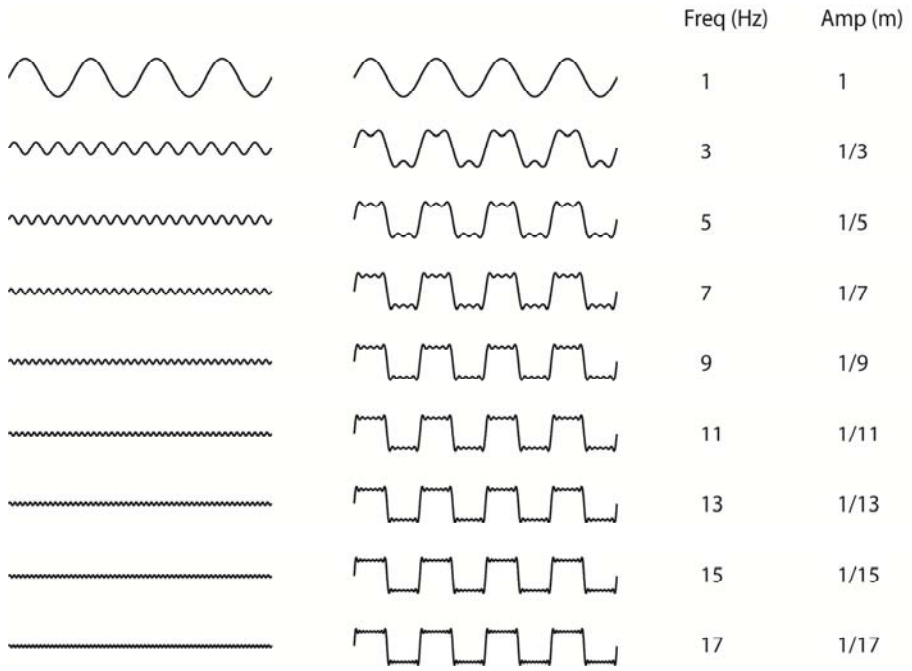

Figure 5. *According to Fourier theory, a square wave can be generated by adding every other harmonic (i.e 3rd, 5th etc) to a sine wave. Here, the 3rd to 17th harmonic are added to a sine wave and the result already resembles a square wave.*

Psychophysical and neurophysiological studies in primates showed that these channels have a relatively limited bandwidth for spatial frequency (±1 octave). Watson and Robson (1981) found that there are several spatial frequency channels between 0.25 and 30 cycles/degree. An additional

channel for low spatial frequencies below 0.2 cycles/degree was found by Hess and Norbdy (1986). Also, long exposure to a grating of a particular orientation and spatial frequency reduces the sensitivity of the visual system to stimuli with that orientation and spatial frequency (Blakemore and Campbell, 1969).

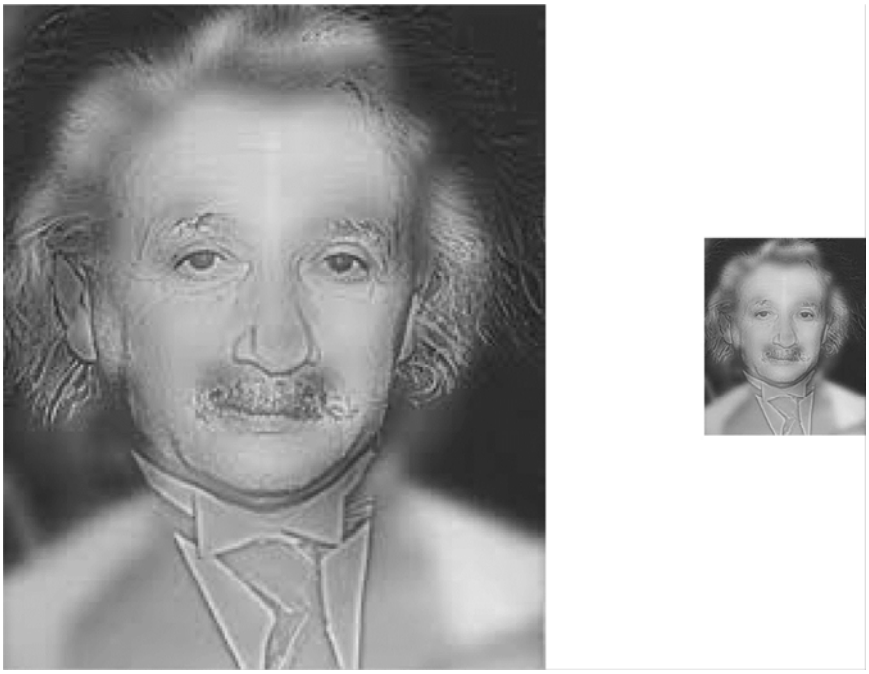

Figure 6. *The Marilyn Monroe-Einstein illusion. This image was created by superimposing two images made up on different spatial scales. The image of Einstein was high pass filtered and contains only high spatial frequencies, making it visible at close range. The picture of Marilyn Monroe is low pass filtered and contains only low spatial frequencies, making it visible at a few metres distance (or when reduced in size). Image © by Aude Oliva.*

Sinusoidal gratings have proven to be more precise in differentiating cells or channels with respect to their tuning properties than stimuli with hard edges, like bars or discs (Thomas, 1986). Stimuli with hard edges contain many Fourier components and these components are broadly distributed across the spatial frequency dimension (see Figure 5), stimulating many

channels at once. The response properties of many cells in the visual cortex are restricted in the Fourier domain: a given cell responds only to a limited bandwidth of spatial frequencies.

Campbell and Robson (1968) compared contrast sensitivity for gratings with that for square waves and found that for all spatial frequencies above 1 cycle/degree, square waves are seen about 1.3 times better than sine waves. However, at their respective contrast thresholds, square wave gratings and sine wave gratings were indistinguishable. In order to be able to distinguish between the two, contrast had to be increased until the third harmonic reached its own threshold. From this, Campbell and Robson concluded: "Thus a picture emerges of functionally separate mechanisms (channels) in the visual system, each responding maximally at some frequency and hardly at all at spatial frequencies differing by a factor of two."

Measuring visual acuity in mice

Mice are not considered to be 'visual animals'. They mainly rely on their olfactory and auditory systems, as well as their whiskers to perceive their surroundings. In order to measure visual acuity and contrast sensitivity in mice, perception of a visual stimulus has to be coupled with some kind of response. This response can be physiological or behavioral. There are many different kinds of tests measure visual function in mice (reviewed by Pinto 2000; see also table 2).

Simple: elevated/plus maze

Most tests are behavioral. The most simple of these tests are visual cliff and elevated plus maze tests. A mouse is placed in an area where visual depth cues are used to create the illusion of local differences in elevation, marking some zones as 'safe' and some 'unsafe'. Visual perception is measured by scoring how much of the time an animal spends in the safe zones. Although these tests can distinguish differences among strains (Fox, 1965), the observable behavior is very random, depending on factors such as fearfulness and the desire to explore (Flint et al, 1995).

Conditioning: avoidance/fear

One way to evoke easily observable behavior is by classical conditioning. Several tests have been described that use fear conditioning (Pinto, 1999) or avoidance learning (shuttle box test; Masu et al, 1995). A mouse is taught that a visual stimulus precedes an unpleasant experience, like a mild electric shock, and the animal will respond to that in a stereotypical way, either by freezing (in fear conditioning) or by moving away from the area where the shock will occur (Jiang et al., 1996). Visual function can be estimated by varying parameters of the stimulus and scoring which ones elicit a response (Smith, 1970; Ray, 1970).

Conditioning: maze

Another approach is to train mice to approach a visual stimulus by conditioning them in a forced choice behavioral paradigm to associate the stimulus with the presence of a reward; either food or safety. The trained mouse is placed in a two armed maze, with a grating stimulus on one side and a blank stimulus on the other, where it can either walk towards food (Gianfranceschi et al, 1999) or swim towards a submerged platform (Prusky et al, 2000; Prusky et al, 2004a; Douglas et al, 2005; Wong et al, 2006). Visual function is inferred by manipulating spatial frequency and contrast of the sine grating and scoring which stimuli elicit a response. Like other conditioning experiments, this approach is rather time consuming. Also, the way stimuli are presented do not always match the way they are perceived by the mouse. For example, the spatial frequency of a stimulus depends on the viewing distance and in a setup where mice are encouraged to move around it is hard to pinpoint the exact location where the animal decides which path to take.

Optomotor: body turns and OKN

Conditioned responses depend on a lot of factors, such as stress levels and inate traits like fearfulness, curiosity and the ability to make new associations. These factors can be excluded by studying optomotor responses, which are reflexive behaviors evoked by stimuli moving about

the animal. As a stimulus rotates about the animal, it evokes an optomotor response when the mouse can see the stimulus. This optomotor response can consist of optokinetic nystagmus (Sinex et al, 1979; Cahill and Nathans, 2008) or full body rotations (Prusky et al, 2004b; Jellali et al, 2005; Schmucker et al, 2005). As stimuli become harder to see, the magnitude of the optomotor response decreases. The experimenter observes the animal to see which stimuli evoke a response.

Two tests do not depend on behavior of a conscious animal: the electroretinogram (ERG) and visual evoked potentials of the cortex (VEPs). ERGs are a useful way to test for retinal degeneration by stimulating the eye with light and measuring electrical responses of various cell types (photoreceptors, ganglion cells, bipolar and amacrine cells) with electrodes placed on or near the eye (Riggs and Schick, 1964, 1968; Karpe, 1948; Balkema et al, 1981). VEPs are evoked by visually stimulating the eye using either flash stimuli or by reversing the dark and light pattern of grating stimuli. These stimuli activate neurons in the geniculo-cortical pathway and the visual cortex, which can be recorded with electrodes either placed on the scalp or subdermally, over the visual cortex (Rose and Lindsley, 1965, 1968).

Table 1 gives an overview of studies that measured visual acuity and contrast sensitivity in mice. Methods consisted of VEP or ERG recordings, two alternative forced choice (2AFC) maze tests and optomotor tests that looked either at full body turns or optokinetic nystagmus (OKN). Most studies used one method, except Douglas (2005) who compared a 2AFC maze test with an optomotor test and found rather different results (see below). Studies using square wave gratings give similar results as studies using sine wave gratings. Visual acuity measured with ERG shows that mice are able to see up to 0.6 cycles/degree (cpd) (Porciatti,et al 2007), which is similar to those recorded with VEPs (Porciatti, 1999; Huang et al, 1999).

Perceived contrasts are generally lower than in behavioral tests, which is probably because behavioral tests have a worse signal to noise ratio. Behavioral tests show more variable results, with thresholds in C57BL6 mice ranging from 0.375 (Wong et al 2006a) to 0.6 cpd (Gianfranchesci, 1999). A contrast sensitivity curve usually has an optimum, and the location of this

optimum varies with the method used. VEP and ERG recordings show an optimum around 0.06 cpd, maze tests find an optimum at 0.2 cpd, full body optomotor responses also show an optimum at 0.06 cpd while OKN optomotor responses have an optimum at 0.125 cpd. The contrast threshold found by OKN studies varies greatly, either 19% or 4% contrast.

Maze tests and optomotor tests give different results. Generally, the maximum spatial acuity is higher in maze tests while optomotor tests show higher contrast sensitivity. One explanation for this is that the optomotor tests measure the visual capabilities on the direct subcortical afferents while they may not be sensitive to detect small decreases in acuity (Douglas, 2005). Another problem in maze tests is that the distance from animal to stimulus can vary, making it harder to define the perceived spatial frequency. The different results can also be explained by the different behavior that is recorded. Maze tests look at all-or-nothing behavior while the optomotor response scales with how well the stimulus is perceived; becoming less vigorous near the threshold (Prusky, 2004b). The behavior in optomotor tests is not quantified; the experimenter looks at the animal and tries to distinguish rotating behavior from other behaviors such as grooming. In chapter 2 we present a method to quantify the visual acuity of mice in terms of its contrast sensitivity at many different spatial frequencies and in chapter 3 we present a practical application of this method by using the decrease in contrast sensitivity as a measure of aging in mutant mice that age rapidly as a result of broken down DNA repair mechanisms.. Unlike the methods described above we do not look only at behavior at the threshold of perception but look at how OKR performance decreases as the stimuli become harder to perceive. This has two advantages. First of all, it removes any biases an observer could have (Douglas, 2005). Also, by looking at a quantifiable response like the OKR, visual behavior can be studied over a large range of stimuli and not just at perceptual thresholds. Thus, this method is also applicable in man, as we demonstrate in chapter 4.

Study	Method	Stimulus	Mice	Max acuity (cpd)	Max contrast (%)
Huang 1999	VEP	Sine grating	C57BL/6J (wt) BDNF mutant	0.6 0.7	3-4 (no cpd) 3-4 (no cpd)
Porciatti 1999	VEP	Sine grating	C57BL/6J	0.48	4 (0.06 cpd)
Porciatti 2007	ERG	Sine grating	C57BL/6J	0.6	10 (0.05 cpd)
Gianfranchesci 1999	2AFC maze	Sine grating	C57BL/6J (wt) blc2 mutant	0.6 0.6	-
Prusky 2000	2AFC maze	Sine grating	C57BL/6J	0.49	-
Prusky 2004a	2AFC maze	Sine grating	C57BL/6J	0.528	16 (0.2 cpd)
Wong 2006a	2AFC maze	Sine grating	C57BL/6J DBA/2J AKR/J (albino) BALB/cByJ (albino) 129S1/SvImJ	0.375 0.375 0.375 0.320 0.245	- - - - -
Wong 2006b	2AFC maze	Sine grating	C57BL/6J DBA/2J D2.*mpclb* B6.*mpclb*	0.48 0.54 0.53 0.48	- - - -
Douglas 2005	2AFC maze Optomotor (body turn)	Sine grating	C57BL/6J	0.5 0.3	16 (0.2 cpd) 5 (0.06 cpd)
Prusky 2004b	Optomotor (body turn)	Sine grating	C57BL/6J	0.4	4 (0.064 cpd)
Umino 2008	Optomotor (body turn)	Sine grating	C57BL/6J	0.48	5 (0.125 cpd)
Jellai 2005	Optomotor (body turn)	Square wave	C57BL/6J 129/SvPas Rd1 Albino CD1	0.52 0.52 0 0	- - - -
Schmucker 2005	Optomotor (body turn)	Square wave	C57BL/6J	0.4	-
Sinex 1979	Optomotor (OKN)	Square wave	C57BL/6J *Reeler*	0.5 0.5	19 (0.12 cpd) 19 (0.12 cpd)
Cahill 2008	Optomotor (OKN)	Square wave	C57BL/6J 129/SvEv	0.5 0.25	4 (0.125 cpd) 8 (0.125 cpd)

Table 2: *Overview of studies that measured visual acuity and contrast sensitivity in mice.*

References

Albus, J. S. (1971). "Theory of Cerebellar Function." Mathematical Biosciences 10(1/2): 25-61.

Baarsma, E. A. and Collewij.H (1974). "Vestibulo-Ocular and Optokinetic Reactions to Rotation and Their Interaction in Rabbit." Journal of Physiology-London 238(3): 603-625.

Babinski, J. (1902). "Sur le rôle du cervelet dans les actes volitionnels necessitant une succession rapide de mouvements (adiadococinésie)." Rev Neurol 10: 1013-1015.

Balkema, G. W., Jr., L. H. Pinto, et al. (1981). "Characterization of abnormalities in the visual system of the mutant mouse pearl." J Neurosci 1(11): 1320-1329.

Batini, C., P. Buisseret, et al. (1974). "Extraocular proprioceptive and trigeminal projections to the Purkinje cells of the cerebellar cortex." Arch Ital Biol 112(1): 1-17.

Birch, D. and G. H. Jacobs (1979). "Spatial contrast sensitivity in albino and pigmented rats." Vision Res 19(8): 933-937.

Blake, R., S. J. Cool, et al. (1974). "Visual resolution in the cat." Vision Res 14(11): 1211-1217.

Blakemore, C. and F. W. Campbell (1969). "On the existence of neurones in the human visual system selectively sensitive to the orientation and size of retinal images." J Physiol 203(1): 237-260.

Bolk, L. (1906). "Das Cerebellum der Säugetiere: eine verglichende anatomische Untersuchung." Haarlem: Fischer.

Boyden, E. S., A. Katoh, et al. (2004). "Cerebellum-dependent learning: the role of multiple plasticity mechanisms." Annu Rev Neurosci 27: 581-609.

Braddick, F. W. C., J Atkinson (1978). Channels in Vision: Basic aspects.

Burr, D. C. and J. Ross (1982). "Contrast sensitivity at high velocities." Vision Res 22(4): 479-484.

Cahill, H. and J. Nathans (2008). "The optokinetic reflex as a tool for quantitative analyses of nervous system function in mice: application to genetic and drug-induced variation." PLoS One 3(4): e2055.

Campbell, F. W. (1983). "Why do we measure contrast sensitivity?" Behav Brain Res 10(1): 87-97.

Campbell, F. W., G. F. Cooper, et al. (1969). "The spatial selectivity of visual cells of the cat and the squirrel monkey." J Physiol 204(2): 120P+.
Campbell, F. W. and D. G. Green (1965). "Optical and retinal factors affecting visual resolution." J Physiol 181(3): 576-593.
Campbell, F. W. and J. G. Robson (1968). "Application of Fourier analysis to the visibility of gratings." J Physiol 197(3): 551-566.
Carter-Dawson, L. D. and M. M. LaVail (1979). "Rods and cones in the mouse retina. I. Structural analysis using light and electron microscopy." J Comp Neurol 188(2): 245-262.
Cenni, M. C., L. Bonfanti, et al. (1996). "Long-term survival of retinal ganglion cells following optic nerve section in adult bcl-2 transgenic mice." Eur J Neurosci 8(8): 1735-1745.
Collewijn, H. (1969). "Optokinetic eye movements in the rabbit: input-output relations." Vision Res 9(1): 117-132.
Collewijn, H. (1972). "Latency and gain of the rabbit's optokinetic reactions to small movements." Brain Res 36(1): 59-70.
Collewijn, H. and A. F. Grootendorst (1979). "Adaptation of optokinetic and vestibulo-ocular reflexes to modified visual input in the rabbit." Prog Brain Res 50: 771-781.
de Zeeuw, C. I., A. M. van Alphen, et al. (1998). "Recording eye movements in mice: a new approach to investigate the molecular basis of cerebellar control of motor learning and motor timing." Otolaryngol Head Neck Surg 119(3): 193-203.
Demer, J. L. (1995). "Evaluation of vestibular and visual oculomotor function." Otolaryngol Head Neck Surg 112(1): 16-35.
Douglas, R. M., N. M. Alam, et al. (2005). "Independent visual threshold measurements in the two eyes of freely moving rats and mice using a virtual-reality optokinetic system." Vis Neurosci 22(5): 677-684.
Drager, U. C. and J. F. Olsen (1981). "Ganglion cell distribution in the retina of the mouse." Invest Ophthalmol Vis Sci 20(3): 285-293.
Eccles, M. I. J. S. J. (1967). The cerebellum as a neuronal machine. New York, Springer Verlag.
Field, G. D. and E. J. Chichilnisky (2007). "Information processing in the primate retina: circuitry and coding." Annu Rev Neurosci 30: 1-30.

Fiorentini, A., N. Berardi, et al. (1995). "Nerve growth factor preserves behavioral visual acuity in monocularly deprived kittens." Vis Neurosci 12(1): 51-55.
Flint, J., R. Corley, et al. (1995). "A simple genetic basis for a complex psychological trait in laboratory mice." Science 269(5229): 1432-1435.
Flourens, P. (1824). "Rechérches expérimentales sur les propriétés et les fonctions du système nerveux dans les animaux vertébrés." Paris: Crevot.
Fox, M. W. (1965). "The visual cliff test for the study of visual depth perception in the mouse." Anim Behav 13(2): 232-233.
Frens, M. A. and J. N. van der Geest (2002). "Scleral search coils influence saccade dynamics." J Neurophysiol 88(2): 692-698.
Gerlai, R. (1996). "Gene-targeting studies of mammalian behavior: is it the mutation or the background genotype?" Trends Neurosci 19(5): 177-181.
Gianfranceschi, L., A. Fiorentini, et al. (1999). "Behavioural visual acuity of wild type and bcl2 transgenic mouse." Vision Res 39(3): 569-574.
Ginsburg, A. P. (2003). "Contrast sensitivity and functional vision." Int Ophthalmol Clin 43(2): 5-15.
Glickstein, M., P. Strata, et al. (2009). "Cerebellum: history." Neuroscience 162(3): 549-559.
Graham, N. (1989). Visual Pattern Analyzers. New York, Oxford University Press.
Hebb, D. O. (1949). The Organization of Behavior. New York, Wiley.
Herculano-Houzel, S. and R. Lent (2005). "Isotropic fractionator: a simple, rapid method for the quantification of total cell and neuron numbers in the brain." J Neurosci 25(10): 2518-2521.
Herman, L. M., M. F. Peacock, et al. (1975). "Bottle-nosed dolphin: double-slit pupil yields equivalent aerial and underwater diurnal acuity." Science 189(4203): 650-652.
Hess, R. F. and K. Nordby (1986). "Spatial and temporal properties of human rod vision in the achromat." J Physiol 371: 387-406.
Holden, A. L. and F. W. Fitzke (1988). "Image size in the fundus: structural evidence for wide-field retinal magnification factor." Br J Ophthalmol 72(3): 228-230.
Holmes, G. (1917). "The symptoms of acute cerebellar injuries due to gunshot injuries. ." Brain 4: 461-535.

Huang, Z. J., A. Kirkwood, et al. (1999). "BDNF regulates the maturation of inhibition and the critical period of plasticity in mouse visual cortex." Cell 98(6): 739-755.
Ito, M. (1982). "Cerebellar control of the vestibulo-ocular reflex--around the flocculus hypothesis." Annu Rev Neurosci 5: 275-296.
Ito, M. (2002). "The molecular organization of cerebellar long-term depression." Nat Rev Neurosci 3(11): 896-902.
Iwashita, M., R. Kanai, et al. (2001). "Dynamic properties, interactions and adaptive modifications of vestibulo-ocular reflex and optokinetic response in mice." Neurosci Res 39(3): 299-311.
Jacobs, G. H., J. Neitz, et al. (1991). "Retinal receptors in rodents maximally sensitive to ultraviolet light." Nature 353(6345): 655-656.
Jacobs, G. H., G. A. Williams, et al. (2004). "Influence of cone pigment coexpression on spectral sensitivity and color vision in the mouse." Vision Res 44(14): 1615-1622.
Jellali, A., M. Hamid, et al. (2005). "The optomotor response: a robust first-line visual screening method for mice." Vision Res 45(11): 1439-1446.
Jeon, C. J., E. Strettoi, et al. (1998). "The major cell populations of the mouse retina." J Neurosci 18(21): 8936-8946.
Jiang, H., A. Lyubarsky, et al. (1996). "Phospholipase C beta 4 is involved in modulating the visual response in mice." Proc Natl Acad Sci U S A 93(25): 14598-14601.
Karpe, G. (1948). "Apparatus and method for clinical recording of the electroretinogram." Doc Ophthalmol 2(1 vol.): 268-276.
Leigh, R. J., Zee, D. S. (2006). The Neurology of Eye Movements, Oxford University Press.
Maffei, L. and A. Fiorentini (1972). "Retinogeniculate convergence and analysis of contrast." J Neurophysiol 35(1): 65-72.
Maffei, L. and A. Fiorentini (1973). "The visual cortex as a spatial frequency analyser." Vision Res 13(7): 1255-1267.
Marr, D. (1969). "A theory of cerebellar cortex." J Physiol 202(2): 437-470.
Masu, M., H. Iwakabe, et al. (1995). "Specific deficit of the ON response in visual transmission by targeted disruption of the mGluR6 gene." Cell 80(5): 757-765.

Migliaccio, A. A., H. G. Macdougall, et al. (2005). "Inexpensive system for real-time 3-dimensional video-oculography using a fluorescent marker array." J Neurosci Methods 143(2): 141-150.
Miller, P. E. and C. J. Murphy (1995). "Vision in dogs." J Am Vet Med Assoc 207(12): 1623-1634.
Morris, R. G. M. (1981). "Spatial Localization Does Not Require the Presence of Local Cues." Learning and Motivation 12(2): 239-260.
Nagao, S. (1983). "Effects of vestibulocerebellar lesions upon dynamic characteristics and adaptation of vestibulo-ocular and optokinetic responses in pigmented rabbits." Exp Brain Res 53(1): 36-46.
Nassi, J. J. and E. M. Callaway (2009). "Parallel processing strategies of the primate visual system." Nat Rev Neurosci 10(5): 360-372.
Olzak, L. A. and J. P. Thomas (1981). "Gratings - Why Frequency Discrimination Is Sometimes Better Than Detection." Journal of the Optical Society of America 71(1): 64-70.
Perry, V. H. and A. Cowey (1985). "The ganglion cell and cone distributions in the monkey's retina: implications for central magnification factors." Vision Res 25(12): 1795-1810.
Pettigrew, J. D., B. Dreher, et al. (1988). "Peak density and distribution of ganglion cells in the retinae of microchiropteran bats: implications for visual acuity." Brain Behav Evol 32(1): 39-56.
Picciotto, M. R. and K. Wickman (1998). "Using knockout and transgenic mice to study neurophysiology and behavior." Physiol Rev 78(4): 1131-1163.
Pinto, L. H. and C. Enroth-Cugell (2000). "Tests of the mouse visual system." Mamm Genome 11(7): 531-536.
Porciatti, V., T. Pizzorusso, et al. (1999). "The visual physiology of the wild type mouse determined with pattern VEPs." Vision Res 39(18): 3071-3081.
Porciatti, V., M. Saleh, et al. (2007). "The pattern electroretinogram as a tool to monitor progressive retinal ganglion cell dysfunction in the DBA/2J mouse model of glaucoma." Invest Ophthalmol Vis Sci 48(2): 745-751.
Prusky, G. T. and R. M. Douglas (2004). "Characterization of mouse cortical spatial vision." Vision Res 44(28): 3411-3418.
Prusky, G. T., R. M. Douglas, et al. (2004). "Visual memory task for rats reveals an essential role for hippocampus and perirhinal cortex." Proc Natl Acad Sci U S A 101(14): 5064-5068.

Prusky, G. T., P. W. West, et al. (2000). "Behavioral assessment of visual acuity in mice and rats." Vision Res 40(16): 2201-2209.
Ray, B. A. (1970). Psychophysical testing of neurologic mutant mice. Animal Psychophysics: The Design and Conduct of Sensory Experiments. W. C. Stebbins. New York: 99-124.
Riggs, L. A., E. P. Johnson, et al. (1964). "Electrical Responses of the Human Eye to Moving Stimulus Patterns." Science 144(3618): 567.
Riggs, L. A. and A. M. Schick (1968). "Accuracy of retinal image stabilization achieved with a plane mirror on a tightly fitting contact lens." Vision Res 8(2): 159-169.
Robinson, D. A. (1963). "A Method of Measuring Eye Movement Using a Scleral Search Coil in a Magnetic Field." IEEE Trans Biomed Eng 10: 137-145.
Rolando, L. (1809). "Saggio sopra le vera struttura del cervello dell'uomo e degli animali e sopra le funzioni del sistema nervoso." Sassari: Stamperia da S.S.R.M.
Rose, G. H. and D. B. Lindsley (1965). "Visually Evoked Electrocortical Responses in Kittens: Development of Specific and Nonspecific Systems." Science 148: 1244-1246.
Rose, G. H. and D. B. Lindsley (1968). "Development of visually evoked potentials in kittens: specific and nonspecific responses." J Neurophysiol 31(4): 607-623.
Rosenblatt, F. (1962). Principles of neurodynamics: Perceptrons and the theory of brain mechanisms. Washington, Spartan Books.
Schmucker, C., M. Seeliger, et al. (2005). "Grating acuity at different luminances in wild-type mice and in mice lacking rod or cone function." Invest Ophthalmol Vis Sci 46(1): 398-407.
Schonewille, M. (2008). Cerebellar codings for control of compensatory eye movements. Neuroscience. Rotterdam, Erasmus MC: 208.
Simpson, J. I. (1984). "The accessory optic system." Annu Rev Neurosci 7: 13-41.
Sinex, D. G., L. J. Burdette, et al. (1979). "A psychophysical investigation of spatial vision in the normal and reeler mutant mouse." Vision Res 19(8): 853-857.
Smith, J. (1970). Conditioned suppression as an animal psychophysical technique. Animal Psychophysics: the Design and Conduct of Sensory Experiments. W. C. Stebbins. New York: 125-159.

Stahl, J. S. (2004). "Using eye movements to assess brain function in mice." Vision Res 44(28): 3401-3410.
Stahl, J. S., A. M. van Alphen, et al. (2000). "A comparison of video and magnetic search coil recordings of mouse eye movements." J Neurosci Methods 99(1-2): 101-110.
Steinhausen, W. (1933). "Uber die Beobachtung der Cupula in den Bogengansampullen des Labyrinths des lebenden Hechts." Pfluegers Arch. Gesamte Physiol 232: 500-512.
Thomas, J. P. (1986). "Spatial vision then and now." Vision Res 26(9): 1523-1530.
Timney, B. and K. Keil (1992). "Visual acuity in the horse." Vision Res 32(12): 2289-2293.
Umino, Y., E. Solessio, et al. (2008). "Speed, spatial, and temporal tuning of rod and cone vision in mouse." J Neurosci 28(1): 189-198.
van Alphen, A. M. and C. I. De Zeeuw (2002). "Cerebellar LTD facilitates but is not essential for long-term adaptation of the vestibulo-ocular reflex." Eur J Neurosci 16(3): 486-490.
van Alphen, B., B. H. Winkelman, et al. (2009). "Age- and sex-related differences in contrast sensitivity in C57BL/6 mice." Invest Ophthalmol Vis Sci 50(5): 2451-2458.
van Hof, M. W. and G. C. Lagers-van Haselen (1975). "Monocular pattern discrimination in rabbits after unilateral ablation of the visual cortex." Exp Neurol 46(1): 257-259.
Watson, A. B. and J. G. Robson (1981). "Discrimination at threshold: labelled detectors in human vision." Vision Res 21(7): 1115-1122.
Watson, A. B. and J. G. Robson (1981). "Discrimination at threshold: labelled detectors in human vision." Vision Res 21(7): 1115-1122.
Westheimer, G. and S. P. McKee (1975). "Visual acuity in the presence of retinal-image motion." J Opt Soc Am 65(7): 847-850.
Wiesenfeld, Z. and T. Branchek (1976). "Refractive state and visual acuity in the hooded rat." Vision Res 16(8): 823-827.
Wikler, K. C. and P. Rakic (1990). "Distribution of photoreceptor subtypes in the retina of diurnal and nocturnal primates." J Neurosci 10(10): 3390-3401.
Wong, A. A. and R. E. Brown (2006). "Visual detection, pattern discrimination and visual acuity in 14 strains of mice." Genes Brain Behav 5(5): 389-403.

Wong, A. A. and R. E. Brown (2007). "Age-related changes in visual acuity, learning and memory in C57BL/6J and DBA/2J mice." Neurobiol Aging 28(10): 1577-1593.

Chapter 2

Age- and Sex-Related Differences in Contrast Sensitivity in C57Bl6 mice

Bart van Alphen, Beerend Winkelman, Maarten Frens

Published in:

Age- and sex-related differences in contrast sensitivity in C57BL/6 mice.
van Alphen, B., Winkelman, B.H.J., Frens, M.A. (2009).
Investigative Ophthalmology and Visual Science 50(5): 2451-2458.

Introduction

The contrast sensitivity function (CSF) shows which contrasts can be seen at a range of spatial frequencies (the number of sine gratings in one degree of visual angle). Maze tests and optomotor tests are most commonly used to test the CSF of mice. Both however, have their drawbacks.

In maze tests, a mouse is trained to distinguish sine gratings from a uniform gray field to obtain a food reward [1] or find a submerged platform in a two armed watermaze [2-4]. The distance from animal to stimulus varies in this test, making it hard or even impossible to define the perceived spatial frequency exactly.

In optomotor tests a mouse is surrounded by a panoramic sine grating. As the stimulus rotates about the animal, it evokes an optomotor response when the mouse distinguishes the stimulus pattern from a homogeneous background. This optomotor response can consist of optokinetic nystagmus [5] or full body rotations [6-9]. The behavior in optomotor tests is often not quantified (except one group who measured full body rotations [8]); the experimenter observes the animal and tries to distinguish which stimuli evoke a response

The optomotor response scales with how well the stimulus is perceived; becoming less vigorous as stimuli are harder to perceive [6]. This makes it hard for observers to see which stimuli evoke responses close to threshold.

Furthermore, maze tests and optomotor tests give different results. Generally, the maximum spatial acuity is reported to be higher in maze tests while optomotor tests show higher contrast sensitivity [6]. Also, the measurements of contrast sensitivity are basically dichotome. When an animal responds, by choosing the correct arm in a maze or by rotating along with the stimulus, it is inferred that the animal sees the stimulus.

We have used a novel way to measure contrast sensitivity in mice. By recording how the gain of the optokinetic reflex (OKR, a gaze stabilization reflex) decreases as moving sine grating stimuli become harder to see, we can look not just at whether an animal reacts to a stimulus but also at the magnitude of that response.

Our first objective was to quantify vision in the most commonly used mouse in behavioural neuroscience, i.e. the C57BL/6J mouse. In addition, we investigated the effect of sex and age on contrast sensitivity function.
To show applicability in pharmacological or genetic studies we also investigated how the contrast sensitivity of mice was affected by pilocarpine, a drug that decreases pupil size and is often used in mice video-oculography [10]. Additionally, we studied the L7-PKCi mouse, a mutant where plasticity in the cerebellum is impaired [11] by bringing a protein kinase C inhibitor to expression. This mutant was reported to perform worse in the Morris water maze; a navigation task requiring accurate vision. This decrease in performance did not occur in a star maze; a maze where navigation is less dependent on vision [12]. It was suggested that the mutation might have an effect on spatial learning. However, the promotor used to express the PKC inhibitor is also found in the retina [13]. Here we tested whether vision was affected in the L7-PKCi mutant.

Materials and methods

Animals

In this study 25 adult mice (10 4- month old and 5 9-month old males and 10 4-month old females) of the C57BL/6J background (Jackson Laboratory, Bar Harbor, ME) strain were used, as well as 10 male L7-PKCi mutants and 10 male wildtype littermates. The L7-PKCi transgenic mouse lacks long term depression at the parallel fibre Purkinje cell synapse [11]. All mice were housed on a 12 h light / 12 h dark cycle with unrestricted access to food and water. Experiments were done during their light phase. All experiments were done with approval of the local ethics committee and were in accordance with the European Communities Council Directive (86/609/EEC) and the ARVO Statement for the Use of Animals in Ophthalmic and Vision Research.

Surgery

Animals were prepared for fixation by head restraint by attaching two metal nuts to the skull using a construct made of a microglass composite (Charisma; Heraues Kulzer GmbH, Hanau, Germany) All surgical

procedures were performed while the animal was anesthetized with a mixture of isofluoran (Isofloran 1–1.5%; Rhodia Organique Fine Ltd, Bristol, UK) and oxygen. After anaesthesia induction a sagittal incision was made across the scalp, exposing lamda and bregma. The periosteum was removed after which the skull was briefly etched using a gel containing phosphoros acid. Then the skull was dried thoroughly and a drop of primer (Optibond Prime, Kerr USA, Orange CA) was applied to the etched part of the skull, followed by a layer of adhesive (Kerr USA, Orange CA) that was light cured until it formed a hard shiny layer that will facilitate a strong bond between skull and composite. Two layers of composite were used to make a pedestal on which a prefabricated construct of two metal nuts (M4) was attached.

Stimulus setup

Optokinetic stimuli were created using a modified Electrohome Marquee 9000 CRT projector (Christie Digital Systems, Cypress CA, USA). The red and blue CRT tubes were replaced by green ones. The three tubes were mounted on the ceiling at a 120° angle from each other. The CRT tubes projected their images via mirrors onto three transparent anthracite screens (156*125 cm) which were placed in a triangular formation around the recording setup (Fig 1A). This created a monochrome panoramic stimulus fully surrounding the animal. The stimuli were programmed in C++ and rendered in openGL. A 360 degrees stimulus consisted of a virtual vertically oriented cylinder with a vertically oriented sine grating on its wall. The spatial resolution of the setup was 1600*1200 pixels per screen, and hence a pixel subtended 4.5 arcminutes. Luminances of the bright (I max) and dark stripes (I min) were measured using a LS-100 luminance meter (Minolta camera co. LTD, Osaka, Japan), after which contrasts were calculated using the Michelson formula:

$$C = \frac{(Imax - Imin)}{(Imax + Imin)}$$

Average luminance was 17.5 cd/m^2 in all stimulus conditions. The minimal luminance of the stimulus was 0.05 cd/m^2, the maximum luminance was 35 cd/m^2).

Recording setup

The animal was placed in a plastic tube which was attached to a set of linear stages that allowed translations in three dimensions as well as rotation about the naso-occipital axis. These stages were used to position the mouse eye in the centre of the visual stimulus, and in front of the eye position recording apparatus, before the experiment. Both the linear stages and the recording setup were attached to a table.

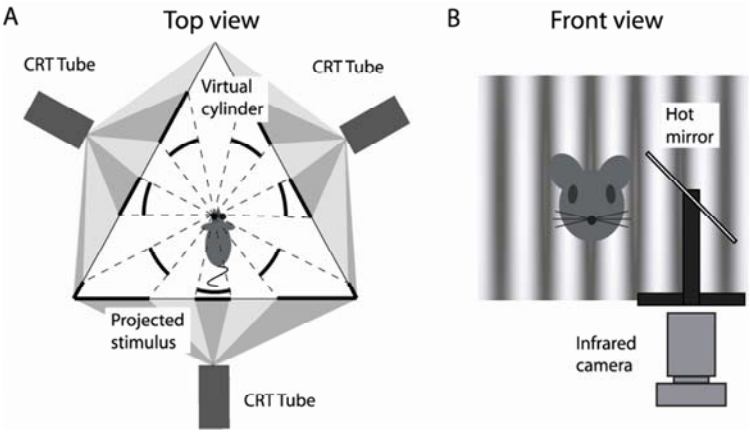

Figure 1*. Schematic representation of the experimental setup. A. Top view. A mouse was placed in the setup, with its left eye in the exact center. It was surrounded by three screens on which the sine gratings are projected. Here the tubes are shown to be surrounding the setup. In the lab the three tubes were mounted on the ceiling at a 120° angle from each other and projected their images via mirrors onto the three screens. The stimulus was programmed in such a way that it appeared as a virtual cylinder from the perspective of the mouse B. Front view. To keep the field of view of the mouse unobstructed we recorded eye movements with an infrared camera that was placed under the set up. The eye was tracked using a hot mirror, a mirror that is transparent to visible light but reflects infrared light.*

Image acquisition

The system resembled the one described by Stahl [10] with some modifications. Eye movements were recorded with an infrared video system (Iscan ETL-

200). Images of the eye were captured at 120 Hz with an infrared sensitive CCD camera. From this image, X and Y positions of the center of the pupil and the corneal reflection (1st Purkinje image) were recorded in pixel positions, giving their location on the 512*256 pixel grid, with a resolution of 1/3 pixel horizontally and 1/10 pixel vertically. These positions were lowpass filtered with a cut off frequency of 300Hz (Axon Cyberamp 380), sampled at 1 kHz and stored for offline analysis.

In order to keep the field of view as free from obstacles as much as possible the camera and lens were mounted under the table surface and recordings were made using a hot mirror, which was transparent to visible light and reflective to infrared light (Fig 1B). The eye was illuminated using two infrared LEDs at the base of the hot mirror. The camera, mirror and LEDs were all mounted on an arm that could rotate about the vertical axis over a range of 26.12º (peak to peak). Eye movement recordings and calibration procedures were similar to those described by Stahl [10], yielding eye position in degrees of visual angle.

Testing procedure

The animal was placed in a plastic tube with its head fixed to a small metal bar. By fixing its head, the exact distance from the eye to the screen is known which allows optimal definition of the stimulus. Additionally, head fixing the mouse is required to record its eye movements with an infrared camera. The left eye of the mouse was positioned at the centre of the virtual cylinder.
Each stimulus showed a sine grating made up of a combination of one of seven spatial frequencies (0.03, 0.05, 0.08, 0.17, 0.25, 0.33, or 0.42 cycles per degree) and one of six contrast value (100%, 75%, 50%, 25%, 10%, 1%). The 42 stimulus combinations were presented in random order.
A stimulus was first projected and was kept stationary for one minute, allowing the eye to adjust to changes in stimulus brightness. Then the stimulus started to move with a constant velocity of 6 º/s. It moved to one direction for two seconds, than it changed direction and moved in the opposite direction for two seconds. This was repeated five times, yielding 10 changes in direction. As the stimulus moved, the position of the left eye was

recorded. The screens were bright enough to allow pupil recordings over the small range of eye movement amplitude.

Data analysis

Recorded eye positions were transformed offline in a velocity signal. Fast phases are removed using a velocity threshold of twice the stimulus velocity (i.e.,12 º/s). The first 200 ms after stimulus onset and before and after each change in direction were removed as well. Because the stimulus velocity was constant and eye data in the first 200 ms after the stimulus direction changes were ignored, average absolute eye velocity could be divided directly by the stimulus velocity to calculate a gain value for each combination of spatial frequency and contrast. The gain is the ratio between average eye velocity and stimulus velocity, and a gain of 1 means that the eye has the same velocity as the stimulus [15]. Experimenters were masked to the experimental conditions. Trials were randomized, mice were assigned a number and the data analysis scripts were automated. All data was analyzed after the experiment.

Statistics

The effect of age, sex, pilocarpine and the L7-PKCi mutation were analyzed using a repeated measures ANOVA with three factors: one between subjects factor with two levels (for example: 'Sex' with 2 levels: male and female) and two within subject factors: 'Contrast' with 6 levels and 'Spatial Frequency' with 7 levels). Post hoc, groups were compared at each contrast by averaging OKR gains over spatial frequencies. Differences between groups were analysed for significance with a student's t-test. A detailed step by step guide of these methods can be found in Appendix A, along with some helpful troubleshooting tips.

Contrast sensitivity in C57BL/6J mice

To investigate whether gender has an effect on contrast sensitivity, we compared OKR gains between 10 male and 10 female 4-months old C57BL/6J mice. To gain more insight in the effect of age on contrast sensitivity, OKR

gains between the 10 4- months old mice and 5 9-months old male C57BL/6J mice.

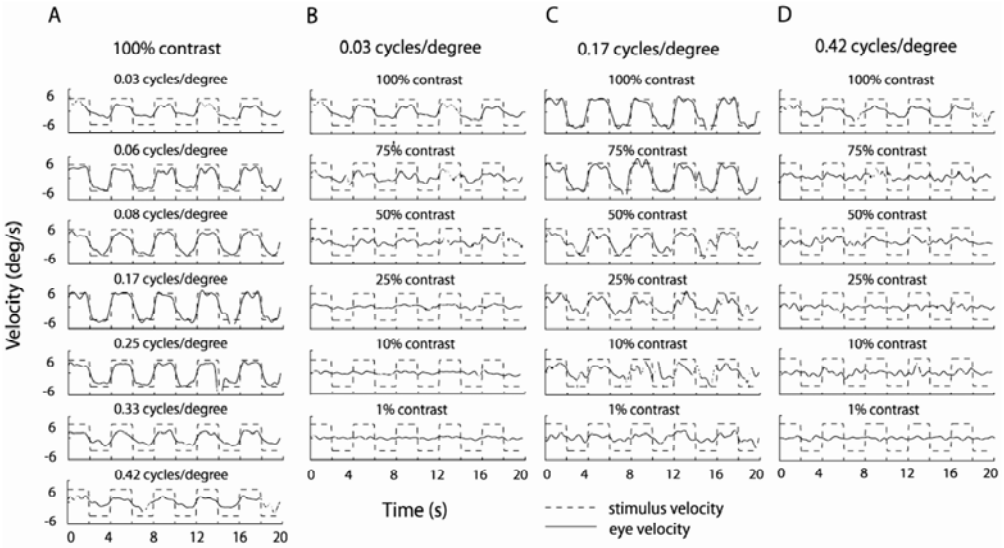

Figure 2. *Eye velocity and stimulus velocity traces. A, Eye and stimulus velocities are plotted for a single C57Bl6/J male (4 months old) at 7 spatial frequencies. Contrast is 100%. Here the response shows an optimum at 0.17 cycles/degree and decreases as the gratings become either larger or smaller than 0.17 cycles/degree. B-D Eye and stimulus velocities of the same mouse at 6 contrast values. The spatial frequency is 0.03 cycles/degree (B), 0.17 cycles/degree (C) and 0.42 cycles/degree (D). As contrast decreases the stimulus becomes harder to see and the eye velocity decreases. At very low contrasts the eye velocity decreases to zero.*

Effect of miotic drugs on contrast sensitivity

When the gaze stabilization reflexes of mice are tested using video-oculography, their pupil size is often reduced in order for the eye movement recordings to work properly. This can be achieved by applying meiotic drugs such as pilocarpine to the cornea.

Pilocarpine acts on a subtype of the muscarinic receptor (M_3) found on the iris sphincter muscle, causing the muscle to contract and the pupil to constrict. A drawback of using Pilocarpine while investigating gaze

stabilization reflexes is that the treatment might affect visual function. We investigated the effect of artificial pupil constriction on contrast sensitivity by applying a 1% pilocarpine hydrochloride solution (Minims, Chauvin Benelux NV, Belgium) to the eyes. We compared OKR gains within these mice before and after treatment of 10 4-month old male C57BL/6J mice using a multivariate repeated measures ANOVA.

Contrast sensitivity of L7-PKCi mutants

In L7-PKCi mice, a protein kinase C inhibitor is expressed in Purkinje cells under the control of the pcp-2(L7) gene promoter [11]. However, the protein pcp-2 (L7) is not only expressed in Purkinje cells, it is also expressed in bipolar cells in the retina [13]. This means that the protein kinase C inhibitor might be expressed in the retina of the L7-PKCi transgenic mouse as well and could result in deteriorated vision. We investigate whether the contrast sensitivity function is affected in the L7-PKCi mutant. Thereto we compared OKR gains between 10 4-month old male L7-PKCi mouse mutants and 10 4-month old wild type littermates.

Results

Effect of sex on contrast sensitivity

We determined OKR gain in 10 male and 10 female mice for the 42 combinations of a contrast and a spatial frequency. We find a main effect of sex (between subject) $F = 17.6$, $p = 0.001$. There were no significant interaction effects: spatial frequency * sex ($F(6,13)=2.56$, $p = 0.073$) and contrast * sex ($F(5,14)=2.82$, $p = 0.058$). Within subjects we find a main effect of spatial frequency ($F(6,13)=141$, $p < 0.001$) and a main effect of contrast ($F(5,14) = 177$, $p < 0.001$).

Post-hoc analysis showed that for each of the six contrasts, the OKR gains averaged over spatial frequencies were significantly lower in female than in male mice (t-test: $p < 0.05$ at 100% contrast; $p < 0.01$ at 1%, 25%, 50% and 75% contrast.; $p < 0.001$ at 10% contrast; Fig 3B-H). The optimum response was at 0.17 cycles/degree for both sexes for all contrasts. With maximum contrast

and optimal spatial frequency the OKR gain was not different between male and female mice (0.97 ± 0.13 vs. 0.85 ± 0.15, t-test, p = 0.1).

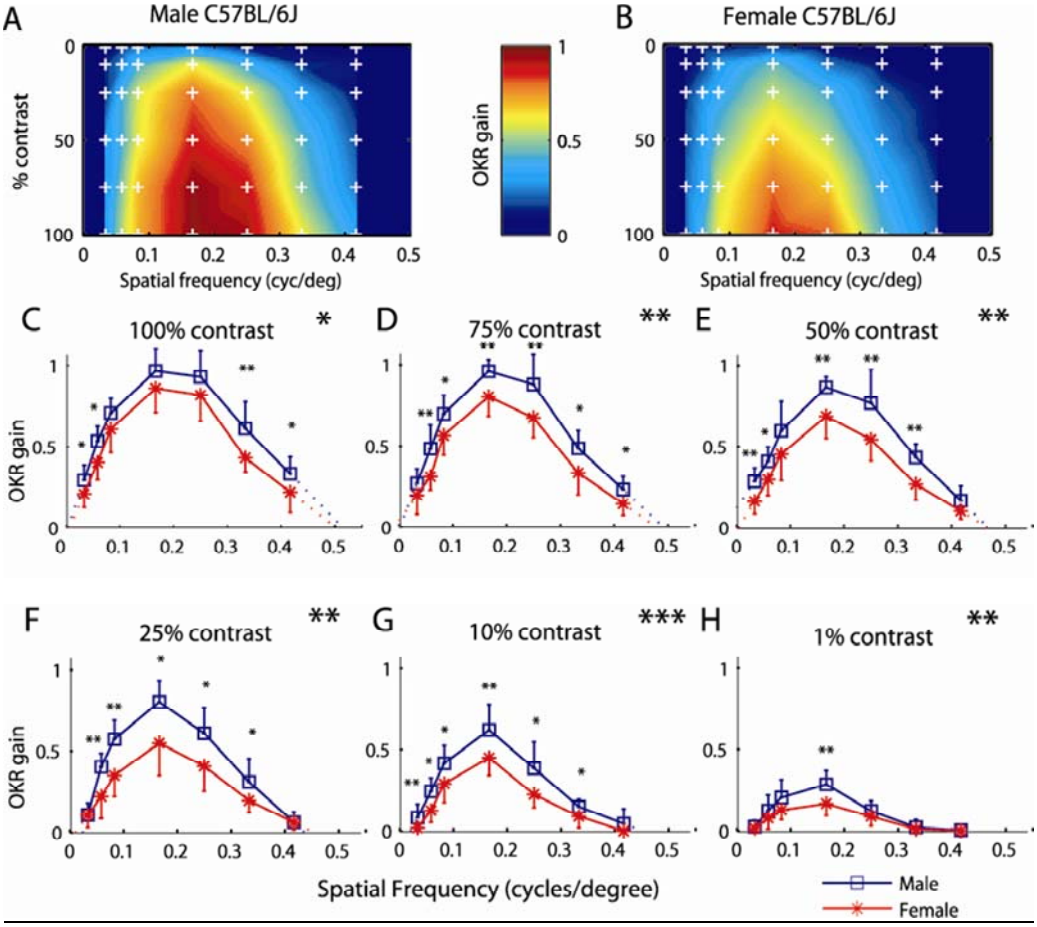

Figure 3. *OKR gains of male and female 4-month C57BL/6J mice. A,B, The color reflects the OKR gain at each of the 42 combinations of contrast and spatial frequency, indicated by the white crosses. The spaces in between the measured points are filled with linear interpolation. C-H, six cross-sections of A and B are plotted, one at each contrast. Error bars indicate standard deviations. Stars in the graphs indicate significant differences between male and female mice (t-test, * = p<0.05; ** = p<0.01; *** = p<0.001). Dotted lines show extrapolation to zero gain.*

When contrast was reduced, the gain of the OKR decreases (Fig 2). For all contrasts, the OKR response was highest in only a small range of spatial frequencies around 0.17 cycles/degree (fig 3C-H). Even stimuli with 1% contrast were able to evoke an OKR (Fig 3H). A stimulus with 0.17 cycles/degree and 1% contrast evoked an OKR with a gain of 0.2. This means that the eye was moving at 20% of the stimulus speed, or 1.2°/s for two seconds.

Velocity gains were extrapolated by elongating the line through the last two points (0.33 and 0.42 cycles/degree) to zero gain in order to estimate the maximum contrast sensitivity for both groups. At 100% contrast the estimated maximal contrast sensitivity of male mice is 0.52 cycles/degree. For females, extrapolation shows an estimated maximum contrast sensitivity of 0.50 cycles/degree at 100% contrast.

Effect of age on contrast sensitivity

Figure 4 shows the OKR gains of 10 young adult males (4 months old) and 5 adult males (9 months old). Between subjects, there is a main effect of age ($F = 17.7$, $p = 0.001$). Within subjects there are main effects of spatial frequency ($F(6,8)=300$, $p < 0.001$) and contrast ($F(5,9) = 168$, $p < 0.001$). There was one significant interaction effect: spatial frequency * age ($F(6,8)=2.56$, $p = 0.01$). The interaction of contrast * age was not significant ($F(5,9)=2.61$, $p = 0.109$)

Post hoc analysis showed that four of the six contrasts the OKR gains of 4-months old mice were significantly lower than those of 9-month old mice (t-test, $p < 0.01$ at 10%, 25%, 50% and 75% contrast, figure 3). Only at highest and lowest contrasts there were no significant differences between the two groups (Fig 4C and H). At maximum contrast and optimal spatial frequency (0.17 cycles/degree) the OKR gain was not different between younger and older mice (0.97 ± 0.12 vs. 0.94 ± 0.03, t-test, $p = 0.76$).

Extrapolation by elongating the line through the last two points (0.33 and 0.42 cycles/degree) to zero shows an estimated maximum contrast sensitivity at 100% contrast of 0.52 for 5 months old mice and 0.54 for 9 months old mice.

Effect of miotic drugs on contrast sensitivity

In the group of 10 4-month old male C57BL/6J mice we tested the effect of pilocarpine. Application of pilocarpine reduced pupil diameter from 0.366 ± 0.096 (SD) mm to 0.216 ± 0.053 mm ($p < 0.001$). The main effect of Pilocarpine ($F = 3.64$, $p = 0.89$), as well as the interactions 'Pilocarpine' with 'Contrast' ($F(5,14) = 2.20$, $p = .20$) and 'Pilocarpine' with 'Spatial Frequency' ($F(6,13) = 1.95$, $p = 0.27$) were not significant. Significant main effects of the factors 'Contrast' ($F(5,14) = 214$, $p < 0.0001$ and 'Spatial Frequency' ($F(6,13) = 123$, $p < 0.0001$) were observed.

Velocity gains were extrapolated by elongating the line through the last two points (0.33 and 0.42 cycles/degree) to zero gain in order to estimate the maximum contrast sensitivity for both groups. At 100% contrast the estimated maximal contrast sensitivty is 0.51 cycles/degree for both groups.

Effect of L7-PKCi mutation on contrast sensitivity

To test the effect of the L7-PKCi mutation on visual performance, we compared the OKR gains of 10 mutants with those of 10 of their wildtype littermates. The main effect of the mutation is not significant ($F = 0.055$, $p = 0.82$) and neither are the interactions of Spatial Frequency with the mutation ($F(6,13)=0.90$, $p = 0.51$) and Contrast with the mutation ($F(5,14)=0.4$, $p = 0.84$). Within subjects there are main effects of Spatial Frequency ($F(6,13)=115$, $p < 0.001$) and Contrast ($F(5,14) = 184$, $p < 0.001$). Figure 6 shows that there is no difference in OKR gains between the two groups. Both groups have similar gains close to 1 at 100% contrast and 0.17 cycles/degree 0.93 ± 0.05 vs. 0.93 ± 0.19, $p = 0.998$).

Extrapolation by elongating the line through the last two points (0.33 and 0.42 cycles/degree) to zero shows an estimated maximum contrast sensitivity at 100% contrast of 0.49 for wildtypes and 0.51 for the mutants.

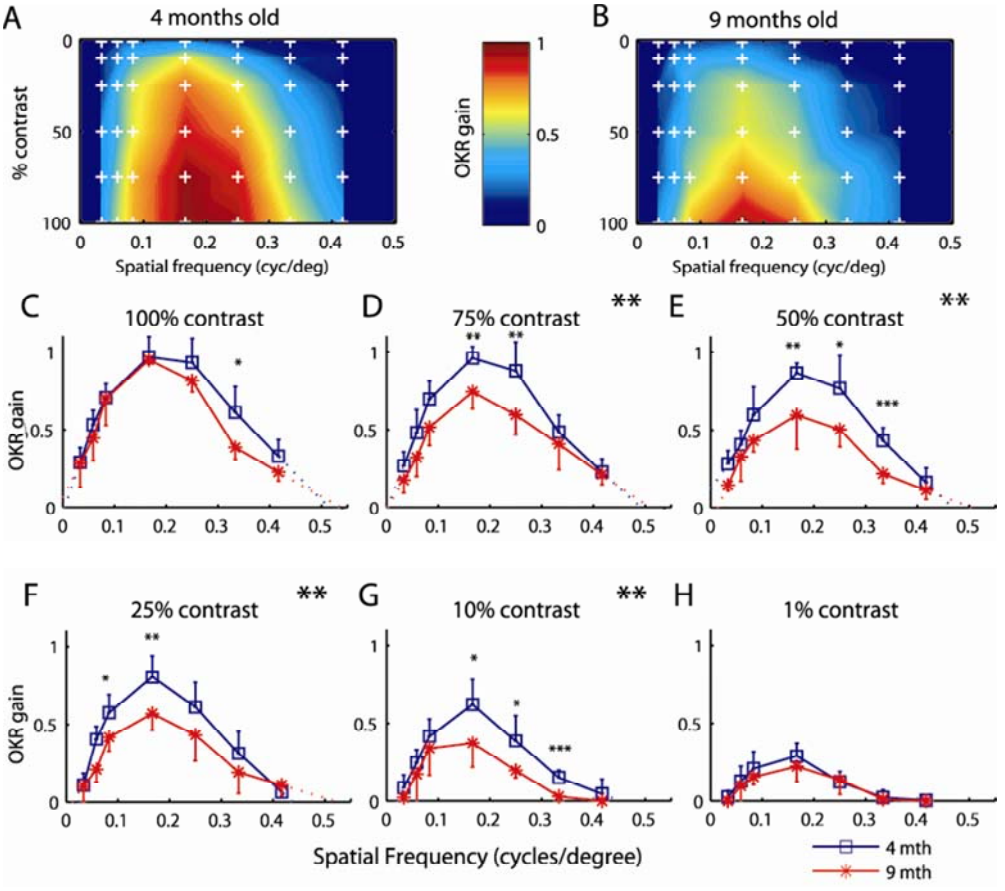

Figure 4. *OKR gains of 10 4-months old and 5 9-months old male C57BL/6J mice. A,B, White crosses show OKR gains at 42 combinations of contrast and spatial frequency. The colour shows the OKR gain at each point. The spaces between the measured points are filled with linear interpolation. C-H, six cross-sections of A and B are plotted, one at each contrast. Errorbars show standard deviations. Stars in the graphs show which points are significantly different between groups (* = p<0.05; ** = p<0.01; *** = p<0.001). OKR response curves in D-G are significantly different (t-test , p<0.01). Dotted lines show extrapolation to zero gain.*

Discussion

By measuring how the gain of the optokinetic reflex (OKR) varies with different contrasts and spatial frequencies the contrast sensitivity function can be inferred.

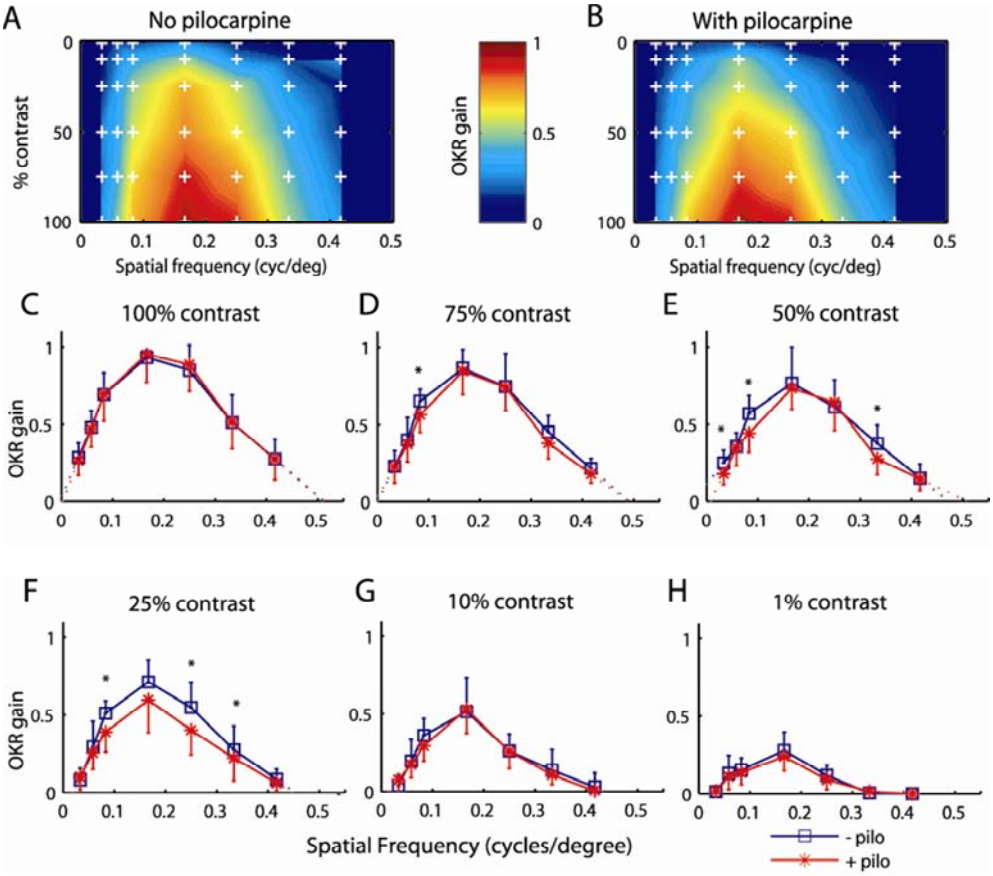

Figure 5. *The effect of Pilocarpine on the OKR gains in 10 male C57BL/6J mice. A,B, White crosses show OKR gains at 42 combinations of contrast and spatial frequency. The color shows the OKR gain at each point. The spaces between the measured points are filled with linear interpolation. C-H, six crosssections of A and B are plotted, one at each contrast. Errorbars show standard deviations Stars in the graphs show which points are significantly different between groups (* = p<0.05, t-test). Dotted lines show extrapolation to zero gain.*

Using this approach, we observed differences in contrast sensitivity between male and female C57BL/6J mice, as well as between younger and older adult C57BL/6J mice. As expected, the effects of spatial frequency and contrast on OKR were highly significant in all experiments. Like other optomotor responses, the OKR becomes less vigorous as stimuli become harder to perceive [14]. However, unlike other optomotor responses, the magnitude of

the OKR can be easily quantified with eye tracking. Such methods are well established [10]. This makes the OKR a sensitive tool to probe visual capabilities, without having to depend on an observer deciding whether an animal responds.

The OKR evoked by gratings of different contrasts and spatial frequencies decreased like the optomotor response of turning rodents [6]. However, the response did not diminish only close to a perceptual threshold but over a much larger range of stimuli (Fig 2). The motor circuits underlying the OKR appeared unaffected in all mice because their OKR has a gain close to 1 at 0.17 cycles/° and 100% contrast, identical to the younger mice (panel C, fig 3-6). Throughout a stimulus presentation, the mice responded with a highly regular OKR-movement (Fig 2).

In order to use the OKR as a tool to investigate contrast sensitivity it is important to understand the properties of this tool. The OKR is a gaze stabilization reflex that is evoked by image motion in the visual field. It causes the eye to move along with the movement in the visual field, thus minimizing retinal slip [15-18]. Rabbit data shows that a quarter of the retinal ganglion cells are sensitive to a pattern moving in a particular direction. These direction selective ganglion cells are most sensitive to low stimulus velocities [14]. This occurs as well in other afoveate species like the rat [19], rabbit [15] and goldfish [20]. The OKR of mice is also velocity tuned and decreases with increasing stimulus velocity [21]. Therefore, the OKR is most useful as a probe to study contrast sensitivity when it is used with low stimulus velocties, where the gain is high.

Umino [9] also report velocity tuning for the optomotor response, under photopic conditions, but find a bell shaped response curve, with an optimum response at a stimulus velocity of 12°/s. An explanation for these differences in velocity tuning might be found in their experimental paradigm. Mice were subjected to stimuli that moved either clockwise or counterclockwise for 5 seconds, at velocities between 1.5 and 24°/s, and an observer decided whether the mice rotated their body along with the stimulus. However, like the OKR the optomotor response decreases as stimuli become harder to perceive [6]. A mouse that responds optimally to a

stimulus that moves for 5 seconds with 1.5°/s will rotate 7.5°. This is analogous to the hand of a clock that moves in five seconds from 12:00 to halfway between 12:01 and 12:02. If a mouse responds with a gain of 0.5 it moves at 0.75°/s and the full body rotation of 3.75° in five seconds becomes very hard to detect by eye.

In this study, we did not search for the highest possible acuity. The highest spatial frequency, 0.417 cycles/°, evoked an OKR with gains above 0.2 in all animals at 100% and 75% contrast. However, extrapolation to zero gain showed an absolute threshold of 0.49-0.52 cycles/° for all groups. This is similar to the 0.5-0.6 cycles/° reported by other experiments [1,8,22] that use optomotor responses to probe the visual system.

We find a significant optokinetic response at the lowest contrast (1%) in all animals. This is much lower than the threshold of 5% contrast that was reported in both maze tests and optomotor tests [6,8]. This lower threshold almost closes the contrast detection gap between mice and men. Humans are able to see up to about 0.5% contrast [23] and up to 60 cycles/° [24]. They have a much better visual acuity than mice (0.5 cycles/°). So the acuity of man is more than 100 times better than that of mice, while the lowest detectable contrast varies only a factor 2. The mouse eye has notoriously poor optics. Two studies measured modulation transfer functions of the mouse eye [25, 26].Both studies show that the ability of the lens to transfer contrasts decreases rapidly as spatial frequency increases. However, the stimuli used in our experiments are no higher than 0.42 cycles/degree, a range at which the reported modulation transfer functions are close to optimal.

In this study we did not correct for refractive errors of the mouse eye so the data reported in this paper might be an underestimation of the contrast sensitivity of C57BL/6J mice. However, this data is very useful to design

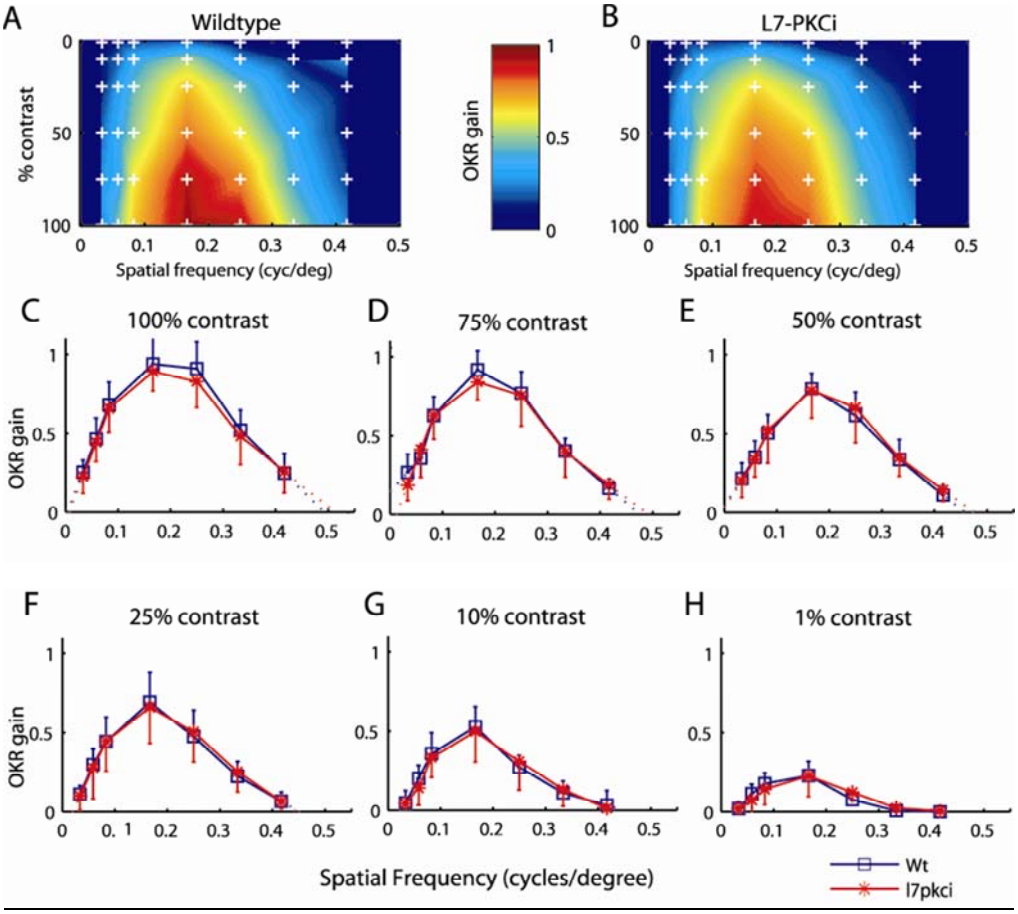

Figure 6. *OKR gains of 10 L7-PKCi mutants and 10 wildtype littermates. A,B, White crosses show OKR gains at 42 combinations of contrast and spatial frequency. The color shows the OKR gain at each point. The spaces between the measured points are filled with linear interpolation. C-H, six cross-sections of A and B are plotted, one at each contrast. Errorbars show standard deviations. There are no significant differences in contrast sensitivity between L7-PKCi mutants and their wildtype littermates (t-test). Dotted lines show extrapolation to zero gain.*

behavioral experiments that require vision and where it is not possible to correct for the refractive errors of the mouse eye. Also, there is not much known about whether mice can accommodate so the close distance to the screen could result in sub-optimal contrast performance.

Effect of sex on contrast sensitivity

Female C57BL/6J mice show consistent lower gains than male mice in almost all stimulus conditions, except for a few spatial frequencies at maximum or minimum contrasts. Because the OKR is similar for males and females under optimal conditions (0.17-0.25 cycles/°, 100% contrast (Fig 3C)) gain differences cannot be explained by differences in the oculomotor system. This result suggests that female mice have lower contrast sensitivity than males. The sex-related difference in CSF cannot be readily explained. It might be a particular trait of the C57BL/6J strain or it might occur for mice in general. One way to gain more insight in this sex-related difference is to test whether it occurs in other strains as well.

However, it strongly argues for a proper matching of animals on sex in any test involving vision, such as watermaze tests. Differences in contrast sensitivity are likely to have an impact of the outcome of these tests. If not controlled for differences in visual function, these outcomes can be misinterpreted as being related to, for instance, learning or motor processes.

Effect of age on contrast sensitivity

After the early years of life, vision deteriorates as man ages. Acuity decreases [27] as does contrast sensitivity [28,29]. Also, contrast sensitivity decreases with age even if all subjects have normal or corrected to normal acuity [30]. The visual acuity threshold of C57BL/6J mice also decreases as they age. In 6 months old C57BL/6J mice the acuity has been reported to be 0.48 cycles/° and to decrease to 0.38 cycles/° in 12 months old C57BL/6J mice [4].
The contrast sensitivity function is lower for nine months old C57BL/6J males than for four month old C57BL/6J males in most stimulus conditions while their maximum response is unaffected (Fig 4C). Even at a five months age difference, there are already large changes in the contrast sensitivity function. A decrease in visual threshold from 0.48 to 0.38 cycles/° was reported earlier for C57BL/6J mice of 6 and 12 months old [4]. Here we show that the effect of age on vision is not limited to a decrease in acuity and that contrast sensitivity decreases dramatically in five months time. Rod and cone numbers and densities do not decrease as mice age [31-33]. However,

maximal voltages (Vmax) of cone-based electroretinograms (ERG) show a substantial age-related decline. The ERG Vmax of 800 days old mice is about half of the ERG Vmax of 100 days old mice[31,33]. So, as mice age, the responsivity of their photoreceptors decreases. Both four and nine months old mice are considered to be adults; they aren't very young or old yet show very different contrast sensitivity. In behavioral tests that require vision, it is essential to use groups matched for age. Otherwise, differences in visual capabilities can influence the test and be misinterpreted as learning- or motor-problems.

Effect of miotic drugs on on contrast sensitivity

Pilocarpine, a receptor agonist in the parasympathetic nervous system, is is often used in mice video-oculography [21]. When it is applied to the eye it causes the iris sphicter muscle to contract and the pupil to constrict. Due to this, the contrast sensitivity function decreases slightly but not significantly (Fig 5). Both groups have gains close to 1 at 100% contrast and 0.17 cycles/° so pilocarpine application has no effect on motor performance. These results suggest that Pilocarpine can be used to reduce pupil size without having a significant impact on contrast sensitivity.

L7-PKCi mutants on contrast sensitivity

The contrast sensitivity function for L7-PKCi mutants is similar to their wildtype littermates. Mutants are reported to be slower than wildtypes in finding a hidden platform in the Morris watermaze task but not in the starmaze task [12]. Our data shows that both mutant and wildtype have identical contrast sensitivities (Fig 6). Differences in navigating the Morris watermaze therefore cannot be explained by differences in contrast sensitivity.

In summary, the methodology outlined in this paper is more sensitive than the methods currently available. Behavior in response to visual stimuli is no longer recorded as an all-or-nothing response but as a graded response. By quantifying eye movement behavior evoked by moving sine gratings information about response magnitudes can be obtained from optomotor

responses. A drawback of this method is that it is not suitable to use for very young (< 3 weeks) animals, or for valuable mutants. In those cases optomotor tests with freely moving animal are better suited. We show that in C57BL/6J mice these response magnitudes vary greatly between sexes and between mice that differ only a few months in age. Therefore, it is important to match groups according to age and sex in experiments that require unimpaired vision such as watermaze experiments and oculomotor studies. Otherwise, impaired vision can be misinterpreted as a learning- or motor-problem. Additionally, this new and sensitive method is useful in characterizing mouse models where vision is affected as a result of mutations, aging, retinal degeneration or neurological impairment of the visual system.

References:

1) Gianfranceschi L, Fiorentini A, Maffei L. Behavioural visual acuity of wild type and bcl2 transgenic mouse. *Vision Res.* 1999;39(3):569-74
2) Prusky, GT Douglas RM. Characterization of mouse cortical spatial vision. *Vision Res* 2004;44(28):3411–3418
3) Douglas RM, Alam, NM, Silver BD, McGill TJ, Tschetter, WW Prusky GT Independent visual threshold measurements in the two eyes of freely moving rats and mice using a virtual-reality optokinetic system. *Vis. Neurosci.* 2005;22(5):677-684
4) Wong, AA, Brown, RE Age-related changes in visual acuity, learning and memory in C57BL/6J and DBA/2J mice. *Neurobiol Aging* 2006;28(10):577-1593
5) Sinex DG, Burdette LJ, Pearlman AL.A psychophysical investigation of spatial vision in the normal and reeler mutant mouse. *Vision Res.* 1979;19(8):853-7
6) Prusky GT, Alam NM, Beckmanand S, Douglas RM. Rapid quantification of adult and developing mouse spatial vision using a virtual optomotor system. *Invest Ophthalmol Vis Sci* 2004;45(12):4611-4616
7) Jellali A, Meziane H, Ouagazzal AM., Rousseau S, Romand R, Auwerx J, Sahel J, Chambon P, Picaud S. The optomotor response: A robust first-line visual screening method for mice. *Vision Res* 2005;45(11):1439-1446.
8) Schmucker C, Seeliger M, Humphries P, Biel M, Schaeffel F. Grating acuity at different luminances in wild-type mice and in mice lacking rod or cone function. *Invest Ophthalmol Vis Sci* 2005;46(1):398-407
9) Umino Y, Solessio E, Barlow RB Speed, Spatial and temporal tuning of rod and cone vision in mouse. *J Neurosci* 2008;28(1):189-198
10) Stahl, JS, van Alphen AM, de Zeeuw CI. A comparison of video and magnetic search coil recordings of mouse eye movements. *J Neurosci Meth* 2000;99(1-2):101–110
11) de Zeeuw CI, Hansel C, Bian F, Koekkoek SKE, van Alphen AM, Linden DJ, Oberdick J. Expression of a protein kinase C inhibitor in Purkinje cells blocks cerebellar long term depression and adaptation of the vestibulo-ocular reflex. *Neuron* 1998;20(3):495-508

12) Burguiere E, Arleo A, Hojjati MR, Elgersma Y, De Zeeuw CI, Berthoz A, Rondi-Reig L. Spatial navigation impairment in mice lacking cerebellar LTD: a motor adaptation deficit? *Nat Neurosci* 2005;8(10):1292-1294
13) Oberdick J, Smeyne RJ, Mann JR, Zackson S, Morgan JI. A promotor that drives transgene expression in cerebellar Purkinje and retinal bipolar neurons. *Science* 1990; 248(4952):223-226
14) Collewijn H. An analog model of the rabbit's optokinetic system. *Brain Res* 1972 36(1):71-88
15) Collewijn H. Optokinetic eyemovements in the rabbit: input-output relations. *Vision Res* 1969;9(1):117-132
16) Nagao S. Effects of vestibulocerebellar lesions upon dynamic characteristics and adaptation of vestibulo-ocular and optokinetic responses in pigmented rabbits. *Exp Brain Res*. 1983;53(1):36-46
17) Katoh A, Kitazawa H, Itohara S, Nagao S. Dynamic characteristics and adaptability of mouse vestibulo-ocular and optokinetic response eye movements and the role of the flocculo-olivary system revealed by chemical lesions. *Proc. Natl. Acad. Sci. USA* 1998 95(13): 7705–7710
18) van Alphen AM, Stahl JS, De Zeeuw CI. The dynamic characteristics of the mouse horizontal vestibulo-ocular and optokinetic response. *Brain Res*. 2001;890(2):296-305.
19) Hess BJM, Savio T, Strata P Dynamic characteristics of optokinetically controlled eye movements following inferior olive lesions in the brown rat, *J Physiology* 1988;397:349–370
20) Rinner O, Rick JM, Neuhauss SC. Contrast sensitivity, spatial and temporal tuning of the larval zebrafish optokinetic response. *Invest Ophthalmol Vis Sci* 2005;46(1):137–142
21) Stahl JS. Using eye movements to assess brain function in mice. *Vision Res* 2004 44(28): 3401-3410
22) Prusky GT, West PW, Douglas RM. Behavioral assessment of visual acuity in mice and rats. *Vision Res.* 2000;40(16):2201-9
23) van Nes FL, Koenderink JJ, Nas H, Bouman MA. Spatiotemporal modulation transfer in the human eye. *J Opt Soc Am.* 1967; 57(9):1082-8
24) Campbell FW, Green DG. Optical and retinal factors affecting visual resolution. *J. Physiol*. 1965; 181(3):576-593

25) de la Cera EG, Rodríguez G, Llorente L, Schaeffel F, Marcos S. Optical aberrations in the mouse eye. *Vision Res*. 2006; 46(16):2546-53.
26) Artal P, de Tejada PH, Tedo CM. Retinal image quality in the rodent eye. *Vis. Neurosci.* 1998; 15 (4): 597-605
27) Salthouse TA, Hancock HE, Meinz EJ, Hambrick DZ. Interrelations of age, visual acuity, and cognitive functioning. *J Geront B-Psychol* 1996;51(6): 317-330
28) Mantyjarvi, M; Laitinen, T. Normal values for the Pelli-Robson contrast sensitivity test. *J Cataract Ref Surg* 2001;27(2):261-266
29) Hohberger B, Laemmer R, Adler W, Juenemann AGM, Horn FK Measuring contrast sensitivity in normal subjects with OPTEC (R) 6500: influence of age and glare *Graff Arch Clin Exp* 2007; 245(12):1805-1814
30) Nomura H, Ando F, Niino N, Shimokata H, Miyake Y. Age-related change in contrast sensitivity among Japanese adults. *Jpn J Opthalmol*: 2003;47(3):299-303
31) Li C, Cheng M, Yang H, Peachey NS, Naash MI. Age-related changes in the mouse outer retina. *Optom Vis Sci*. 2001 Jun;78(6):425-30
32) Trachimowicz RA, Fisher LJ, Hinds JW. Preservation of retinal structure in aged pigmented mice. *Neurobiol Aging*. 1981;2(2):133-41
33) Williams GA, Jacobs GH. Cone-based vision in the aging mouse. *Vision Res*. 2007 Jul;47(15):2037-46

Chapter 3

Optomotor impairments in Ercc d-mouse mutants

Bart van Alphen, Marcella Spoor, Maarten Frens

Introduction

DNA encodes the genetic information that is necessary for the development and functioning of all living organisms. It is constantly under attack from exogenous (UV, radiation, chemicals) and endogenous (reactive oxygen species, alkylation) agents that threaten to damage and distort genetic information. Even though evolution is driven by random changes occurring in the genome it is essential for organisms that their DNA is overall stable. Damage to the genome can interfere with vital cellular processes and can have severe consequences for the organism.

Defects in these repair mechanisms have severe consequences for the overall organismal survival. Both cancer (Hoeijmakers, 2001) and aging (Hasty et al, 2003; Mitchell and Hoeijmakers, 2003) are proposed consequences of unrepaired DNA damage. Likewise, defective DNA repair mechanisms in mature neural tissue have been linked to Parkinson's disease (Bender et al, 2006) and Alzheimer's disease (Nouspikel and Hanawalt, 2003).

To protect the integrity of the information stored in DNA molecules cells are equipped with a variety of mechanisms that recognize and repair lesions. Several repair pathways deal with damage to a single strand and use the other strand as template. These pathways are Nucleotide Excision Repair (NER), Base Excision Repair (BER) and Transcription-coupled repair (TCR). Other mechanisms deal with strand breaks (Homologous Recombination and Non-homologous End Joining (NHEJ). These mechanisms are well conserved in evolution and occur in all eukaryotes. Prokaryotes have similar mechanisms, which illustrates their importance.

Nucleotide Excision Repair (NER) deals with helix-distorting damage to a single strand caused by ultraviolet light or chemicals. NER is a multistep 'cut and paste' mechanism that involves a cascade of proteins that are involved in damage recognition, local helix opening, damage verification, dual incision and gap-filling of the damaged strand, using the undamaged strand as template for repairs (reviewed by Schumacher and Hoeijmakers, 2008). A major function of NER is to protect against carcinogenic effects of ultraviolet light. Inherited defects in NER have been associated with three human

syndromes: Xeroderma Pigmetosum (XP), Cockayne Syndrome (CS) and a photosensitive form of the brittle hair disorder Trichothiodystrophy (TTD) (Bootsma et al., 2001; Lehmann, 2003; Nance & Berry, 1992). The symptoms of these syndromes are often severe and range from severe developmental delay, increased cancer predisposition and progeriod symptoms like accelerated aging.

Vision is often impaired in most syndromes that are caused by dysfunctional or impaired DNA repair mechanisms (reviewed by Dollfus et al, 2003). Patients suffering from Xeroderma Pigmentosum, have been reported with visual impairment and photobia (Goyal et al, 1994, Kraemer, 1994). Cockayne syndrome is characterized by pigmentary degeneration of the retina in 60-100% of the cases (Traboulsi et al, 1992, Nance and Berry, 1992, Cockayne EA 1936). Visual acuity is often low, pupil dilation is poor and in 3 out of 8 cases spontaneous nystagmus occurs (Traboulsi et al, 1992). The main visual impairment in Trichothiodystrophy is cataract (Itin and Pittelkow, 1990).

To study the pathofysiology caused by unrepaired DNA damage, numerous mouse models were generated with deficiencies in NER (reviewed by Niedernhofer, 2008) by knocking out genes that are essential for one or more steps in the NER pathway, or by knocking in disease causing human mutations. One of these mutants is the Ercc1 -/- mutant. In this mutant the Ercc1-XPF nuclease is deleted, an essential component of the NER pathway and interstrand cross-link repair. This results in dramatically increased aging and other symptoms, including aging-like skin abnormalities, reduced growth, liver and kidney dysfunction, typically culminating in death by four weeks, (Niedernhofer et al, 2006) (compared to two to three years in normal mice that are kept in captivity). These extreme symptoms make the Ercc 1 knockout mutant a less than ideal candidate to study aging. The Ercc d/- mutant lacks Ercc 1 in one allele and has a truncated version in the other (Niedernhofer et al, 2004) has less severe symptoms. It still ages rapidly, and has a lifespan of 24-30 weeks.

In man, senescent changes in vision include declines in visual acuity and spatial contrast sensitivity (Spear, 1993). Studies on the effect of age on the spatial contrast sensitivity curve have shown a decrease in high frequency sensitivity in middle age (Derefeldt et al., 1979; Owsley et al., 1983; Arundale, 1878) leading to intermediate and high spatial frequency attenuation above 60 years of age (Derefeldt et al., 1979; Owsley et al., 1983). Shefrin et al., (1988) found age related decline in contrast sensitivity across all spatial frequencies under scotopic conditions. In adult C57Bl6 mice the contrast sensitivity function was conspicuously lower for 9-month-old than for 4-month-old mice (Chapter 2).

Aging impairs the central nervous system capability to process vestibular signals responsible for maintaining body balance, as well as for reducing the capacity of modifying vestibular guided adaptive reflexes (Baloh and Enrietto, 2001). In mice, a modest age-related decrease in vestibular guided eye movements was found already above 12 weeks of age (Shiga et al, 2005). It is likely that senescence of the vestibular pathways plays a role in age-related decline in balance. Senescent hair cell loss has been documented in the saccule, utricle, and cristae ampullares of the vestibular organ, as well as a neural loss of the primary afferent neurons, Scarpa's ganglia, and its afferent nerves (Ishiyama, 2009).

Gaze stabilization reflexes like the optokinetic reflex (OKR) and the vestibule ocular reflex (VOR) are known to decrease with age. OKR gains declines with age, at high frequencies as well as at high velocities (Leigh & Zee, 2006; Paige, 1994) due to an impaired sensori-motor system. The elderly show a decrease in VOR gain, predominantly at low frequencies of stimulation and high speeds of rotation. These findings are probably related to the senescence of the velocity storage mechanism and senescent loss of hair cell and neurons within the vestibular system (Leigh and Zee, 2006). Neuro-anatomical studies of the vestibular end-organs in older people have consistently shown attrition of neural and sensory cells as a function of age (Richter, 1980 and Rosenhall, 1973).

Furthermore, there is a decrease in the gain of visual enhanced vestibular responses at low frequencies of sinusoidal stimulation over time (Baloh,

Enrietto, Jacobsen and Lin, 2001). The Cervico-ocular Reflex seems to compensate this loss in humans, as its gain increases with age (Kelders et al, 2003). The deterioration in the visual modification of the VOR is most likely secondary to changes in the central visual motor pathways. Neuronal degeneration or loss of synaptic activity in any structure that make up these pathways could explain the deterioration of visual-vestibular responses with aging.

In order to gain more insight in the progressive nature of neurological deficiencies caused by impaired DNA mechanisms we studied how the visual and vestibular system are affected by accelerated aging. The visual system was studied by measuring the contrast sensitivity function in Ercc1 d/- mutants and their wild type littermates at three different ages: 6 weeks, 10 weeks and 14 weeks.

Sensory motor integration was studied by measuring two gaze stabilization reflexes: the optokinetic reflex (OKR) and the vestibulo-ocular reflex (VOR). Together, these two reflexes combine visual and vestibular information to minimize image slip over the retina, thus providing a moving organism with a stable image of the outside world. The combined effect of both reflexes is the visually enhanced vestibulo-ocular reflex (VVOR).

Materials and methods

Animals

Experiments were performed in accordance with the "Principles of laboratory animal care" (NIH publication no. 86-23) and the guidelines approved by the Erasmus University animal care committee and were in accordance with the European Communities Council Directive (86/609/EEC). The generation of ERCC1- and ERCC1d alleles has been previously described (Weeda et al, 1997). ERCC1d/- mice were obtained by crossing ERCC1- with ERCC1d/+ mice of C57Bl6J and FVB backgrounds to yield ERCC1d/- with C57Bl6J/FVB hybrid background. Wild-type littermates were used as controls. In this study 14 Ercc1 d/- mutants were used as well as 14 wild type littermates. All mice were housed on a 12 h light / 12 h dark cycle

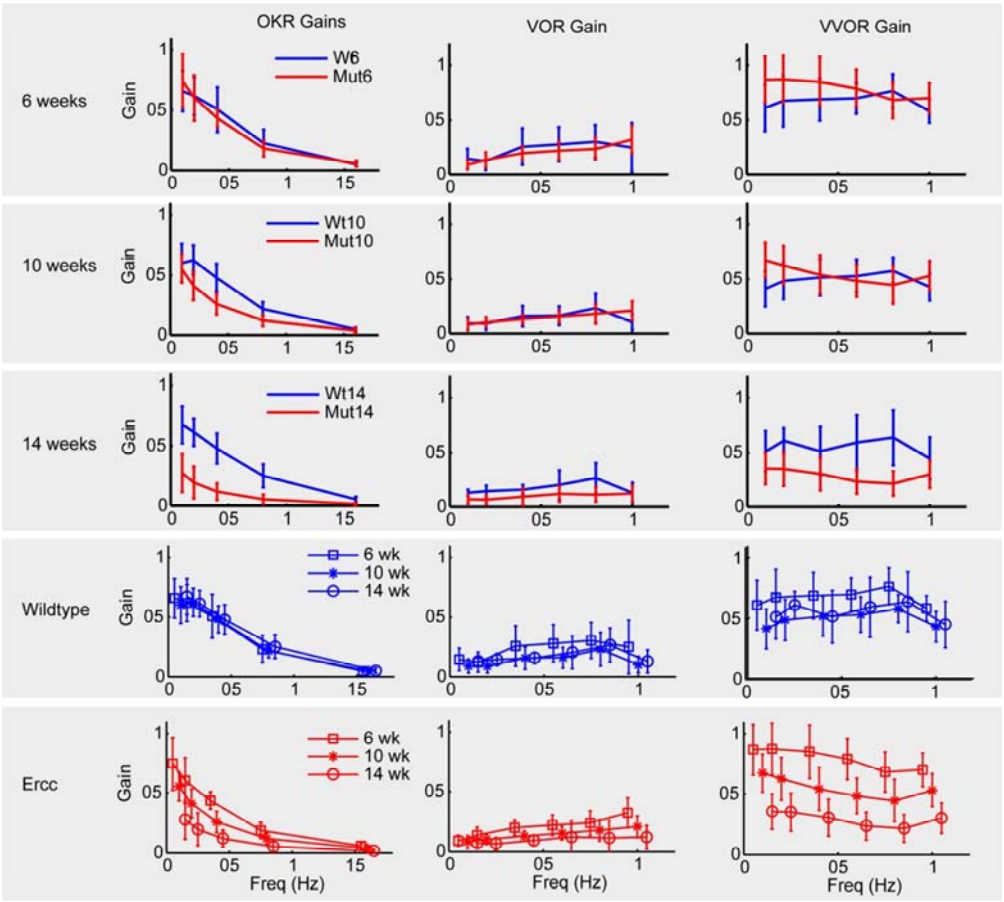

***Figure 1**: Gaze stabilization reflexes for Ercc d/- mutants and their wildtype littermates. In Ercc d/- mutants the OKR, VOR and VVOR gains strongly decrease in eight weeks. Error bars show STD. **A)** At 6 weeks of age, there is no significant difference in OKR, VOR and VVOR gains. **B)** At 10 weeks, there is a significant decrease in OKR in the mutant, but not in the VOR and VVOR. **C)** At 14 weeks, OKR, VOR and VVOR deteriorated strongly in the Ercc d/- mutant. **D)** OKR, VOR and VVOR do not change in wild type mice during the experiment. **E)** As Ercc d/- mice age, the gains of all gaze stabilization reflexes decreases.*

with unrestricted access to food and water. Experiments were done during their light phase.

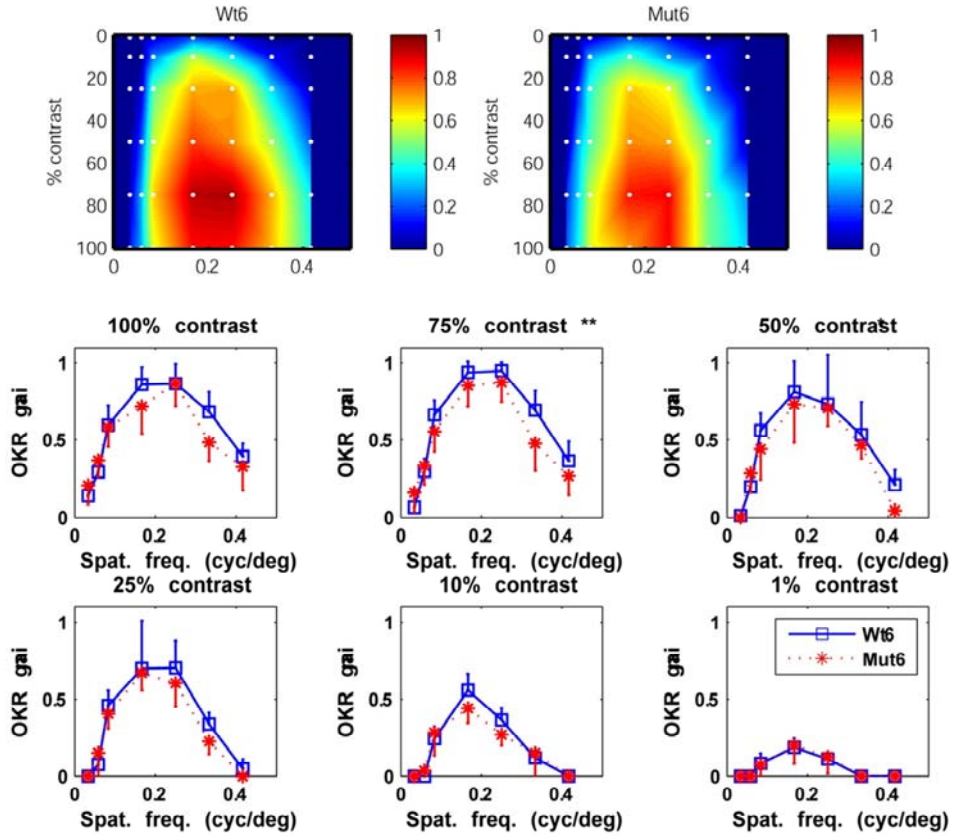

Figure 2: *Contrast sensitivity at 6 weeks of age for wild type and Ercc d/- mutants.* ***A, B)*** *The color reflects the OKR gains at 42 different combinations of spatial frequency and contrast. Spaces between measured points are filled with linear interpolation.* ***C-H)*** *Six cross sections of A and B are plotted, one for each contrast. Error bars indicate standard deviation, stars indicate significance (** = p < 0.01).*

Surgery

Animals were prepared for fixation by head restraint by attaching two metal nuts to the skull using a construct made of a micro-glass composite. The full procedure is described in van Alphen et al, 2009.

Stimulus setup

Optokinetic stimuli were created using a modified Electrohome Marquee 9000 CRT projector (Christie Digital Systems, Cypress CA, USA) that projected stimuli via mirrors onto three transparent anthracite screens (156*125 cm) which were placed in a triangular formation around the recording setup (Fig 1A). This created a monochrome panoramic stimulus fully surrounding the animal. The stimuli were programmed in C++ and rendered in openGL and consisted of a virtual vertically oriented cylinder with a vertically oriented sine grating on its wall. A pixel subtended 4.5 arcminutes. Contrasts (C) were calculated using the Michelson formula:

$$C = \frac{I_{\max} - I_{\min}}{I_{\max} + I_{\min}}$$

Where I_{max} and I_{min} are the maximum and minimum luminance of the stimulus, respectively. Average luminance was 17.5 cd/m^2 in all stimulus conditions. The minimal luminance of the stimulus at 100% contrast was 0.05 cd/m^2, the maximum luminance was 35 cd/m^2).

Eye movement recordings

The animal was placed in a plastic tube which was attached to a set of linear stages that allowed translations in three dimensions such that the mouse eye was placed in the centre of the visual stimulus, in front of the eye position recording apparatus.

Eye movements were recorded with an infrared video system (Iscan ETL-200). Images of the eye were captured at 120 Hz with an infrared sensitive CCD camera (see Chapter 2 for more details). The camera, mirror and LEDs were all mounted on an arm that could rotate about the vertical axis over a range of 26.12º (peak to peak). Eye movement recordings and calibration procedures were similar to those described by Stahl and van Alphen (2000), yielding eye position in degrees of visual angle.

Experiments

Contrast sensitivity function

Contrast sensitivity was determined by presenting moving visual stimuli to the mice and recording optokinetic eye movements evoked by those stimuli (Chapter 2). Each stimulus showed a sine grating made up of a combination of one of seven spatial frequencies (0.03, 0.05, 0.08, 0.17, 0.25, 0.33, or 0.42 cycles per degree) and one of six contrast values (100%, 75%, 50%, 25%, 10%, 1%). The stimulus evokes a compensatory eye movement when a mouse can distinguish it from a homogenous background. The 42 stimulus combinations were presented in random order.
A stimulus was first projected and was kept stationary for one minute, allowing the eye to adjust to changes in stimulus brightness. Then the stimulus started to move with a constant velocity of 6 º/s. It moved to one direction for two seconds, than it changed direction and moved in the opposite direction for two seconds. This was repeated five times, yielding 10 changes in direction. As the stimulus moved, the position of the left eye was recorded.

Recorded eye positions were transformed offline into a velocity signal. Fast phases were removed using a velocity threshold of twice the stimulus velocity (i.e.,12 º/s). The first 200 ms after stimulus onset and before and after each change in direction were removed as well. Because the stimulus velocity was constant and eye data in the first 200 ms after the stimulus direction changes were ignored, average absolute eye velocity could be divided directly by the stimulus velocity to calculate a gain value for each combination of spatial frequency and contrast. The gain is the ratio between average eye velocity and stimulus velocity, and a gain of 1 means that the eye has the same velocity as the stimulus (Collewijn, 1969).
Experimenters were masked to the experimental conditions. Trials were randomized, mice were assigned a number and the data analysis scripts were automated. All data was analysed after the experiment.

The effect of the Ercc d/- mutation was analyzed using a repeated measures ANOVA with three factors: one between subjects factor with two levels

('Mutation' with 2 levels: wild type and Ercc d/-) and two within subject factors: 'Contrast' with 6 levels and 'Spatial Frequency' with 7 levels). Post hoc, groups were compared at each contrast by averaging OKR gains over spatial frequencies. Differences between groups were analysed for significance with a student's t-test.

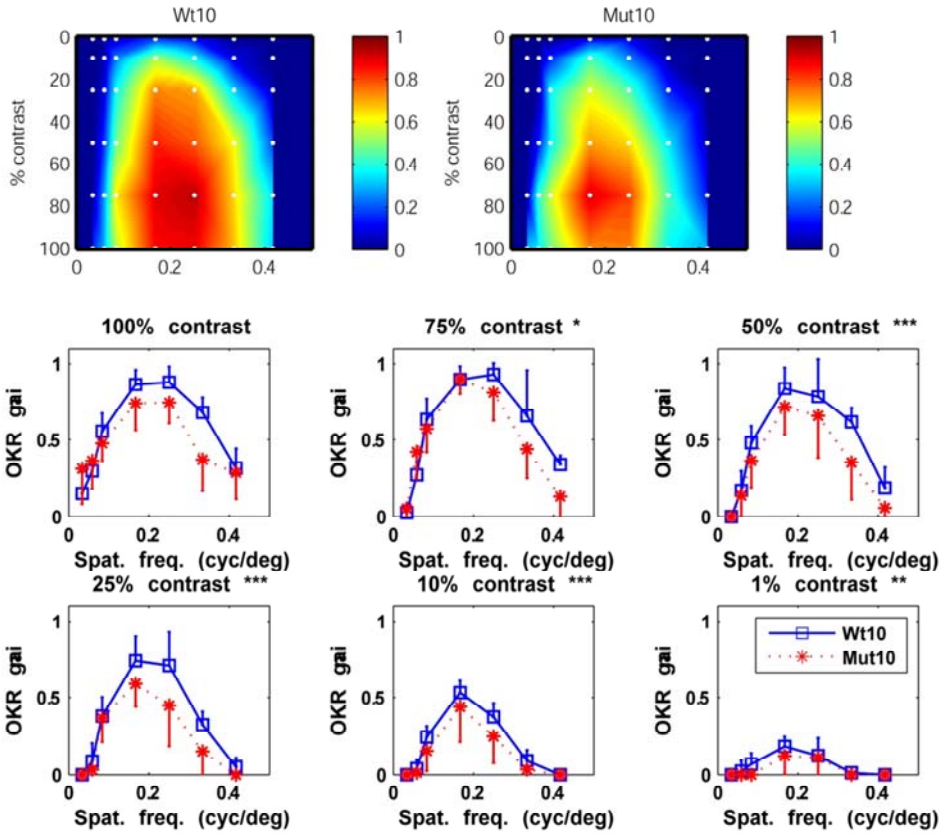

Figure 3: *Contrast sensitivity at 10 weeks of age for wild type and Ercc d/- mutants.* ***A, B)*** *The color reflects the OKR gains at 42 different combinations of spatial frequency and contrast. Spaces between measured points are filled with linear interpolation.* ***C-H)*** *Six cross sections of A and B are plotted, one for each contrast. Error bars indicate standard deviation, stars indicate significance (* = $p < 0.05$, ** = $p < 0.01$, ** = $p < 0.001$).*

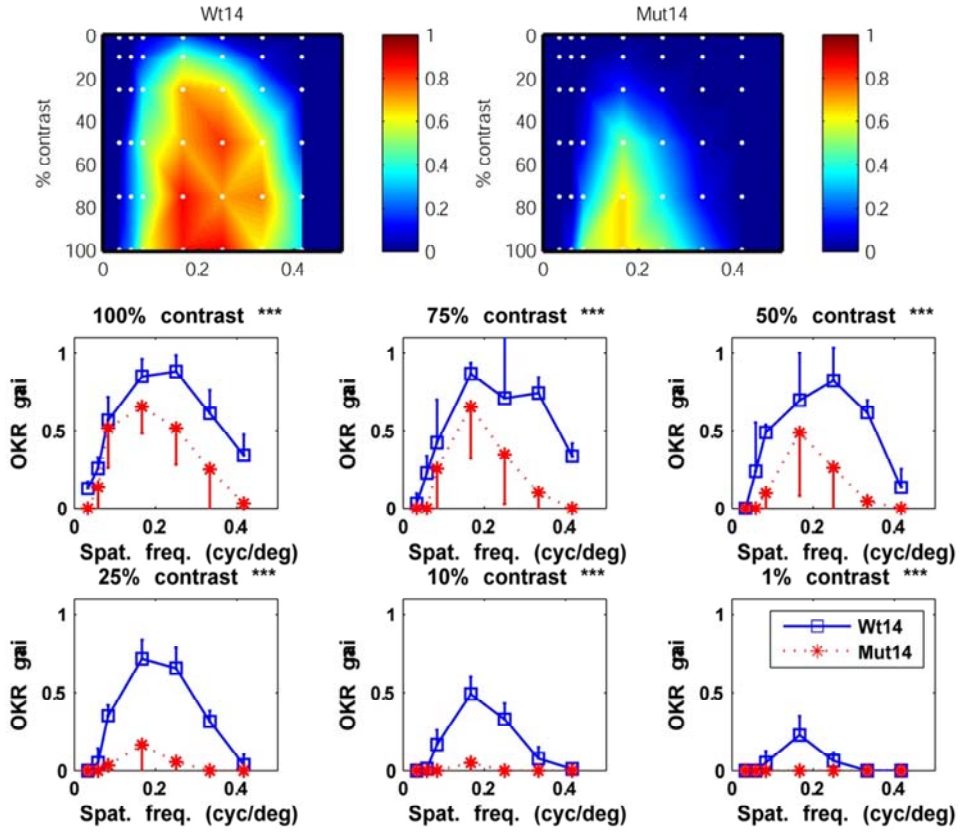

Figure 4: *Contrast sensitivity at 14 weeks of age for wild type and Ercc d/- mutants.* ***A, B)*** *The color reflects the OKR gains at 42 different combinations of spatial frequency and contrast. Spaces between measured points are filled with linear interpolation.* ***C-H)*** *Six cross sections of A and B are plotted, one for each contrast. Error bars indicate standard deviation, stars indicate significance (* = $p < 0.05$, ** = $p < 0.01$, ** = $p < 0.001$).*

Sensorimotor integration

OKR gains are used as a probe to measure contrast sensitivity. To determine whether the neuronal circuitry driving gaze stabilization reflexes (like the OKR) are affected, either by the mutation itself or by accumulated, unrepaired DNA damage, we recorded a baseline OKR curve for both the mutants and their wild type.

The stimulus consisted of 1592 green dots that were equally spaced on a virtual sphere that has its center at eye height above the center of the table. This is a very powerful stimulus for evoking compensatory eye movements.

The stimulus oscillated sinusoidally about the earth vertical axis at a constant amplitude of 5º and 100% contrast. By using different oscillation frequencies (0.1, 02, 0.4, 0.8, 1.6 Hz) the peak velocity of the stimulus was varied. The OKR is a velocity dependent reflex (Collewijn, 1969). During the optokinetic stimulation the eye position was recorded and stored to be analysed offline.

Additionally, we determined if vestibular driven gaze stabilization reflexes were altered. In order to record the VOR and VVOR, mice were rotated on a turntable, either in the dark to measure the VOR or in the light to measure the VVOR. Vestibular stimuli were created by oscillating the mouse about the earth vertical axis at six different frequencies (0.1, 0.2, 0.4, 0.6, 0.8 and 1 Hz) with constant amplitude of 5 º.

In the OKR, VOR and VVOR data the fast phases and blinks were removed and the signal was differentiated to get eye velocity. A sine wave was fitted through the velocity trace. OKR gain was calculated by dividing the peak velocity of the fitted eye velocity by the peak velocity of the stimulus (Stahl and van Alphen, 2000)

Pupil dilation

Photobia and poor pupil dilation are symptoms of Cockayne syndrome (Traboulsi et al, 1992) and Xeroderma Pigmentosa (Goyal et al, 1994). To test whether mouse mutants with a NER deficiency also have these symptoms we measured pupil diameter changes at transitions from light to dark. The full field visual stimulus alternated from bright to dark every 20 seconds. Ten light-dark cycles were shown.

Results

Compensatory eye movements were evoked, either by rotating a visual stimulus about the animal to measure OKR or by rotating the animal itself to measure (V)VOR. These results are shown in Figure 1. Gains were recorded in Ercc d/- mutants and their wild type littermates at three different ages; at 6, 10 and 14 weeks. As the mice age OKR, VOR and VVOR decrease in the Ercc d/- mutant but not in their wild type littermates.

At 6 weeks of age, there are no significant differences between wild type and mutants for the OKR (repeated measures ANOVA, $p = 0.8418$), VOR (repeated measures ANOVA, $p = 0.5514$), and VVOR (repeated measures ANOVA, $p = 0.072$). At 10 weeks, OKR is significantly different (repeated measures ANOVA, $p < 0.001$) but VOR and VVOR are not (VOR: repeated measures ANOVA, $p = 0.9163$; VVOR: repeated measures ANOVA, $p = 0.2788$). However, at low stimulus velocity (3 º/s) there is no significant difference between both groups (t-test, $p < 0.01$), which means that the OKR can be used to estimate contrast sensitivity. At 14 weeks of age, there are large differences between wild type and mutant for all three reflexes (repeated measures ANOVA, $p < 0.001$).

Since the OKR for low stimulus velocities was unaffected in 6 and 10 weeks old Ercc mutants, OKR gain changes were used to infer contrast sensitivity (cf van Alphen et al, 2009). Results are shown in Figures 2 (6 weeks old), 3 (10 weeks old) and 4 (14 weeks old).

At six weeks of age, overall contrast sensitivity is similar for both groups (Figure 2). The only exception is at 75% contrast, where contrast sensitivity is slightly lower in Ercc d/- mutants. Both groups show a similar optimum for all contrasts, at 0.17-0.25 cycles per degree. There were no differences in contrast sensitivity between male and female mice.

At ten weeks of age, contrast sensitivity deteriorates in Ercc d/- mutants (Figure 3). At 100% contrast, there is no difference between both groups, but at lower contrasts, Ercc d/- mice perform worse than their wild type littermates. Gains are lower and the window in which responses occur

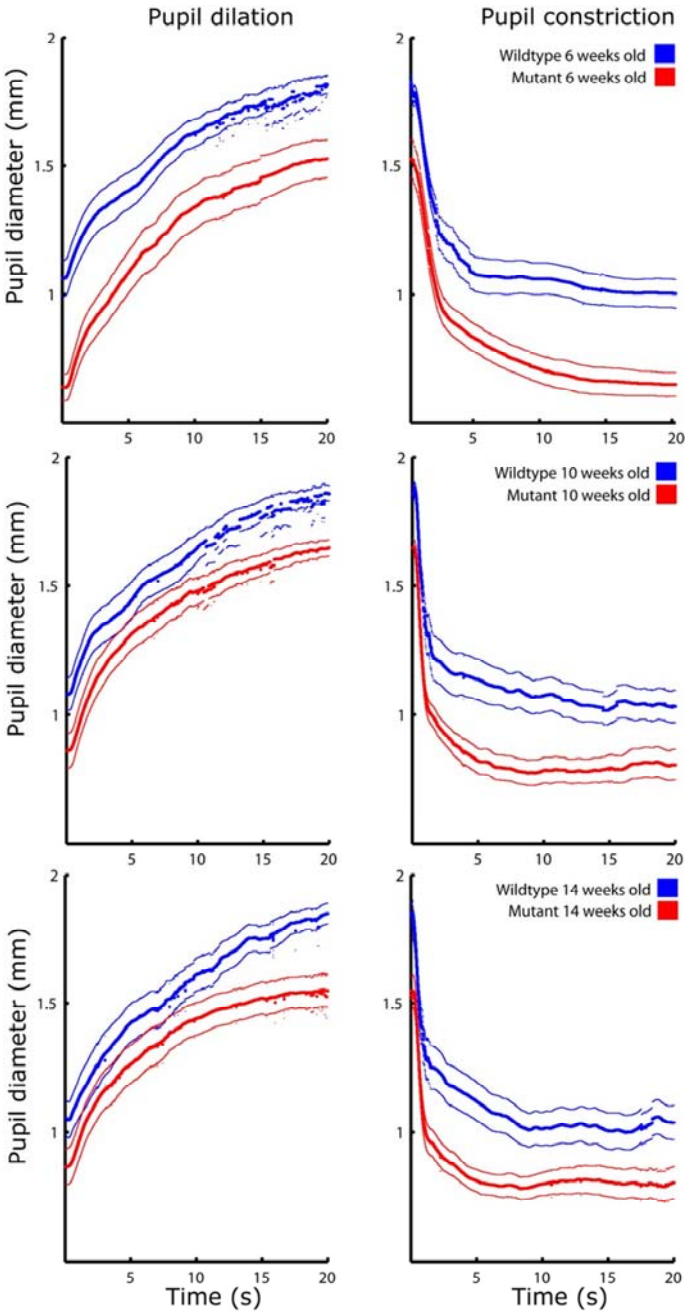

Figure 5: *Pupil dilation and contraction at three different ages.* ***A)*** *6 weeks,* ***B)*** *10 weeks,* ***C)*** *14 weeks. Thick lines show the mean pupil diameter, thin lines show standard error.*

narrows, i.e. the highest (0.42 cpd) and lowest (0.03 cpd) spatial frequencies do not elicit a response in mutant mice. Because the OKR gains are similar at the stimulus velocity used in this experiment (3 º/s, see Figure 1 B, left panel) these differences cannot be explained by changes in the oculomotor circuitry.

Four weeks later, at 14 weeks of age, contrast sensitivity is strongly reduced in Ercc d/- mutants. The response window narrows further, i.e. no responses occur below 0.08 cycles per degree or over 0.25 cycles per degree. Below 50% contrast, hardly any response is observed. Even though OKR gains are also reduced in Ercc d/- mutants (see Figure 1 C, left panel), the reduction in contrast sensitivity cannot be fully explained by deterioration of the oculomotor system of Ercc d/- mice, as they are still able to reach gains up to 0.65 (Figure 4 C and D), provided contrast is high enough.

Pupil dilation and constriction was measured by exposing mice of both groups to stimuli alternating between dark and bright every 20 seconds (Figure 5). Pupil diameters are approximately 40% smaller in Ercc d/- mice., which is similar to the weight rations between six week old wildtypes and Ercc1 d/- mutants (de Waard et al, 2010). Despite the size difference, both pupil dilation and constriction followed a similar pattern. At the transition from dark to light, pupil dilation starts after a 300 ms delay after which pupil size increases with 80% in wildtype and 100% in Ercc. Half of the diameter increase occurs during the first five seconds. Pupil constriction occurs faster, with a delay of approximately 100 ms in both groups after which pupil diameter drops sharply during the first second and levels off during the next five seconds. In wildtype mice, minimal and maximal pupil sizes do not change with age, even though average bodyweight increases with 15% from 6-14 weeks. In Ercc mice, minimum pupil diameter increases from 0.64 ± 0.05 to 0.86 ± 0.07 mm between weeks 6 and 10, after which it stays at that diameter. Weights did not increase during this time. There are no other significant changes with age in both groups.

Discussion

As Ercc d/- mice age, their visual function and gaze stabilization reflexes deteriorate in a matter of weeks. In man VVOR and OKR gains are known to decrease slightly with age (Paige 1994) but the OKR in mice does not change as they age from 4 to 24 months (Stahl 2006). This decrease is marginal when compared to Ercc mice, where all gaze stabilization reflexes fail to adequately compensate for either visually or vestibularly induced image motion. The findings in this paper are consistent with earlier work that shows age dependent motor neuron degeneration and progressive loss of neuromuscular connectivity in Ercc1 d/- mice (de Waard et al, 2010).

After the first six weeks of life, there are no neurological differences between wild type and Ercc mutants, even though they differ in size. Both male and female Ercc1 d/- mice weigh 12-15 g, while wild type females weigh ~18 g and wild type males weight ~28 g (de Waard et al, 2010). Gaze stabilization reflexes in both mutants are similar. In both groups, OKR gains show similar low pass filter characteristics, with high gains at low stimulus frequencies and low gains at high stimulus frequencies. Likewise, the VOR shows similar high pass filter characteristics, even though gains are low in the measured frequency range when compared to C57Bl6. This might be a trait of the background strain. The synergetic effect of both reflexes is shown in the VVOR, which is constant over the whole measures frequency range.

Gains measured during contrast sensitivity experiments are generally higher than those measured during OKR and VOR recordings. This is probably caused by different stimulus paradigms. VOR and OKR were recorded using sinusoidal stimuli and gains were calculated by dividing peak eye velocity by peak stimulus velocity. Due to the sinusoidal character of the stimulus, the eye has only a moment to reach a similar velocity. Contrast sensitivity measurements used constant velocity stimuli, which allowed the eye more time to reach stimulus velocity.

In six weeks old mice, there are no differences in contrast sensitivity between wild type and mutant. The contrast sensitivity function shows a profile that is very similar to that of the C57Bl6 mice (van Alphen et al, 2009).

Gains are highest at 75-100% contrast and a spatial frequency of 0.17–0.25 cycles per degree and decrease as contrast decreases or the spatial frequency falls outside this optimal window. Unlike C57Bl6 mice, there are no differences in contrast sensitivity between male and female mice.

During the next four weeks, the first signs of oculomotor deterioration are observed, as gains of the optokinetic reflex decrease at higher stimulus frequencies. VOR and VVOR are not significantly lower. Because OKR gains are not significantly different at the stimulus velocity used to measure contrast sensitivity, OKR gains can be used reliably to infer contrast sensitivity. Contrast sensitivity begins to decrease at contrasts below 100%. Also, sensitivity to the highest and lowest spatial frequencies disappears as responses to those stimuli decrease to 0 for contrasts below 50%. This decrease in contrast sensitivity follows a similar pattern as was reported for C57Bl6 mice (van Alphen 2009), where the ability to perceive low contrasts and very high or low spatial frequencies disappears first.

At 14 weeks of age, the oculomotor circuits are affected by accumulated DNA damage and both OKR and VOR gains are approximately halved. Thus OKR gains are no longer a reliable measure of contrast sensitivity. However, the reduction in contrast sensitivity cannot be fully explained by deterioration of the oculomotor system of Ercc d/- mice, as they are still able to reach gains up to 0.65 (Figure YY3 C and D), provided contrast is high enough. Contrast sensitivity has decreased to the point where the mouse is only able to observe a small set of contrast-spatial frequency combinations, in the same window that was optimal for 6 weeks old mice (0.17-0.25 cpd, 74-100% contrast).

Photobia and poor pupil dilation are symptoms of Cockayne syndrome (Traboulsi et al 1992) and Xeroderma Pigmentosa (Goyal et al 1994). To test whether mouse mutants with a NER deficiency also have these symptoms we measured pupil diameter changes at transitions from light to dark and from dark to light.In Ercc d/- mice, the minimum pupil diameter increases from 0.64 ± 0.05 to 0.86 ± 0.07 mm between weeks 6 and 10, after which it stays constant. Because body weight does not change , this diameter increase might be a compensation for photorecpetor loss that occurs as Ercc mutants

age. Pupil constriction and dilation are not affected in Ercc d/- mice and occur at the same rate as in wildtype mice. Both the increased pupil diameter and the unaffected pupil dilation and constriction rates suggest that Ercc mice are not photobic.

Previous studies in human on the effect of age on the spatial contrast sensitivity function (CSF) curve have shown a decline in high frequency sensitivity in middle age (Derefeldt et al., 1979; Owsley et al., 1983; Arundale, 1978), leading to intermediate and high spatial frequency attenuation with increasing age (Derefeldt et al., 1979; Owsley et al., 1983) due to optical and neural degeneration. Also in mice, the contrast sensitivity function is known to decrease as function of age (Chapter 2).

Ercc1 d/- mice age rapidly and develop severe neurological impairments in a matter of weeks. During the first six weeks of their life, their sensory and motor systems function as well as those of their litter mates. At ten weeks, vision starts to deteriorate and the gain of the optokinetic reflex is decreased for all but the slowest visual stimuli. Another four weeks later, Ercc mice are almost blind and their gaze stabilization reflexes are strongly impaired. This is not merely a result of reduced visual input, as the VOR (which is measured in the dark) is affected as well. Both the decline in contrast sensitivity and the reduced VOR and OKR (and thus VVOR) are symptoms of aging, and the Ercc mice displays severe aging effects only 14 weeks after birth. The Ercc d/- mutants' gradual development of neurological impairments described in this paper make it an ideal candidate to study aging and possible strategies to reduce accumulation of DNA damage.

References

Arundale, K. (1978). "An investigation into the variation of human contrast sensitivity with age and ocular pathology." Br J Ophthalmol 62(4): 213-215.
Baloh, R. W., J. Enrietto, et al. (2001). "Age-related changes in vestibular function: a longitudinal study." Ann N Y Acad Sci 942: 210-219.
Bender, A., K. J. Krishnan, et al. (2006). "High levels of mitochondrial DNA deletions in substantia nigra neurons in aging and Parkinson disease." Nat Genet 38(5): 515-517.
Bootsma, D. (2001). "The "Dutch DNA Repair Group", in retrospect." Mutat Res 485(1): 37-41.
Cockayne, E. (1936). "Dwarfism with retinal atrophy and deafness." Archives of Disease in Childhood 11.
Collewijn, H. (1969). "Optokinetic eye movements in the rabbit: input-output relations." Vision Res 9(1): 117-132.
de Waard, M. C., I. van der Pluijm, et al. (2010). "Age-related motor neuron degeneration in DNA repair-deficient Ercc1 mice." Acta Neuropathol.
Derefeldt, G., G. Lennerstrand, et al. (1979). "Age variations in normal human contrast sensitivity." Acta Ophthalmol (Copenh) 57(4): 679-690.
Dollfus, H., F. Porto, et al. (2003). "Ocular manifestations in the inherited DNA repair disorders." Surv Ophthalmol 48(1): 107-122.
Goyal, J. L., V. A. Rao, et al. (1994). "Oculocutaneous manifestations in xeroderma pigmentosa." Br J Ophthalmol 78(4): 295-297.
Guarente, L. and C. Kenyon (2000). "Genetic pathways that regulate ageing in model organisms." Nature 408(6809): 255-262.
Hasty, P., J. Campisi, et al. (2003). "Aging and genome maintenance: lessons from the mouse?" Science 299(5611): 1355-1359.
Hoeijmakers, J. H. (2001). "DNA repair mechanisms." Maturitas 38(1): 17-22; discussion 22-13.
Ishiyama, G. (2009). "Imbalance and vertigo: the aging human vestibular periphery." Semin Neurol 29(5): 491-499.
Itin, P. H. and M. R. Pittelkow (1990). "Trichothiodystrophy: review of sulfur-deficient brittle hair syndromes and association with the ectodermal dysplasias." J Am Acad Dermatol 22(5 Pt 1): 705-717.
Jaspers, N. G., A. Raams, et al. (2007). "First reported patient with human ERCC1 deficiency has cerebro-oculo-facio-skeletal syndrome with a mild

defect in nucleotide excision repair and severe developmental failure." Am J Hum Genet 80(3): 457-466.
Johnson, T. E. (1990). "Increased life-span of age-1 mutants in Caenorhabditis elegans and lower Gompertz rate of aging." Science 249(4971): 908-912.
Kelders, W. P., G. J. Kleinrensink, et al. (2003). "Compensatory increase of the cervico-ocular reflex with age in healthy humans." J Physiol 553(Pt 1): 311-317.
Kraemer, K. H. (1994). "Nucleotide excision repair genes involved in xeroderma pigmentosum." Jpn J Cancer Res 85(2): inside front cover.
Lehmann, A. R. (2003). "DNA repair-deficient diseases, xeroderma pigmentosum, Cockayne syndrome and trichothiodystrophy." Biochimie 85(11): 1101-1111.
Leigh, R. J., Zee, D. S. (2006). The Neurology of Eye Movements, Oxford University Press.
Mitchell, J. R., J. H. Hoeijmakers, et al. (2003). "Divide and conquer: nucleotide excision repair battles cancer and ageing." Curr Opin Cell Biol 15(2): 232-240.
Nance, M. A. and S. A. Berry (1992). "Cockayne syndrome: review of 140 cases." Am J Med Genet 42(1): 68-84.
Nance, M. A. and S. A. Berry (1992). "Cockayne syndrome: review of 140 cases." Am J Med Genet 42(1): 68-84.
Niedernhofer, L. J. (2008). "Nucleotide excision repair deficient mouse models and neurological disease." DNA Repair (Amst) 7(7): 1180-1189.
Niedernhofer, L. J., G. A. Garinis, et al. (2006). "A new progeroid syndrome reveals that genotoxic stress suppresses the somatotroph axis." Nature 444(7122): 1038-1043.
Niedernhofer, L. J., H. Odijk, et al. (2004). "The structure-specific endonuclease Ercc1-Xpf is required to resolve DNA interstrand cross-link-induced double-strand breaks." Mol Cell Biol 24(13): 5776-5787.
Nouspikel, T. and P. C. Hanawalt (2003). "When parsimony backfires: neglecting DNA repair may doom neurons in Alzheimer's disease." Bioessays 25(2): 168-173.
Owsley, C., R. Sekuler, et al. (1983). "Contrast sensitivity throughout adulthood." Vision Res 23(7): 689-699.

Paige, G. D. (1994). "Senescence of human visual-vestibular interactions: smooth pursuit, optokinetic, and vestibular control of eye movements with aging." Exp Brain Res 98(2): 355-372.
Partridge, L., M. D. Piper, et al. (2005). "Dietary restriction in Drosophila." Mech Ageing Dev 126(9): 938-950.
Richter, E. (1980). "Quantitative study of human Scarpa's ganglion and vestibular sensory epithelia." Acta Otolaryngol 90(3-4): 199-208.
Rosenhall, U. (1973). "Degenerative patterns in the aging human vestibular neuro-epithelia." Acta Otolaryngol 76(2): 208-220.
Schumacher, B., G. A. Garinis, et al. (2008). "Age to survive: DNA damage and aging." Trends Genet 24(2): 77-85.
Shefrin, S. L., D. S. Goodin, et al. (1988). "Visual evoked potentials in the investigation of "blindsight"." Neurology 38(1): 104-109.
Shiga, A., T. Nakagawa, et al. (2005). "Aging effects on vestibulo-ocular responses in C57BL/6 mice: comparison with alteration in auditory function." Audiol Neurootol 10(2): 97-104.
Spear, P. D. (1993). "Neural bases of visual deficits during aging." Vision Res 33(18): 2589-2609.
Stahl, J. S., R. A. James, et al. (2006). "Eye movements of the murine P/Q calcium channel mutant tottering, and the impact of aging." J Neurophysiol 95(3): 1588-1607.
Stahl, J. S., A. M. van Alphen, et al. (2000). "A comparison of video and magnetic search coil recordings of mouse eye movements." J Neurosci Methods 99(1-2): 101-110.
Traboulsi, E. I., I. De Becker, et al. (1992). "Ocular findings in Cockayne syndrome." Am J Ophthalmol 114(5): 579-583.
van Alphen, B., B. H. Winkelman, et al. (2009). "Age- and sex-related differences in contrast sensitivity in C57BL/6 mice." Invest Ophthalmol Vis Sci 50(5): 2451-2458.
Weeda, G., I. Donker, et al. (1997). "Disruption of mouse ERCC1 results in a novel repair syndrome with growth failure, nuclear abnormalities and senescence." Curr Biol 7(6): 427-439.

Chapter 4

Measuring contrast sensitivity in man using the ocular following response

Behdokht Hosseini, Bart van Alphen, Marcella Spoor, Jos van der Geest, Maarten Frens

Introduction

Vision is the ability to observe the world by interpreting visual light that is reflected on the surroundings and reaches the retina. The visual system is the best developed sensory system in man and functional vision is important for many parts of life. Fear of the dark (nyctophobia) is prevalent in young children. Loss of visual function affects a person's ability to eat, dress, read, write and travel, which can result in a decrease of the quality of life for many visually impaired persons (Armbrecht et al, 2004, Warrian et al 2010). Loss of vision can be caused by ocular diseases, such as retinitis pigmentosa, a disorder where the rod cells in the retina lose their ability to respond to light, macular degeneration which is a major cause of visual impairment in older adults above 50 (de Jong 2006), or glaucoma, a disease where the optic nerve is damaged. Loss of vision can also occur as a symptom of other diseases like Multiple Sclerosis (Compston and Coles, 2008) or diabetic retinopathy.

Currently, visual function is mainly assessed by measuring central visual acuity which yields highly variable results (Gibson and Sanderson, 1980, Pandit 1994). Snellen acuity, named after the Dutch ophthalmologist who developed the test in 1862, is the standard measure of vision. In this test, a subject has to read increasingly smaller letters on a chart. A person with normal acuity (20/20 vision) can see standardized symbols on the chart at a distance of 20 feet (~6m). A person with 20/30 vision can see symbols on the chart from 20 feet that a person with normal vision could see from 30 feet. Other similar tests use the E-Chart or the Landolt C test; subjects are asked to report the orientation of a capital E or C. Thus, Snellen acuity measures the highest resolution that that the visual system can perceive and is useful to determine refractive errors of the eye. However, Snellen acuity does not provide an accurate measure of the quality of visual function because it only measures a small subset of what the visual system can perceive (see Figure 1): objects with high spatial frequencies at very high contrast (Ginsburg, 2003). The last point on the main curve in Figure 1 is a measure of Snellen acuity. It represents the smallest resolvable image at 100% contrast.

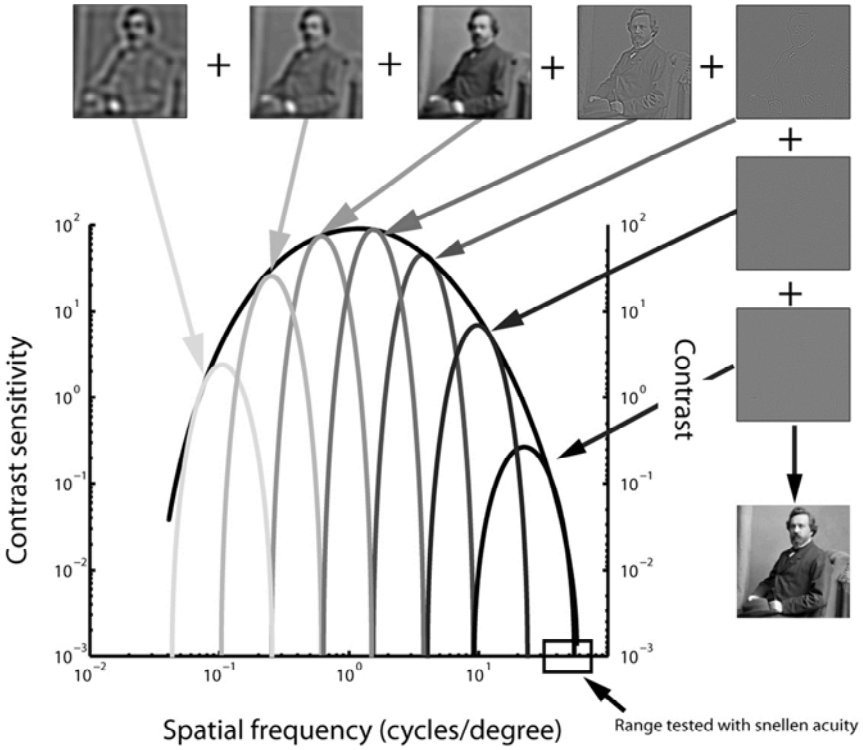

Figure 1. *Visual information is processed by different channels that are sensitive to a particular range of spatial frequencies. Full contrast sensitivity is depicted by the black curve spanning the figure. Underneath this curve, the different channels are depicted in shades of grey. Superimposition of those channels provides a detailed picture, in this case of F.C. Donders. Snellen acuity only measures a small subset of the full range of human vision, consisting of high spatial frequencies measured at high contrast, as is shown by the black box in the lower right of the graph.*

A more thorough way to look at vision is to measure contrast sensitivity, the ability to detect small increments in shades of gray on a uniform background. This function measures the least amount of contrast needed to detect a visual stimulus and provides a more complete quantification of a person's visual capabilities. A contrast sensitivity test measures two variables, size and contrast. Contrast sensitivity is measured by presenting an observer with sine-wave gratings as targets instead of the letters or

symbols. Sine-wave gratings possess useful mathematical properties and early stages of visual processing are optimally "tuned" to such targets (Maffei, 1973; Watson, et al., 1983). Each sine-wave grating consists of a given spatial frequency (i.e., the number of sinusoidal luminance cycles per degree of visual angle). The contrast of the target grating is then varied while the observer's contrast detection threshold is determined (see figure 1). Thus, a 20/20 result in visual acuity will not always uncover a possible hidden loss in contrast sensitivity.

During the last decade, attempts were made to develop treatments that restore vision for visually impaired patients, such as retinal prosthetics (Loewenstein et al, 2004), transplants of retinal epithelium (Aramant and Seiler, 2004; Thomas et al, 2006), stem cells (Young 2005), or neuroblast progentitor cells (Seiler and Aramant, 2005). Visual function tests in low vision patients (patients with impaired eye sight that cannot be corrected by conventional means) often depend on self-reported changes in visual function and acuity, which can be highly inaccurate (Skeel et al, 2003, Warrian et al 2010). Thus, more sensitive tests of visual function are required to evaluate the effects of potential treatments.

Technique	Selected references
Psychophysics (forced choice, preferential looking)	Burg, 1966; Campbell, 1965; Banks, 1978; Rogers, 1987; Leguire, 1989; Cox, 1990; Drover, 2009; Campos, 1985
Visually evoked potentials (VEPs)	Katsumi, 1986; Atkinson, 1979; Norcia, 1986; Harris; 1976; Campos, 1984; Levi, 1974;
Optokinetic nystagmus (OKN)	Reinecke, 1958; Wolin; 1964; Voipio; 1966; Lewkonia; 1969; Schor, 1980;; Hainline, 1985;; Atkinson, 1989, Leguire, 1991;Wester, 2007; Cetinkaya, 2008
Ocular following response	Millodot, 1973; Goldmann, 1943; Bouman, 1951; DeLaet 1959

Table 1. *Different techniques to study contrast sensitivity in man. The references show some studies using these techniques. This list is by no means exhaustive.*

The contrast sensitivity function has become a well-established tool to probe the functional integrity of the visual system (Leguire, 1991) and over the last decades, many techniques have been described to measure the contrast sensitivity function. See table 1 for an indication.

New methods are still being developed (Wester et al, 2007; Drover et al, 2009) so no gold standard has been met. Here we describe a technique that uses the ocular following response (OFR), a gaze stabilization reflex that drives the eye to follow moving stimuli in the visual field, to infer contrast sensitivity. This technique was originally developed for mice and demonstrated subtle age and sex related differences in contrast sensitivity, as well as much lower contrast sensitivity than previously reported in mice (chapter 2). Using a quantifiable measure, like OFR gains has two benefits. First, it is completely objective and not subject to user reported bias, which often occurs in perception tasks where the stimulus is close to the perceptual threshold. Also, the response is not binomial but graded, as the gain of the OFR decreases as stimuli become harder to see (van Alphen 2009, Cahill and Nathans, 2008). This makes the method ideally suited to screen for small changes in visual function caused either by degenerative diseases or new by treatment methods that aim to improve visual function in low vision patients. Also, because no patient response is required, this method can be very useful to study vision in small children or mentally impaired patients. This study is a proof of principle only, and shows how responses to moving Gabor patches with different contrasts and spatial frequencies correlate with regular Snellen acuity.

Methods

Subjects

40 eyes from 36 subjects were recorded. Their average age was 29. Two eyes had myopia as well as astigmatism, one was amblyopic and 37 eyes were only myopic.

Visual acuity

Snellen acuity was assessed using a Landolt-C chart, which requires subjects to detect the location of a gap in a series of consecutively smaller C's. The

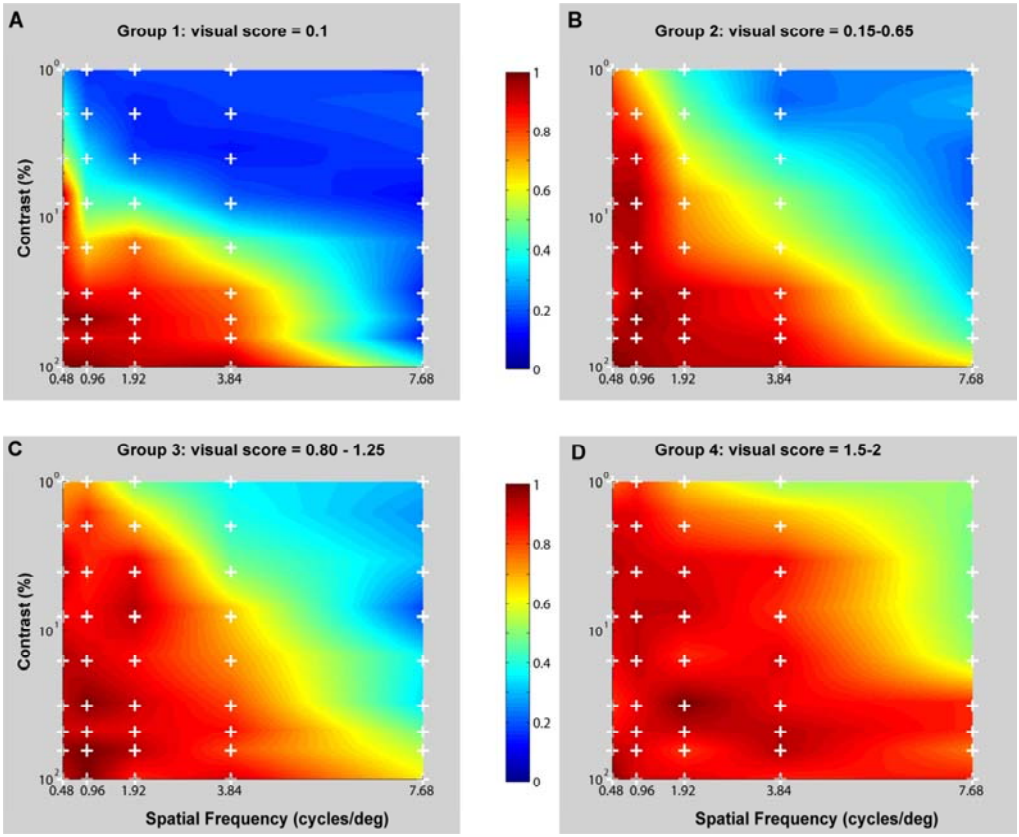

Figure 2. *Normalized OFR gains for each of the four subject groups. The colour reflects the OFR gains at 45 combinations of contrast and spatial frequency. White crosses indicate measurements.. Spaces between the measured points are linearly interpolated.*

score of the line prior to the line in which the subject could not perceive any or most of the letters was considered as the visual acuity score of the subject. Subjects were divided into four groups based on their visual scores (table 2). Subjects in group A scored 0.1 or less, those in group B had visual acuity scores between 0.15 and 075, group C's scores are between 0.8 and 1.25 and group D has visual scores from 1.5 to 2.

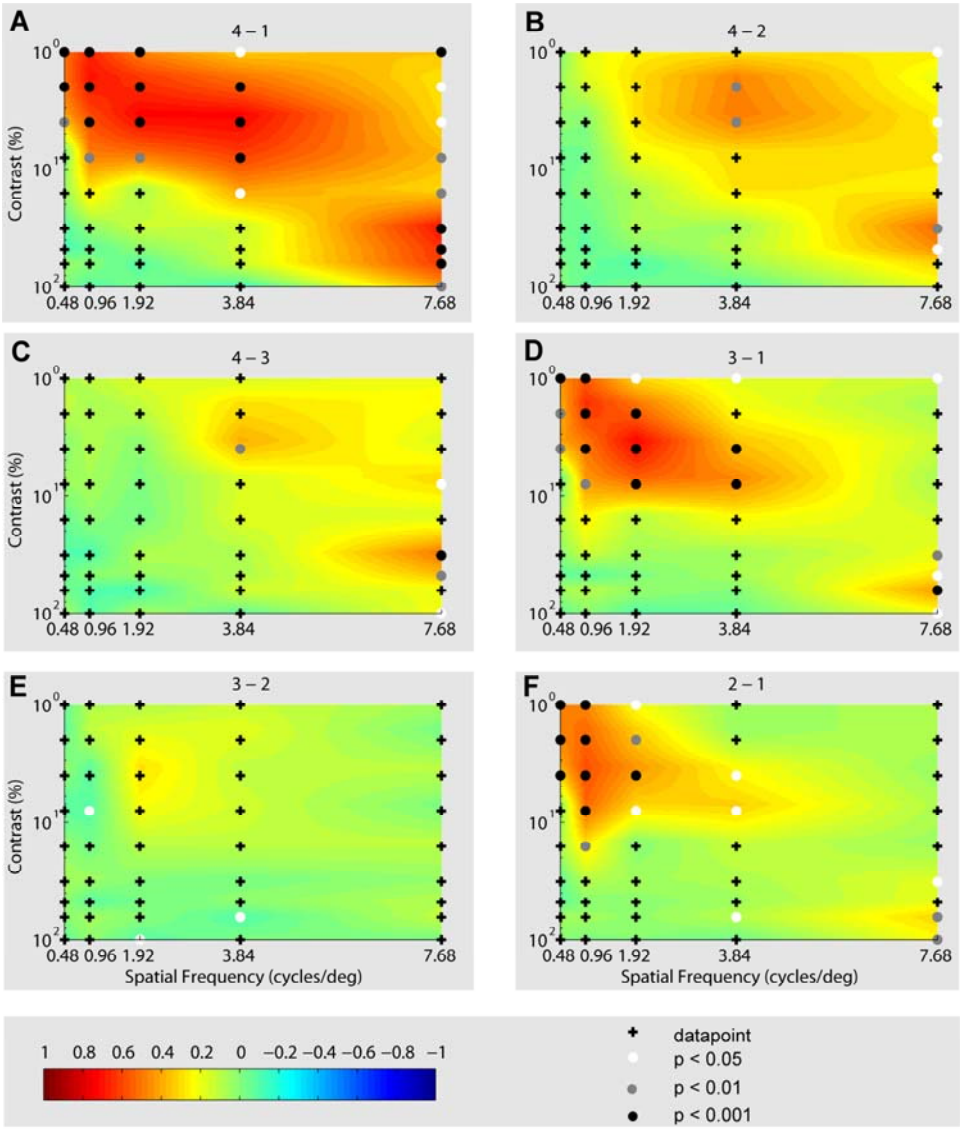

Figure 3. *Differences between normalized gains of the four groups of subjects. Each panel shows the subtraction of two groups, where the group with the lower visual score is always subtracted from the higher score group. Red and yellow shades show where in stimulus space the gains of the first group are higher and blue shades show regions where the second group has higher gains. Significant differences in measurements are labelled with white, grey or black dots. Other data points are marked with crosses.*

Total number of eyes with refractive errors	Visual Acuity Score			
	Group A <0.1	Group B 0.15-0.75	Group C 0.8-1.25	Group D 1.5-2
40	13	12	9	6

Table 2. *Subjects grouped by visual score.*

Contrast sensitivity measurements

In this study, we measured contrast sensitivity using a modified approach originally developed for mice (van Alphen et al, 2009). Optokinetic eye movements were evoked by moving a Gabor patch from left to right, in a pendular way. By recording how the gain of the OFR decreases as moving Gabor patches become more difficult to see, we were able measure not just whether a subject responded to a stimulus, and thus was able to see it, but also measure the magnitude of that response, which indicates how well the stimulus was seen. In mice, this approach uncovered differences in contrast sensitivity between male and female C57Bl6 mice that were undetectable by other methods (van Alphen et al, 2009).

Stimulus setup

Visual stimuli consisted of Gabor patches generated in Matlab 6.5 (The MathWorks, Natick, MA). The standard deviation of each Gabor patch was 5 degrees visual angle in diameter and was back-projected on a transparent screen (135 * 99 cm) using a digital projector with a resolution of 1024 * 768 pixels. Images were projected via a set of movable, computer controlled mirrors that diverged the projector beam to smoothly move the Gabor patch over the screen, creating fluent motion. Mirror movement was PC-controlled (Spike-2 4.20, Cambridge electronic design), and generated a movement that consisted of three cycles of a sinusoidal motion of 0.1 Hz with peak velocity of 5 degrees per second. Each stimulus showed a Gabor patch composed of a combination of 1 of 5 spatial frequencies (0.48, 0.96, 1.93, 3.87, 7.74 cycles per degree) and 1 of 9 contrast values (1, 2, 4, 8, 16, 32, 48, 64, 100). The 45 stimulus combinations were presented in random order. The used spatial frequencies do not even approach 60 cycles per degree, which is the limit of normal human vision at maximum contrast (Campbell and Green, 1965) but

focus on the low frequency component of vision instead, due to limitations of the projector.

Viewing distance was 305 cm. Subjects were head fixed using a bite board. Monocular eye movements were recorded using an Eyelink system infrared camera system (SensoMotoric instruments GmbH, Teltow, Germany) at a 250Hz sampling rate. Calibration and calibration-accuracy validation were performed before the experiments using the standard Eye-link routine. All experiments were performed in a darkened room so that only the stimulus was visible. The eye that was not being tested was covered with a pirate patch.

Data Analysis

Recorded eye positions were transformed offline using commercial programming language (Matlab; The MathWorks, Natick, MA) in a velocity signal by taking the first derivative. Fast phases were removed with a velocity threshold. A sine wave was fitted to the resulting velocity trace. Gains were calculated by dividing the peak eye velocity by peak stimulus velocity (5 deg/s) and normalized by setting the highest gain for each subject to 1.

Results

Even though this test only measured the low frequency component of human vision, some differences between the four groups are immediately apparent. In the normal vision group (Figure 2D, visual score 1.5-2), gains were high for all but a few stimulus condition. However, at 7.68, contrast sensitivity drops sharply off in the lower contrast range, below 16%. OFR gains in the low vision group (visual score < 0.1) are not able to see contrasts below 16 % in all but the lowest spatial frequency. Even at maximal contrast, their gains drop sharply from 1 to 0.4 over a range of a few degrees in spatial frequency, from 3.87 to 7.74. Groups B and C are almost identical over the range of stimuli in this experiment.

Differences between groups are shown in Figure 3. Each of the panels shows the result of subtracting a group with lower visual score from a group with a

higher visual score. Similar stimulus conditions in both groups were compared using an unpaired t-test. Subjects in group 1 perform significantly worse than all other groups. Surprisingly, we didn't find any significant difference between groups B and C with the current range of stimulus conditions, except a few unrelated points, which can be expected with 45 measurements at $p<0.05$, which suggests two false positive results. However, it is not unlikely that differences between both groups can be found at higher spatial frequencies. There are also some differences between group 4 and groups 2 and 3 at the higher spatial frequencies.

Discussion

As in mice, OFR gains in man decrease as stimuli become harder to see. Even though we only tested a small range of spatial frequencies, instead of measuring all the way up to 60 cycles per degree, we are able to demonstrate differences between four groups of subjects visual scores ranging from very low to better than normal. Thus, this method shows promise to study subtle changes in contrast sensitivity as a result of ageing, disease or treatments meant to improve vision. Using OFR gains as a measure of how well a stimulus is seen provides researchers with an extra dimension of data: that of response magnitude.

With the current range of stimuli, we could only demonstrate differences between subjects with very low visual scores, < 0.1 and the other groups. Also, subjects in group 4 performed better than groups 2 and 3 at the highest two spatial frequencies. Surprisingly, there were no obvious differences between groups 2 and 3 with the current range of stimuli. However, at higher spatial frequencies, differences are expected to be found.

There are some technical challenges to measure high spatial frequencies, as this requires up to 60 sine gratings to be displayed in a small area covering 1 degree of visual angle. For example, when you stretch your arm, the nail of your thumb will be about 1-2 degrees visual angle in size. An average 24" widescreen LCD monitor is approximately 48 cm wide and has a horizontal resolution of 1920 pixels, or 40 pixels per centimetre, which means maximally 20 square wave gratings can be constructed in one cm. To create a

minimal sine grating, 4 pixels are required per centimetre. Thus, at a viewing distance of approximately 170 cm, a square wave grating of 60 cycles/degree can be constructed. For sine gratings, the viewing distance has to be doubled.

Using this approach, with stimuli covering the whole range of human vision, small changes in a person's contrast sensitivity could be detected. This is especially important since contrast sensitivity decreases with age (Sekuler et al, 1980; Greene and Madden, 1987) and changes in contrast sensitivity are generally not picked up with the regular Snellen test. In elderly persons, decreased contrast sensitivity contributes to a poor postural stability which leads to a 2x increase in the likelihood of falling (Turano et al, 1994).

Several studies confirmed a correlation between CSF and driving ability. One study described how impaired contrast sensitivity in elderly drivers was strongly associated with self-reported difficulty in day and night driving (Rubin et al, 1994). Also, elderly drivers with a cataract induced monocular reduction in contrast sensitivity are three times more likely to be involved in an at-fault crash. This increased to a six-fold greater risk in patients with binocular impairment of contrast sensitivity (Owsley et al, 2001). Likewise, most people drive considerably less during the hours of darkness. Despite this, more than half of all fatal motor vehicle collisions occur after dark, a difference which cannot be fully attributed to altered driver behaviour associated with nightfall, such as fatigue or alcohol consumption (Plainis, 2006).

In a recent study, contrast perception was studied in depressed patients using pattern electroretinograms (Bubl, 2010). Both medicated and unmedicated patients showed dramatically lower retinal contrast gains, thus showing that depressed people have reduced sensitivity to contrast, and therefore may indeed experience the world as being less colorful. This study also suggests that depression can be diagnosed by objectively, by measuring contrast sensitivity. It's still unclear, however, whether reduced contrast sensitivity is a specific marker of depression. The same effect could possibly occur in patients with other neuropsychiatric conditions such as

schizophrenia, and this is could be investigated in future work. Interestingly enough, the size of the olfactory bulb is decreased in depressed patients, compared to healthy patients, and their olfactory sensitivity is decreased (Negoias et al 2010).

Thus, accurate measurements of contrast sensitivity are important, especially in the elderly and in patients where contrast sensitivity can be expected to decrease as a result of illness. Also, the approach outlined in this paper can be helpful to those researchers seeking to improve vision in low vision patients.

References

Aramant, R. B. and M. J. Seiler (2004). "Progress in retinal sheet transplantation." Progress in Retinal and Eye Research 23(5): 475-494.
Armbrecht, A. M., P. A. Aspinall, et al. (2004). "A prospective study of visual function and quality of life following PDT in patients with wet age related macular degeneration." Br J Ophthalmol 88(10): 1270-1273.
Atkinson, J. (1984). "Human visual development over the first 6 months of life. A review and a hypothesis." Hum Neurobiol 3(2): 61-74.
Atkinson, J. and O. Braddick (1979). "Assessment of vision in infants: applications to amblyopia." Trans Ophthalmol Soc U K 99(3): 338-343.
Banks, M. S. and P. Salapatek (1978). "Acuity and contrast sensitivity in 1-, 2-, and 3-month-old human infants." Invest Ophthalmol Vis Sci 17(4): 361-365.
Bouman, M. A., Ten Doesschate. J., DuMarchie Sarvass, G.J. (1951). "A modification of Goldmann's apparatus for the objective determination of the visual acuity." Ophthalmologica 122: 368-374.
Bubl, E., E. Kern, et al. (2010). "Seeing gray when feeling blue? Depression can be measured in the eye of the diseased." Biol Psychiatry 68(2): 205-208.
Burg, A. (1966). "Visual acuity as measured by dynamic and static tests: a comparative evaluation." J Appl Psychol 50(6): 460-466.
Cahill, H. and J. Nathans (2008). "The optokinetic reflex as a tool for quantitative analyses of nervous system function in mice: application to genetic and drug-induced variation." PLoS One 3(4): e2055.
Campbell, F. W. and D. G. Green (1965). "Optical and retinal factors affecting visual resolution." J Physiol 181(3): 576-593.
Campos, E. C. and C. Chiesi (1985). "Critical analysis of visual function evaluating techniques in newborn babies." Int Ophthalmol 8(1): 25-31.
Campos, E. C., M. L. Prampolini, et al. (1984). "Contrast sensitivity differences between strabismic and anisometropic amblyopia: objective correlate by means of visual evoked responses." Doc Ophthalmol 58(1): 45-50.
Cetinkaya, A., S. Oto, et al. (2008). "Relationship between optokinetic nystagmus response and recognition visual acuity." Eye (Lond) 22(1): 77-81.
Compston, A. and A. Coles (2008). "Multiple sclerosis." Lancet 372(9648): 1502-1517.

Cox, I. and B. A. Holden (1990). "Soft contact lens-induced longitudinal spherical aberration and its effect on contrast sensitivity." Optom Vis Sci 67(9): 679-683.
de Jong, P. T. (2006). "Age-related macular degeneration." N Engl J Med 355(14): 1474-1485.
De Laet, H. A., Szucs, A. (1959). "La mesure objective de l'acuite visuelle au moyen de l'appareil de
Goldmann." Bull Soc Belg Ophtalmol 120: 527-538.
Drover, J. R., L. M. Wyatt, et al. (2009). "The teller acuity cards are effective in detecting amblyopia." Optom Vis Sci 86(6): 755-759.
Gibson, R. A. and H. F. Sanderson (1980). "Observer variation in ophthalmology." Br J Ophthalmol 64(6): 457-460.
Ginsburg, A. P. (2003). "Contrast sensitivity and functional vision." Int Ophthalmol Clin 43(2): 5-15.
Goldmann, H. (1943). "Objektive Sehcharfenstimmung." Ophthalmologica 105: 240-252.
Greene, H. A. and D. J. Madden (1987). "Adult age differences in visual acuity, stereopsis, and contrast sensitivity." Am J Optom Physiol Opt 64(10): 749-753.
Hainline, L. and I. Abramov (1985). "Saccades and small-field optokinetic nystagmus in infants." J Am Optom Assoc 56(8): 620-626.
Harris, L., J. Atkinson, et al. (1976). "Visual contrast sensitivity of a 6-month-old infant measured by the evoked potential." Nature 264(5586): 570-571.
Katsumi, O., T. Hirose, et al. (1986). "A new method to measure the pattern reversal visual evoked response in infants and young children." Jpn J Ophthalmol 30(4): 420-430.
Leguire, L. E. (1989). "Caution advised in interpreting contrast sensitivity results." Ophthalmology 96(5): 731-732.
Leguire, L. E., B. S. Zaff, et al. (1991). "Contrast sensitivity of optokinetic nystagmus." Vision Res 31(1): 89-97.
Levi, L. (1974). "Blackbody temperature for threshold visibility." Appl Opt 13(2): 221.
Lewkonia, I. (1969). "Objective assessment of visual acuity by induction of optokinetic nystagmus." Br J Ophthalmol 53(9): 641-644.

Loewenstein, J. I., S. R. Montezuma, et al. (2004). "Outer retinal degeneration: an electronic retinal prosthesis as a treatment strategy." Arch Ophthalmol 122(4): 587-596.
Maffei, L. and A. Fiorentini (1973). "The visual cortex as a spatial frequency analyser." Vision Res 13(7): 1255-1267.
Millodot, M., D. Miller, et al. (1973). "Evaluation of an objective acuity device." Arch Ophthalmol 90(6): 449-452.
Norcia, A. M., C. W. Tyler, et al. (1986). "Electrophysiological assessment of contrast sensitivity in human infants." Am J Optom Physiol Opt 63(1): 12-15.
Owsley, C., B. T. Stalvey, et al. (2001). "Visual risk factors for crash involvement in older drivers with cataract." Arch Ophthalmol 119(6): 881-887.
Pandit, J. C. (1994). "Testing acuity of vision in general practice: reaching recommended standard." BMJ 309(6966): 1408.
Plainis, S., I. J. Murray, et al. (2006). "Road traffic casualties: understanding the night-time death toll." Inj Prev 12(2): 125-128.
Reinecke, R. D. and D. G. Cogan (1958). "Standardization of objective visual acuity measurements; opticokinetic nystagmus vs. Snellen acuity." AMA Arch Ophthalmol 60(3): 418-421.
Rogers, G. L., D. L. Bremer, et al. (1987). "The contrast sensitivity function and childhood amblyopia." Am J Ophthalmol 104(1): 64-68.
Rubin, G. S., K. B. Roche, et al. (1994). "Visual impairment and disability in older adults." Optom Vis Sci 71(12): 750-760.
Schor, C. M. and D. M. Levi (1980). "Disturbances of small-field horizontal and vertical optokinetic nystagmus in amblyopia." Invest Ophthalmol Vis Sci 19(6): 668-683.
Seiler, M. J. and R. B. Aramant (2005). "Transplantation of neuroblastic progenitor cells as a sheet preserves and restores retinal function." Semin Ophthalmol 20(1): 31-42.
Sekuler, R., L. P. Hutman, et al. (1980). "Human aging and spatial vision." Science 209(4462): 1255-1256.
Skeel, R. L., A. Nagra, et al. (2003). "The relationship between performance-based visual acuity screening, self-reported visual acuity, and neuropsychological performance." Clin Neuropsychol 17(2): 129-136.

Thomas, B. B., R. B. Aramant, et al. (2006). "Retinal transplantation. A treatment strategy for retinal degenerative diseases." Adv Exp Med Biol 572: 367-376.
Turano, K., G. S. Rubin, et al. (1994). "Visual stabilization of posture in the elderly: fallers vs. nonfallers." Optom Vis Sci 71(12): 761-769.
van Alphen, B., B. H. Winkelman, et al. (2009). "Age- and sex-related differences in contrast sensitivity in C57BL/6 mice." Invest Ophthalmol Vis Sci 50(5): 2451-2458.
Voipio, H. and L. Hyvarinen (1966). "Objective measurement of visual acuity by arrestovisography." Arch Ophthalmol 75(6): 799-802.
Warrian, K. J., U. Altangerel, et al. (2010). "Performance-based measures of visual function." Surv Ophthalmol 55(2): 146-161.
Watson, A. B. and J. G. Robson (1981). "Discrimination at threshold: labelled detectors in human vision." Vision Res 21(7): 1115-1122.
Wester, S. T., J. F. Rizzo, 3rd, et al. (2007). "Optokinetic nystagmus as a measure of visual function in severely visually impaired patients." Invest Ophthalmol Vis Sci 48(10): 4542-4548.
Wolin, L. R. and A. Dillman (1964). "Objective Measurement of Visual Acuity. Using Optokinetic Nystagmus and Electro-Oculography." Arch Ophthalmol 71: 822-826.

Chapter 5

Three dimensional optokinetic eye movements in the C57BL/6J mouse

Bart van Alphen, Beerend HJ Winkelman, Maarten A Frens

Published in:

Three-dimensional optokinetic eye movements in the C57BL/6J mouse.
van Alphen, B., Winkelman, B.H.J., Frens, M.A. (2010)
Investigative Ophthalmology and Visual Science 51(1):623-30.

Introduction

Compensatory eye movements are a popular model system for connecting neurophysiology and behavior as well as studying the neural correlates of behavioral plasticity. It is a system where the sensory input can be fully defined. The output, reflexive compensatory eye movements and electrophysiological activity, can be recorded and correlated with the sensory input. Additionally, by manipulating those reflexive eye movements by using different combinations of sensory input, motor learning can be studied in a well-controlled environment. Oculomotor studies focus more and more on mice [1-3]. Their small size and fast reproduction rates make them attractive, especially when combined with the availability of many techniques to generate and characterize mutants. Inducing mutations in the oculomotor system or more generally in the cerebellum is a highly useful tool to gain more insight in the function of the oculomotor or cerebellar system.

Compensatory eye movements combine visual and vestibular sensory information to provide an organism with a stable retinal image, either during head motion or during motion in the outside world. In afoveate species, this is achieved by the combination of two reflexes, the vestibulo-ocular reflex (VOR) and the optokinetic reflex (OKR). Foveate species also use smooth pursuit to track a moving target in the outside world. The VOR and OKR work in tandem, the VOR functioning best at high frequency head movements while the OKR operates best at low angular velocities of the visual surround [3-7]. The combined, synergistic action of these two reflexes results in a good ocular stability over the entire frequency range of natural head rotations [8].

To accomplish that the VOR and OKR work in close synergy the oculomotor system needs to transform the visual and vestibular sensory input into a common coding in three dimensional space. Head rotations occur in all directions. Therefore, the gaze stabilization reflexes need to operate in three dimensions as well. Vestibular information, the change in rotational velocity, is already perceived as three dimensional due to the architecture of the

vestibular canal system. Each organ consists of three semi-circular canals that are approximately orthogonal to each other, resulting in a 3-D reference frame with an earth-vertical axis and two horizontal axes, at angles of 45º and 135º clockwise of the naso-occipital axis.

In the retina, information about image motion is split into several separate channels as well. Direction-selective ganglion cells in the retina respond to retinal slip. This flow-detection by ganglion cells and subsequent neuronal stages is organized in three different channels that are approximately collinear with the best response axes of the vestibular system. The segregation in three channels is also found anatomically in the Accessory Optic System [9, 10] and the inferior olive [11].There are different anatomical and physiological zones in the flocculus that respond to optokinetic stimulation about horizontal and vertical axes. These zones have been described for the Inferior Olive of monkeys [12], cats [13], rabbits [14-16], rats [17, 18] and mice [19].

So far, the properties of 3D compensatory eye movements have been described in several species (e.g. primates [20], rabbits [21], chameleons [22]. Data from mice however are still lacking. In this study we record 3D optokinetic eye movements in wildtype C57BL/6J mice, the most commonly used mouse model in oculomotor neurophysiology.

Materials and Methods

To investigate how the mouse eye moves in three dimensions we used a technique to record eye movements using an infrared video system and three artificial reflective markers that are painted on the cornea. This method merges two earlier methods [23, 24] for recording eye movements using video-oculography. Pupil tracking, the most commonly used video-oculographic method, is unable to capture the full 3D orientation of the eye, because rotation about the pupillary axis (torsion) is not measured. On the other hand, scleral search coils [25, 26] are known to interfere too much with the eye movement dynamics [24].

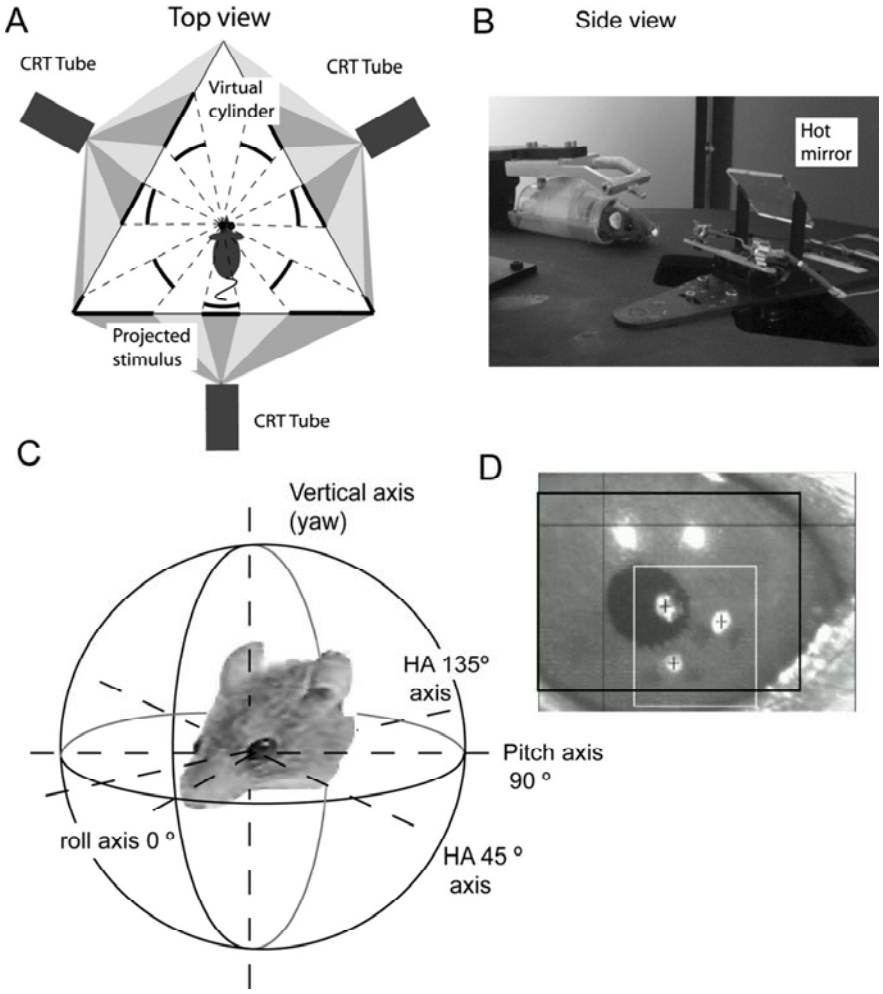

Figure 1. *Schematic representation of the experimental setup.* **A.** *Top view. A mouse was placed in the setup, with its left eye in the exact center. It was surrounded by three screens on which the stimulus is projected in such a way that it appeared as a virtual sphere from the perspective of the mouse.* **B.** *Front view. To keep the field of view of the mouse unobstructed we recorded eye movements with an infrared camera that was placed under the setup. The eye was tracked through a hot mirror.* **C.** *Stimuli were rotated about the five axes indicated with dashed lines.* **D.** *Screenshot of a mouse eye with three markers, shown in the white box. The other two dots are corneal reflections of the illumination LEDs. Black crosses indicate the marker centroids.*

Animal preparation

In this study, five adult male mice of the C57BL/6J strain were used. They were housed on a 12 h:12 h light: dark cycle with unrestricted access to food and water. Experiments were done during the light phase. All surgical procedures and experimental protocols were carried out in accordance with the guidelines set by the Animal Welfare Committee of the Erasmus University and were in accordance with the European Communities Council Directive (86/609/EEC) and the ARVO Statement for the Use of Animals in Ophthalmic and Vision Research.

Setup and eye movement recording

Animals were prepared for head fixation and placed in a virtual reality setup that displays panoramic monochrome stimuli fully surrounding the animal, allowing a 360º field of view (Figure 1A). Eye movements were recorded with an infrared video system (Iscan ETL-200). All procedures and equipment have been described earlier [27].

Marker placement

Before each recording session, the animal was anesthetized briefly with a mixture of Isofluoran and oxygen. Its left eye was topically anesthetized (benoxinate hydrochloride 0.4 %, Minims). A small area of the cornea (0.5 mm * 0.5 mm) was dried with a paper tip after which the markers were placed using a blunt needle to apply three dots of titanium dioxide pigment (art. Nr 650, Custom Tattoo Supplies Europe). These markers can be placed anywhere on the cornea, as long as they remain visible at all times. They are temporary, staying on the eye for 4 to 12 hours after which they wash off without leaving a trace.

Optokinetic Stimuli

The stimulus was rendered using openGL (Silicon Graphics Inc.) and consisted of 1592 green dots, each 2º visual angle in diameter, that were equally spaced on a virtual sphere that had its center at the left eye, which in turn was positioned above the table axis, in the center of the triangular screen configuration. The dots were rotated about an axis that ran through the eye. We used sinusoidally moving stimuli with fixed amplitude of 5º and frequencies of 0.1, 0.2, 0.4, 0.6, 0.8 and 1 Hz. Peak velocities were therefore

3.14, 6.28, 12.57, 18.85, 25.13 and 31.42 º/s respectively. The stimuli oscillated about the pitch (interaural), roll (naso-occipital) and yaw (earth vertical) axis, as well as the 45º and 135º horizontal axes (Figure 1C).

Calibration procedure

Positions of the markers were recorded in head-fixed camera coordinates: x for the horizontal axis and y for the vertical axis. The optical axis of the camera was defined as the z-axis. The unique orientation of the eye can be computed when the 3D position of the markers is known. However only the x and y coordinates of the markers are recorded. When assumed that the eye is spherical and moves exclusively with rotation about a single center of rotation, all marker positions are bound to a sphere on which they travel when the eye rotates. Because the camera records a near orthogonal projection of the markers onto a flat surface, the 3D coordinates of the markers can straightforwardly be computed when the projection of the center of rotation onto the camera image and the radius of the projected sphere are known. Before each experiment a calibration procedure was performed to find these parameters.

Procedure for locating the center of rotation:

Four IR LEDs were placed in a square formation around the lens of the camera, equidistant from the optic axis of the camera. When the camera's optic axis is perfectly orthogonal with the center of curvature of a reflective, spherical object (such as a mouse eye), the reflections of the four LEDs recorded by the camera are also equidistant from the center pixel of the recorded image, retaining their square arrangement. This gives the virtual x- and y-coordinates of the center of the sphere over which the markers move. This method was described earlier [23].

Procedure for determining the radius:

A reference LED was placed on the camera, aligned in the vertical plane with its optical axis, creating a corneal reflection. By continuously oscillating the camera while translating the mouse in its longitudinal direction until the recorded CR displacement was minimal we moved the center of the corneal curvature on the rotation axis of the camera arm (and hence the center of the stimulus setup). Then the camera was placed multiple times in its two most

extreme positions, at -13.06º and +13.06º. At each position the x-coordinate of the corneal reflection and the marker closest to the center of the pupil was recorded (c_1 and c_2, p_1 and p_2 respectively). The radius of rotation of the marker was then approximated using the following formula:

$$Radius \cong 26.12 \cdot \pi \cdot (d_1 - d_2)/180 \quad \text{where} \quad d_i = c_i - p_i$$

This method was previously described [24] to determine the radius of rotation of the pupil.

Data Analysis

Marker positions were converted into rotation matrices, aligned with the stimulus after which instantaneous angular eye velocity was determined (see Appendix and Supplementary figure 1). All data was analyzed after the experiment using Matlab (The MathWorks Inc.). Experimenters were masked to the experimental conditions. Trials were randomized, mice were assigned a number and the data analysis scripts were automated. Eye velocity was smoothed with a Gaussian filter (σ = 100 ms). To correct for the camera delay, the velocity signal was shifted 28 ms back in time. Fast phases were removed using a velocity threshold of twice the stimulus velocity. The time periods that were cut out were extended from 50 ms before the first threshold crossing to 100 ms after the second threshold crossing. Average amplitude and phase values of sinusoidal fits were calculated by multiple linear regression of eye velocity to sine and cosine components of the phase of the stimulus. Gain values were calculated as the ratio between the fitted eye velocity amplitude and stimulus velocity amplitude. The best response axis to each stimulus condition was defined as the axis corresponding to the first principal component of the eye velocity data matrix. All statistical analysis was performed using SPSS 16 (SPSS Inc).

A step by step guide of these methods can be found in Appendix B, along with some helpful troubleshooting tips.

Results

Pupil tracking compared to marker tracking

OKR responses to yaw stimuli were measured two times, once using marker tracking and once using pupil tracking [24]. Stimuli consisted of sinusoidal oscillations about the yaw axis, at six different frequencies (0.1, 0.2, 0.4, 0.6, 0.8 and 1 Hz) with constant amplitude of 5°, resulting in stimulus velocities ranging from 3.14°/s to 31.42°/s. Both methods show very similar gain (Figure 2A) and phase plots (Figure 2B), with high gains at low stimulus velocities, dropping off as stimulus velocity increases. Differences between the two recording methods were tested for significance using a repeated measures ANOVA with two factors: one between subjects factor with two levels ('Recording Method' with 2 levels: Marker tracking and Pupil tracking) and one within subject factors: 'Stimulus Frequency' with 6 levels). We found no main effect of 'Recording method' (between subject) $F = 1.041$, $p = 0.365$. There was no significant interaction effect: Stimulus Frequency * Recording Method ($F=1.322$, $p = 0.317$). Within subjects we found a main effect of Stimulus Frequency ($F = 177.635$, $p < 0.001$). These results indicate that marker tracking is a viable alternative for pupil tracking.

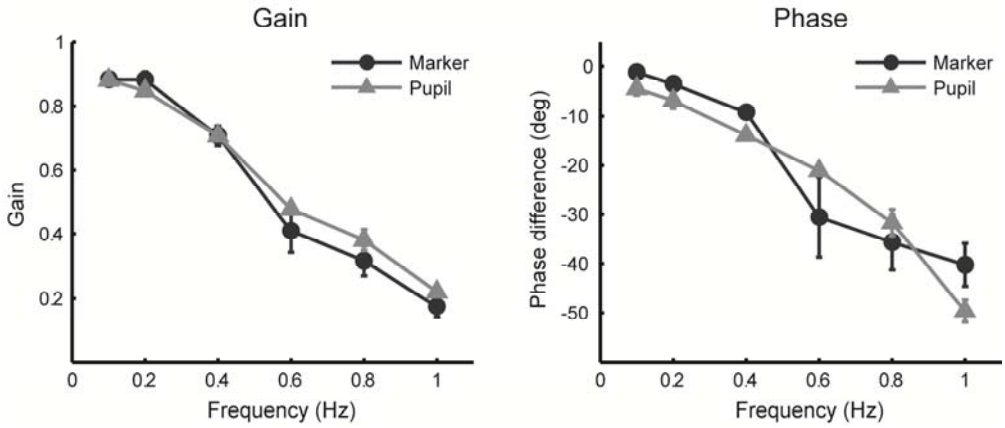

Figure 2: Marker tracking vs pupil tracking **A.** *Gains and* **B.** *phases recorded with pupil tracking (grey line) and marker tracking (black line). Gains and phases were not significantly different (repeated measures ANOVA, F = 1.041, p = 0.365). n = 5, errorbars show SEM.*

Best axis responses

The optokinetic reflex over the best response axis showed highly uniform response magnitudes for all stimulus conditions, being close to unity at low stimulus velocities and decreasing with increased stimulus velocity. Similarly, phase differences (the lag between stimulus and resulting eye movement) were small at low stimulus velocities and increased as the stimulus oscillated faster. These results show that, at low stimulus velocities, the OKR achieves almost perfect compensation for image motion across the retina, regardless whether the retinal image slip is from left to right (Figure 3A), up-down (Figure 3B)), torsional (Figure 3C) or a combination of both (Figure 3D,E). At higher stimulus frequencies/velocities this compensation deteriorates more or less uniformly for all stimulus directions.

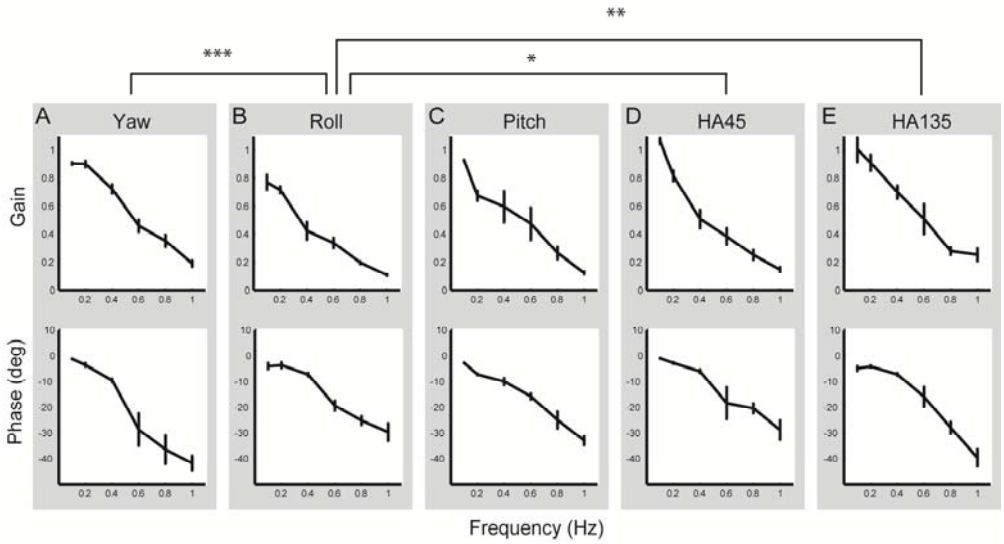

Figure 3. *Best axis responses for stimuli rotating about one of the five stimulation axes. Top panels show gains at six frequencies; bottom panels show phase differences between stimulus and eye movement. n = 5, errorbars show SEM. Responses are highly uniform for all conditions.*

3D components of the optokinetic reflex

Optokinetic responses were decomposed into pitch, roll and yaw components (Figure 4). At all stimulus velocities, yaw stimulation resulted in an almost pure horizontal eye movement, i.e. movement about the yaw axis of the eye (see Figure 1C for the five different stimulation axes). Likewise, roll stimulation resulted in a vertical eye movement (rotation about the Roll axis) and pitch stimulation in a combined vertical and torsional eye movement. Stimulation about the HA 45 and HA 135 axis resulted in a combined torsional and vertical eye movement of similar magnitude, resulting in an eye movement that was practically on-axis.

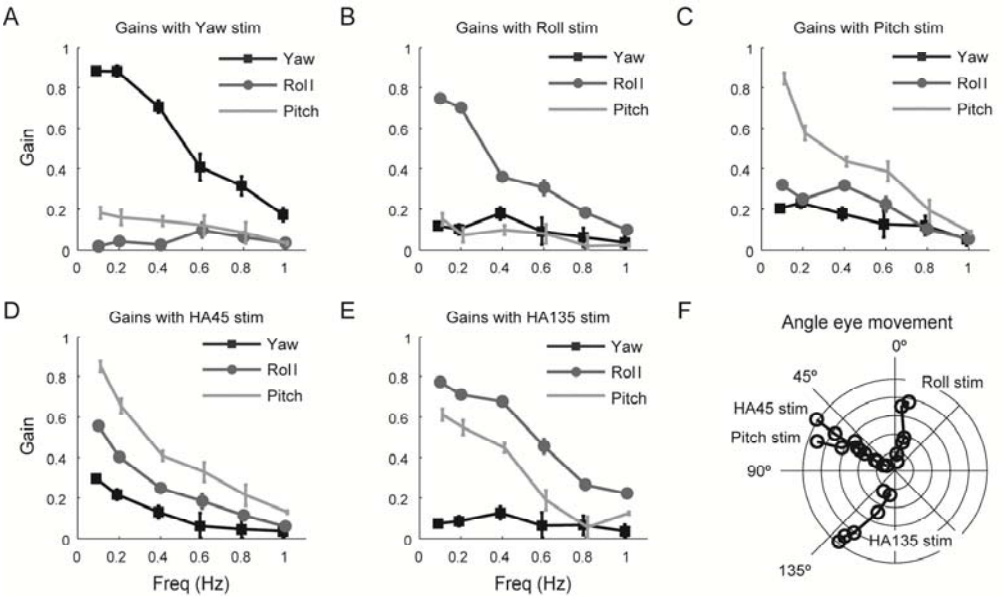

Figure 4: A-E. *Gains of the three dimensional components (roll, pitch and yaw) of the optokinetic response to stimuli oscillating about one the five axes (Figure 1C) are shown. n = 5, errorbars show SEM. Curves were moved one tick over the x-axis to avoid overlapping errorbars.* **F.** *Angle of eye movement (black lines) for all horizontal stimulation axes.*

Discussion

The present experiments demonstrate for the first time that optokinetic eye movements in mice are equally well developed in all directions and hence have a uniform input-output relation for all optokinetic stimuli (Figure 3). At low frequency (0.1 Hz; velocity = 3.14º/s), gains were close to unity and phase differences were minimal (~1º) for all stimulus conditions, which indicates that eye movement largely compensates for image motion over the retina, regardless of stimulus orientation. As stimulus peak velocity increases with frequency, OKR gains decrease and phase lags become larger. The gain and phase of the eye movement response are consistent with reports about horizontal optokinetic eye movements in mice [4, 7, 28, 29], rabbit [21, 30]and cat [31].

The 3D eye movements show slight deviation from the stimulation axis for all stimuli, except Pitch stimuli, where the response is very similar to that of HA45 stimulation. Generally the eye movement follows the stimulus well in both amplitude and direction. The direction of movement does not change as stimulus velocity increases (Figure 4F), even when magnitude of the response decreases (Figure 4A-E) with stimulus velocity.

Mice show torsion responses with gains close to unity at low stimulus frequency and velocity. This is much larger than the 0.36 gain that was reported in man [32] but similar to the rabbit [21]. A possible explanation for this can be found in the anatomy of the mouse retina, which differs in anatomy from the human retina. The human retina contains a fovea, a specialized area for vision in which photoreceptors are densely packed within an area that covers 1° of the visual field. In order to see the world at high spatial resolution, the foveas of both eyes are aimed with fast ballistic movements (saccades) at interesting regions in the field of view. Once a target is fixated, it can be tracked with smooth pursuit movements and the image is stabilized on the retina using compensatory eye movements. In mice, photoreceptors are distributed almost homogenously over the retina, which means that a mouse sees equally well with all parts of its retina; there is no fovea that has to be aimed to get a clearer view. Afoveate animals see optimally when they

fully compensate for blurring caused by image motion across the retina, using compensatory eye movements.

A lot of research on the control of 3D eye movements focuses on primates [20]. By using mice in these studies, with all the genetic tools that are available, new approaches can be used to tackle 3D motor control problems. Of course there are several important differences between mice and primates; most notably the lack of a fovea and related pursuit and saccade systems. This simplicity can be a benefit, because mice face similar challenges as higher vertebrates when controlling compensatory eye movements and have to combine visual, vestibular and ocular information to achieve optimal compensation.

Under natural conditions, when the animal is unrestrained, the OKR works closely together with the vestibulo-ocular reflex (VOR) to keep a stable image on the retina. The OKR compensates for low velocity retinal slip while the VOR compensates for high frequency head movements. Together, these two reflexes are able to keep a stable image on the retina for a large range of natural head movements [8]. Because the murine OKR works equally well for all stimulus directions used in these experiments, we hypothesize that the VOR of mice will also function equally well for sinusoidal oscillations about the yaw, pitch, roll, HA 45 and HA 135 axes. This hypothesis can be tested using a 3-D motion platform, in combination with a setup as described in this paper.

We recorded three dimensional eye movements by tracking the position of three markers that were painted on the eye (Figure 1 D). When recording horizontal optokinetic eye movements, evoked by a stimulus that oscillates sinusoidally about the yaw axis, marker tracking and pupil tracking give similar results (figure 2 A,B). Even though one or more markers can be directly in front of the pupil, it is unlikely that this affected acuity or OKR performance. In an earlier paper [27] we demonstrated that OKR gains decrease as stimuli becomes harder to see and that a 40% reduction in pupil size did not have a significant effect on visual acuity and optokinetic performance. If visual acuity was affected by markers in front of the pupil,

OKR gains recorded using marker tracking would be lower than OKR gains recorded with pupil tracking.

The use of video-oculography to track eye movements abolishes the need to use implanted search coils [26] which can affect eye movements in several ways. Physically they obstruct free eye rotation, a problem that becomes more apparent in smaller animals [24] but that has also consequences for human eye movements [33, 34].

In this paper we used temporary markers that disappear after 4 to 12 hours. Permanent markers would be more desirable. Keratography, the technique of tattooing the cornea, is successfully used for patients where the iris was damaged or the eye discolored. A plastic surgeon can tattoo a new, artificial iris and pupil on the cornea that looks remarkably real [35]. We tried tattooing markers on the cornea but all of those attempts failed because the mouse cornea is very thin (0.1mm), very tough and very flexible. In order to successfully tattoo a marker on the cornea the pigment needs to be injected in the stroma, the middle layer of the cornea that consists of connective tissue. Tattooing markers should be no problem in species with large eyes like rabbits, cats and primates.

Appendix

The rotation matrix $\boldsymbol{R}_{eye}$ describing the unique eye orientation relative to the reference position of the eye expressed in head-fixed coordinates can be decomposed into a sequence of two passive rotations, a torsional rotation about the z-axis followed by a rotation about an axis in the horizontal/vertical plane:

$$\boldsymbol{R}_{eye} = \boldsymbol{R}_2(\varphi) \cdot \boldsymbol{R}_1(\psi)$$

The horizontal/vertical rotation matrix $\boldsymbol{R}_2(\varphi)$ describes the direction of the circumcenter of the marker array (Figure 2A, black arrow) relative to the direction of the circumcenter when the eye is in reference position (Figure S1A, gray arrow). $\boldsymbol{R}_2(\varphi)$ is similar to the rotation matrix calculated with pupil tracking techniques. The torsional rotation matrix $\boldsymbol{R}_1(\psi)$ additionally describes rotation about the axis pointing towards the circumcenter (Figure S1B). Both matrices can be deduced from the marker positions.

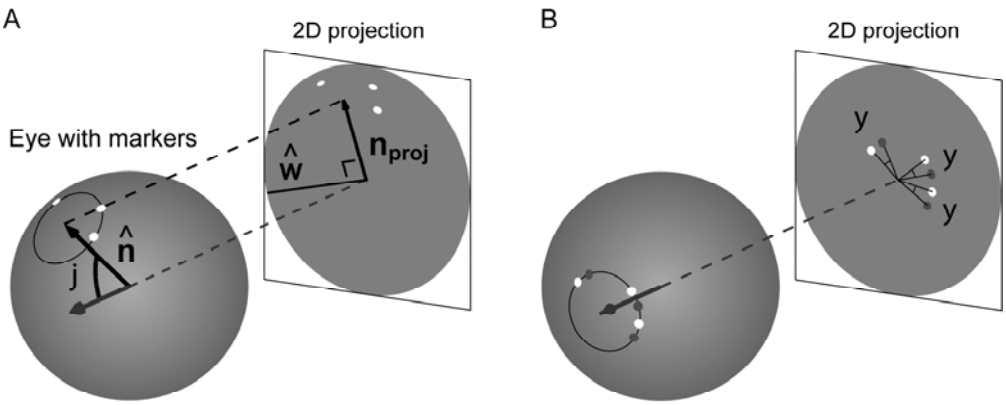

Supplementary Figure 1.A: *Schematic diagram illustrating the calculation of the horizontal/vertical rotation matrix* $\boldsymbol{R}_2(\varphi)$. *White dots indicate the marker array. Rotation axis* $\hat{\boldsymbol{\omega}}$ *and angle* φ *can be deduced from the projected unit normal vector* $\boldsymbol{n}_{proj}$ *of the marker array.* **B:** *Calculation of the torsional rotation matrix* $\boldsymbol{R}_1(\psi)$. *Using* $\boldsymbol{R}_2(\varphi)$ *to align normal vector of the marker array with the z-axis, the torsion angle* ψ *is the angle between any marker in the actual position (white) and the same marker in reference position (gray) relative to the center of rotation.*

The first step consists of finding the matrix M containing the 3D coordinates of the marker array:

$$\boldsymbol{M} = [\widehat{\boldsymbol{m}}_{\boldsymbol{1}}\ \widehat{\boldsymbol{m}}_{\boldsymbol{2}}\ \widehat{\boldsymbol{m}}_{\boldsymbol{3}}] = \begin{bmatrix} m_{1x} & m_{2x} & m_{3x} \\ m_{1y} & m_{2y} & m_{3y} \\ m_{1z} & m_{2z} & m_{3z} \end{bmatrix}$$

The x- and y-coordinate (m_x and m_y) of each marker on the unit sphere is determined by subtraction of the projected center of rotation and division by the radius of rotation. The z-coordinate can then straightforwardly be found using Pythagoras' rule:

$$m_z = \sqrt{1 - m_x^2 - m_y^2}$$

Once the 3D coordinates of the markers are known, the surface normal vector $\widehat{\boldsymbol{n}}$ of the marker array pointing towards its circumcenter can be found by calculating the cross-product of two sides of the triangle:

$$\widehat{\boldsymbol{n}} = \begin{bmatrix} n_x \\ n_y \\ n_z \end{bmatrix} = \boldsymbol{k} \cdot sign(k_z) \cdot |\boldsymbol{k}|^{-1} \qquad \text{where} \qquad \boldsymbol{k} = (\widehat{\boldsymbol{m}}_{\boldsymbol{2}} - \widehat{\boldsymbol{m}}_{\boldsymbol{1}}) \times (\widehat{\boldsymbol{m}}_{\boldsymbol{3}} - \widehat{\boldsymbol{m}}_{\boldsymbol{1}}).$$

The axis $\widehat{\boldsymbol{\omega}}$ (Figure S1A, black dotted line) of the horizontal/vertical rotation $\boldsymbol{R}_2(\varphi)$ is perpendicular to the projection of $\widehat{\boldsymbol{n}}$ onto the camera image ($\boldsymbol{n}_{proj}$):

$$\widehat{\omega} = \begin{bmatrix} \omega_x \\ \omega_y \\ \omega_z \end{bmatrix} = \begin{bmatrix} -n_y \\ n_x \\ 0 \end{bmatrix} \left|n_{proj}\right|^{-1} \qquad \text{where} \qquad \boldsymbol{n}_{proj} = \begin{bmatrix} n_x \\ n_y \\ 0 \end{bmatrix}.$$

The angle of rotation φ can be calculated from the magnitude of $\boldsymbol{n}_{proj}$:

$$\varphi = \sin^{-1}\left|\boldsymbol{n}_{proj}\right|.$$

The rotation matrix $\boldsymbol{R}_2(\varphi)$ can then be found using Rodrigues' rotation formula[36]:

$$\boldsymbol{R}_2(\varphi) = \begin{bmatrix} \omega_x^2(1-n_z)+n_z & \omega_x\omega_y(1-n_z) & n_x \\ \omega_x\omega_y(1-n_z) & \omega_y^2(1-n_z)+n_z & n_y \\ -n_x & -n_y & n_z \end{bmatrix}.$$

To find the torsional rotation matrix $\boldsymbol{R}_1(\psi)$ the marker array M was first rotated back over axis $\hat{\boldsymbol{\omega}}$ using the transpose of the previously found matrix $\boldsymbol{R}_2(\varphi)$, so that $\hat{\boldsymbol{n}}$ was now aligned with the z-axis (Figure S1B, gray arrow):

$$\boldsymbol{M'} = \boldsymbol{R}_2^{\boldsymbol{T}}(\varphi) \cdot \boldsymbol{M}$$

In this position, the difference in orientation of the marker array relative to an arbitrary reference position (with the same alignment of $\hat{\boldsymbol{n}}$ with the z-axis) gives the torsion angle ψ, which in turn is used to create $\boldsymbol{R}_1(\psi)$:

$$\boldsymbol{R}_1(\psi) = \begin{bmatrix} \cos\psi & -\sin\psi & 0 \\ \sin\psi & \cos\psi & 0 \\ 0 & 0 & 1 \end{bmatrix} \text{ where } \qquad \psi = \cos^{-1}\left(\frac{\boldsymbol{m'}\cdot\boldsymbol{m'}_{ref}}{|\boldsymbol{m'}||\boldsymbol{m'}_{ref}|}\right).$$

To determine the instantaneous angular eye velocity, the rotation matrix yielding the rotation from the previously sampled eye orientation to the next eye orientation was computed. The resulting rotation matrix was in turn converted into axis-angle format [37] and multiplied by half the sampling frequency. Because the eye velocity was computed relative to the camera, which in turn was positioned at 70° azimuth from straight ahead, a final multiplication with matrix $\boldsymbol{R}_3(\theta)$ was necessary to align the coordinate system with the stimulus (roll, pitch, yaw). This consisted of swapping the y- and z-components, rotation of the x- and y-components about the z-axis by angle θ = -20° and an inversion of the x-axis, which makes the coordinate system right-handed:

$$\boldsymbol{R}_3(\theta) = \begin{bmatrix} -\cos\theta & -\sin\theta & 0 \\ 0 & 0 & 1 \\ -\sin\theta & \cos\theta & 0 \end{bmatrix}$$

References

1. de Zeeuw CI, van Alphen AM, Koekkoek SK, et al. Recording eye movements in mice: a new approach to investigate the molecular basis of cerebellar control of motor learning and motor timing. *Otolaryngol Head Neck Surg* 1998;119:193-203.
2. Picciotto MR, Wickman K. Using knockout and transgenic mice to study neurophysiology and behavior. *Physiol Rev* 1998;78:1131-1163.
3. Stahl JS. Using eye movements to assess brain function in mice. *Vision Res* 2004;44:3401-3410.
4. Faulstich M, van Alphen AM, Luo C, du Lac S, De Zeeuw CI. Oculomotor plasticity during vestibular compensation does not depend on cerebellar LTD. *J Neurophysiol* 2006;96:1187-1195.
5. Katoh A, Yoshida T, Himeshima Y, Mishina M, T H. Defective control and adaptation of reflex eye movements in mutant mice deficient in either the glutamate receptor delta2 subunit or Purkinje cells. *Eur J Neurosci* 2005;21:1315-1326.
6. Kimpo RR, Boyden ES, Katoh A, Ke MC, Raymond JL. Distinct patterns of stimulus generalization of increases and decreases in VOR gain. *J Neurophysiol* 2005;94:3092-3100.
7. van Alphen AM, Stahl JS, De Zeeuw CI. The dynamic characteristics of the mouse horizontal vestibulo-ocular and optokinetic response. *Brain Res* 2001;890:296-305.
8. Baarsma E, Collewijn H. Vestibulo-ocular and optokinetic reactions to rotation and their interaction in the rabbit. *J Physiol* 1974;238:603-625.
9. Simpson JI, Leonard CS, Soodak RE. The accessory optic system. Analyzer of self-motion. *Ann N Y Acad Sci* 1988;545:170-179.
10. Soodak RE, Simpson JI. The accessory optic system of rabbit. I. Basic visual response properties. *J Neurophysiol* 1988;60:2037-2054.
11. Leonard CS, Simpson JI, Graf W. Spatial organization of visual messages of the rabbit's cerebellar flocculus. I. Typology of inferior olive neurons of the dorsal cap of Kooy. *J Neurophysiol* 1988;60:2073-2090.
12. Lisberger SG, Fuchs AF. Role of primate flocculus during rapid behavioral modification of vestibuloocular reflex. II. Mossy fiber firing patterns during horizontal head rotation and eye movement. *J Neurophysiol* 1978;41:764-777.

13. Groenewegen HJ, Voogd J. Olivocerebellar climbing fiber projections in the cat. An autoradiographic and degeneration study [proceedings]. *Acta Morphol Neerl Scand* 1976;14:247-249.
14. De Zeeuw CI, Gerrits NM, Voogd J, Leonard CS, Simpson JI. The rostral dorsal cap and ventrolateral outgrowth of the rabbit inferior olive receive a GABAergic input from dorsal group Y and the ventral dentate nucleus. *J Comp Neurol* 1994;341:420-432.
15. Tan J, Epema AH, Voogd J. Zonal organization of the flocculovestibular nucleus projection in the rabbit: a combined axonal tracing and acetylcholinesterase histochemical study. *J Comp Neurol* 1995;356:51-71.
16. Van der Steen J, Simpson JI, Tan J. Functional and anatomic organization of three-dimensional eye movements in rabbit cerebellar flocculus. *J Neurophysiol* 1994;72:31-46.
17. Ruigrok TJ, Osse RJ, Voogd J. Organization of inferior olivary projections to the flocculus and ventral paraflocculus of the rat cerebellum. *J Comp Neurol* 1992;316:129-150.
18. Sugihara I, Ebata S, Shinoda Y. Functional compartmentalization in the flocculus and the ventral dentate and dorsal group y nuclei: an analysis of single olivocerebellar axonal morphology. *J Comp Neurol* 2004;470:113-133.
19. Schonewille M, Luo C, Ruigrok TJ, et al. Zonal organization of the mouse flocculus: physiology, input, and output. *J Comp Neurol* 2006;497:670-682.
20. Crawford JD, Martinez-Trujillo JC, Klier EM. Neural control of three-dimensional eye and head movements. *Curr Opin Neurobiol* 2003;13:655-662.
21. Collewijn H. The optokinetic system of the rabbit. *Doc Ophthalmol* 1971;30:205-226.
22. Sandor PS, Frens MA, Henn V. Chameleon eye position obeys Listing's law. *Vision Res* 2001;41:2245-2251.
23. Migliaccio AA, Macdougall HG, Minor LB, Della Santina CC. Inexpensive system for real-time 3-dimensional video-oculography using a fluorescent marker array. *J Neurosci Methods* 2005;143:141-150.
24. Stahl JS, van Alphen AM, De Zeeuw CI. A comparison of video and magnetic search coil recordings of mouse eye movements. *J Neurosci Methods* 2000;99:101-110.

25. Collewijn H. Optokinetic eye movements in the rabbit: input-output relations. *Vision Res* 1969;9:117-132.
26. Robinson DA. A Method of Measuring Eye Movement Using a Scleral Search Coil in a Magnetic Field. *IEEE Trans Biomed Eng* 1963;10:137-145.
27. van Alphen B, Winkelman BH, Frens MA. Age- and sex-related differences in contrast sensitivity in C57BL/6 mice. *Invest Ophthalmol Vis Sci* 2009;50:2451-2458.
28. Iwashita M, Kanai R, Funabiki K, Matsuda K, Hirano T. Dynamic properties, interactions and adaptive modifications of vestibulo-ocular reflex and optokinetic response in mice. *Neurosci Res* 2001;39:299-311.
29. Katoh A, Kitazawa H, Itohara S, Nagao S. Dynamic characteristics and adaptability of mouse vestibulo-ocular and optokinetic response eye movements and the role of the flocculo-olivary system revealed by chemical lesions. *Proc Natl Acad Sci U S A* 1998;95:7705-7710.
30. Nagao S. Effects of vestibulocerebellar lesions upon dynamic characteristics and adaptation of vestibulo-ocular and optokinetic responses in pigmented rabbits. *Exp Brain Res* 1983;53:36-46.
31. Godaux E, Gobert C, Halleux J. Vestibuloocular reflex, optokinetic response, and their interactions in the alert cat. *Exp Neurol* 1983;80:42-54.
32. Kingma H, Stegeman P, Vogels R. Ocular torsion induced by static and dynamic visual stimulation and static whole body roll. *Eur Arch Otorhinolaryngol* 1997;254 Suppl 1:S61-63.
33. Smeets JB, Hooge IT. Nature of variability in saccades. *J Neurophysiol* 2003;90:12-20.
34. van der Geest JN, Frens MA. Recording eye movements with video-oculography and scleral search coils: a direct comparison of two methods. *J Neurosci Methods* 2002;114:185-195.
35. Schaller UC, van der Velden EM, Drost BH, Weede S, Klauss V. [Keratography (corneal tattooing) in corneal leukoma]. *Ophthalmologe* 2001;98:147-150.
36. Rodrigues B. Mémoire sur l'attraction des sphéröıdes. *Correspondance sur l'École Impériale Polytechnique* 1816;3:361–385.
37. van Opstal A. Representation of eye position in three dimensions. In: Berthoz A (ed), *Multisensory control of movement.* Oxford: Oxford University Press; 1993:27-41.

Chapter 6

General Discussion

This thesis describes how three dimensional eye movements can be recorded using video oculography (Chapters 2-4) and how 3-D optokinetic eye movements in mice can be described using this method (Chapter 5). We find that the OKR in mice works equally well for all stimulus orientations. The OKR can also be used as a sensitive probe to study contrast sensitivity in mice by measuring how the gain of the optokinetic reflex (OKR) varies when properties of the visual stimulus (contrast and spatial frequency) are altered. Using this approach, we observed differences in contrast sensitivity between male and female C57BL/6J mice, as well as between four months old and nine months old C57BL/6J mice (Chapter 2). Additionally, we used this method to in a longitudinal study, where we measured how the contrast sensitivity function of mutant mice with impaired DNA repair mechanisms decreased over time (Chapter 3). These mice age very quickly, their vision deteriorates from normal to being almost blind within four months. In chapter 4 we describe how contrast sensitivity can be measured in man, using the ocular following response that is elicited by moving Gabor patches. Finally, in chapter 5 we describe how three dimensional eye movements in mice can be measured by tracking artificial markers using video-oculography.

Contrast sensitivity

The contrast sensitivity function can be inferred by measuring how the gain of the OKR varies with different contrasts and spatial frequencies. With this approach, we observed differences in contrast sensitivity between male and female C57BL/6J mice and between younger and older adult C57BL/6J mice. As expected, the effects of spatial frequency and contrast on OKR were highly significant in all experiments. Like other optomotor responses, the OKR becomes less vigorous as stimuli become more difficult to perceive (Collewijn, 1972). Unlike other optomotor responses, however, the magnitude of the OKR can be easily quantified with eye tracking. Such methods are well established (Stahl, 2000) making the OKR a sensitive tool for probing visual capabilities without the need for an observer to decide whether an animal responds.

Previous studies used optomotor responses that are not quantifiable. Only the occurrence of a response was scored, which results in low resolution data that consists of a threshold that divides the visible and invisible world. Exceptions are Cahill and Nathans (2008) who counted resetting saccades and Schmucker et al (2005) who quantified body turns. Neither method is very accurate though. Schmuckers approach showed large error margins and Cahill and Nathans' approach actually measures eye position but then only counts nystagmus eye movements, instead of measuring eye velocity.

The method to record contrast sensitivity that is described in this thesis differs from the other methods (See table 1 in chapter 1). Instead of using a stair case procedure to determine a percpetual threshold we determine contrast sensitivity by using a fixed set of stimuli, consisting of 42 combinations of spatial frequency and contrast and measuring with what magnitude a mouse responds to them. By interpolating between these 42 responses we can estimate contrast sensitivity over a full spectrum of contrast-spatial frequency combinations.

The contrast sensitivity functions described in this thesis look like inverted V's, with the peak of the V at 0.17 cycles/degree (cpd) at all groups that were studied. There is only a small area in which the response is optimal, i.e. where eye velocity equals stimulus velocity. This area is represented by the dark red colors in figure 3-6 in chapter X and falls between 0.17 and 0.25 cpd and 75-100% contrast. Outside that area, OKR gains decrease rapidly. In chapter X we did not record maximal acuities. These however, were estimated by extrapolating the data to gains of zero, which resulted in a maximal acuity of 0.49-0.52 cpd for all groups, which is very similar to results found by other studies (see chapter 1, table 1).

Because the use of compensatory eye movements to infer contrast sensitivity has an excellent signal to noise ratio, we find a significant optokinetic response at the lowest contrast (1%) in all animals. This is much lower than the threshold of 4-5% contrast that was reported in both maze tests and optomotor tests (see chapter 1, table 1). However, Cahill and Nathans still found strong nystagmus response in C57BL/6J mice at 4% contrast, which was the lowest value tested. This supports our claim that the actual contrast

threshold is well below 4%. This lower threshold almost closes the contrast detection gap between mice and men. Humans are able to see up to about 0.5% contrast (van Nes, 1967) and up to 60 cpd (Campbell, 1965). They have a much better visual acuity than mice (0.5 cpd). So the acuity of man is more than 100 times better than that of mice, while the lowest detectable contrast varies only a factor 2.

The strength of this method lies in the ability to study sub-threshold behavior. We described response magnitudes over a large range of stimuli and found that these response magnitudes were only optimal in a small area in stimulus space. Outside that area, response magnitudes decrease until they become undistinguishable from 'noise', i.e. the way the mouse eye moves when there is no moving visual stimulus. By extrapolating our data in chapter 2, we inferred that the maximal perceivable spatial frequency is ~0.5 cpd.

There are several benefits to the approach described in chapter 2:

By restraining the mouse, the distance from the mouse eye to the stimulus is known exactly, and the stimulus can thus be defined with very high precision. Most studies so far looked at choice behavior in a two armed maze or full body turns in response to a rotating stimulus. In both cases, the animal moves constantly and its distance from the stimulus changes as well. This means that some stimulus properties change with the movement of the mouse. For example, spatial frequencies will decrease as a mouse approaches a sine grating, making the 'bars' appear to be wider. When that happens, an experimenter cannot know what the exact stimulus properties were when the mouse responded.

Experimenter bias can influence experiments where an observer has to watch an animal and decide whether or not it responds to a stimulus (Douglas et al, 2005). This bias can be excluded by measuring eye movement gains in response to a fixed set of stimuli and analyzing the data after the experiment in conditions where the experimenters are masked to the experimental conditions (i.e., randomizing trials, assigning numbers to mice and using automated scripts).

Recording response magnitudes instead of response occurrences adds an extra dimension to the data: i.e. one can not only see whether a mouse responds to a stimulus but also measure how large that response is. This adds a whole new dimension to the data, describing not only where the perceptual thresholds are but also showing sub-threshold data. And that is where things get interesting, as is shown in chapter 2. If these groups were compared with conventional methods, a threshold would be found that runs along the edge of the light blue and the dark blue zones. These thresholds look very much alike and the maximal acuity of all groups would be ~ 0.5 cpd. The big difference between these groups is found in the sub-threshold data.

Sex dependent contrast sensitivity

Female C57BL/6J mice showed consistently lower gains than male mice in almost all stimulus conditions except for a few spatial frequencies at maximum or minimum contrast. Because the OKR was similar for males and females under optimal conditions (0.17– 0.25 cpd, 100% contrast; chapter 2, Fig. 3C), gain differences could not be explained by differences in the oculomotor system. This result suggests that female mice have lower contrast sensitivity than male mice. The sex-related difference in CSF cannot be readily explained. It is unlikely that it is caused by hormonal differences because Andreescu et al (2007) showed that estradiol does not influence motor performance (VOR, OKR, VVOR). However, it does influence motor learning. Jellai et al (2005) measured head turns evoked by moving bar stimuli and found that male C57BL/6J mice make significantly more head turns than female C57BL/6J mice. This difference did not occur in mice from the 129/SvPas strain or in the wildtype controls used in chapter 3, which consist of a mixed C57Bl6J and FVB backgrounds, suggesting that this sex dependent difference is a trait of the inbred C57BL/6J strain. This sex-related difference strongly argues for a proper matching of animals on sex in any test involving vision, such as oculomotor tests and water maze tests. Differences in contrast sensitivity are likely to have an impact of the outcome of these tests. If not controlled for differences in visual function, these outcomes can be misinterpreted as related to, for instance, learning or motor processes.

Age dependent contrast sensitivity

Likewise, the differences in contrast sensitivity between four and nine months old C57BL/6J mice could not have been found with any of the conventional techniques (with a possible exception for Cahill and Nathans (2008)). The contrast sensitivity function is lower for nine months old C57BL/6J males than for four month old C57BL/6J males in most stimulus conditions while their maximum response is unaffected (Chapter 2, Fig 4C). Even at a five months age difference, there are already large changes in the contrast sensitivity function. The visual acuity threshold of C57BL/6J mice also decreases as they age. In 6 months old C57BL/6J mice the acuity has been reported to be 0.48 cpd and to decrease to 0.38 cpd in 12 months old C57BL/6J mice (Wong and Brown, 2007). We show that at nine months of age, visual acuity is similar to that at four months (~0.5 cpd). Here we show that the effect of age on vision is not limited to a decrease in acuity and that contrast sensitivity decreases dramatically in five months time. Rod and cone numbers and densities do not decrease as mice age (Trachimowicz et al, 1981; Li et al, 2001; Williams and Jacobs, 2007) 31-33. However, maximal voltages (Vmax) of cone-based electroretinograms (ERG) show a substantial age-related decline. The ERG Vmax of 800 days old mice is about half of the ERG Vmax of 100 days old mice (Li et al, 2001; Williams and Jacobs, 2007). So, as mice age, the responsivity of their photoreceptors decreases. Both four and nine months old mice are considered to be adults; they aren't very young or old yet their contrast sensitivity is very different. In behavioral tests that require vision, it is essential to use groups matched for age. Otherwise, differences in visual capabilities can influence the test and be misinterpreted as learning- or motor-problems.

Caveats

Using compensatory eye movements to quantify contrast sensitivity has some drawbacks. It is not suitable to use for very young (< 3 weeks) animals because they are too small and fragile to be fitted with a pedestal. Also, a mouse needs at least several days to recover from the surgery. Also, when studying valuable mutants that have to undergo many different tests where a pedestal would influence those tests (for example, swimming through a

water maze) it is better not use the approach outlined in this thesis. In those cases optomotor tests with freely moving animal are better suited.

The neuronal circuits involved in the OKR must not be damaged or dysfunctional, which is not unlikely when studying cerebellar mutants, because then it becomes hard to distinguish between motor control defects and visual defects. This may be the case if even the highest response of mutant mice in a contrast sensitivity diagram is significantly lower than that of its wild type littermates.

There are two ways to work around this: OKR gains can be normalized, where the highest gain becomes 1 in both mutant and wild type group. However, this may distort the data and make it harder to draw conclusions. Another option is to discard response magnitudes as unreliable and only look whether a response occurred or not. In that case one has to decide on an arbitrary threshold to determine which stimuli evoke a response. In most 2AFC paradigms, the threshold of detection is set at those stimuli where the accuracy of animals to distinguish the stimulus falls below 70% (Prusky et al 2000, 2004; Gianfranchesci et al 1999; Wong and Brown, 2006; Umino et al 2008).

Practical applications

When studying how mutations in the brain of a mouse affect its behavior, there always is a possibility that the mutation has more than one effect. When behavioral tests depend on vision, like the water maze or oculomotor tests, it is important to screen for visual defects to rule out that vision plays a role in those tests, as we did for the L7 PKCi mutant (chapter 2). Because the contrast sensitivity tests described in this thesis only take a bit over an hour (surgery + experiment) they should be used on every mutant that will participate in OKR/VOR recordings because those mice will already be outfitted with a pedestal and won't suffer much additional discomfort from this procedure. When testing mice participating in tests where a pedestal is not required, it would be better to use less invasive tests (like regular optomotor responses; cf Prusky et al (2004)) to quickly screen mice for major visual defects.

In chapter 2 we demonstrate that contrast sensitivity decreases with age and in chapter 3 we demonstrate how contrast sensitivity measures can be used to quantify deterioration of the visual system in Ercc d/- mutants, where the NER DNA repair pathway is not functional. At six weeks of age, there is no difference between wild type and mutants as both show identical contrast sensitivity functions and gaze stabilization reflexes. However, within eight weeks both contrast sensitivity and gaze stabilization reflexes deteriorate rapidly.

This approach is more reliable than measuring photoreceptor degeneration because vision in mice is not limited by the number of photoreceptors but by the amount of retinal ganglion cells, on which approximately ten photoreceptors converge. Also, the sensitivity of the test make it very well suited for longitudinal studies of aging, retinal degeneration or impairments if the visual system because mice don't have to be sacrificed, so the effect of a treatment or intervention on a single mouse can be measured at different points in time.

There are links between dietary restriction and aging, which show that lifespan can be extended by suppressing the insulin/insulin growth factor signalling pathway, either by genetically manipulating this system or by caloric restriction. This has been demonstrated in *C. elegans* (Johnson, 1990), *Drosophila melanogaster* (Partridge et al, 2005) and mammals (Guarente and Kenyon, 2000). In order to test the effect of dietary restriction of mice with damaged DNA repair pathways, one needs a reliable way to measure the damage inflicted. This damage has to be progressive with age and highly reproducible among afflicted individuals.

Human contrast sensitivity

Measuring contrast sensitivity in man has a long history, as outlined in chapter 4, as the contrast sensitivity describes the quality of visual function in much more detail than Snellen acuity. In chapter 4 we presented pilot data that use the gain of the compensatory eye movements to measure if a grating stimulus was detected. As reported in other studies, gain decreased with increasing spatial frequency (Joshi et al, 2009; Joshi et al, 2010).

Maximum gains were much lower than those reported by Joshi et al (2009, 2010), which were 0.7 in control subjects. However, gains in those studies dropped off quickly to about 0.1 at a spatial frequency of 2.5 cycles/degree. In our study, subjects with good vision still have good gains at high contrast gratings of 7.48 cycles/degree. Future studies should reveal how gains change at higher spatial frequencies.

Contrast sensitivity in man has several important clinical applications. Because a CSF test gives much more information about visual function that a regular Snellen acuity test (see Chapter 4), a fast and accurate test to measure contrast sensitivity is required. Using the gain of the ocular following response is an objective behavioural measure that is independent of patient interpretation. It is also very suited for fully automated experiments, where a large set of combinations of spatial frequency and contrast can be presented in a short time. There are two different approaches to describe visual function in a fast and accurate way. One method is outlined in this thesis (chapters 2-4) where a fixed set of contrast-spatial frequency combinations is presented, and scores between data points are interpolated. This approach gives a quick and rough overview of the whole range of vision that can be used to measure how one's visual function changes with age of medical complications.

An alternate approach uses an adaptive staircase procedure (Klein, 2001) to determine the threshold of the visual function by searching for those combinations of contrast and spatial frequency where the gain of the OFR equals zero. In this approach, a subject starts with an initial estimate of his visual contrast sensitivity function, for example by drawing a line similar to the one in Figure 4 in chapter 1. As gains decrease when grating stimuli become harder to see (c.f. Figure 2, chapter 2), upper and lower limits of vision can be determined by changing stimulus spatial frequencies at maximal contrast, looking for those high and low frequencies that are just able to elicit a response. Then at several intermediate spatial frequencies, contrast can be gradually modulated around the initial threshold until gains are no longer measurable. This approach is useful when subtle changes in contrast sensitivity have to be studied.

Recent developments in eye tracking hardware make this approach more feasible and user friendly, as modern eye trackers like the Tobii Ey Tracker (Tobii Technology, Stockholm, Sweden) no longer require subjects to be head fixed.

Perspectives

In summary, this thesis outlined several approaches to study vision and eye movements, both in mice and men, that are useful when studying patients of mouse models where vision is affected as a result of disease, mutations, aging, retinal degeneration or neurological impairment of the visual system. Also, these approaches will be valuable when evaluating treatments that aim to improve or restore visual function in low vision patients. Likewise, the method outlined in chapter 5 will be useful to study eye movements generated by three dimensional vestibular stimulation, and will provide more insight in how the brain integrates visual and vestibular information to generate accurate three dimensional compensatory eye movements

References

Andreescu, C. E., B. A. Milojkovic, et al. (2007). "Estradiol improves cerebellar memory formation by activating estrogen receptor beta." J Neurosci 27(40): 10832-10839.

Cahill, H. and J. Nathans (2008). "The optokinetic reflex as a tool for quantitative analyses of nervous system function in mice: application to genetic and drug-induced variation." PLoS One 3(4): e2055.

Campbell, F. W. and D. G. Green (1965). "Optical and retinal factors affecting visual resolution." J Physiol 181(3): 576-593.

Collewijn, H. (1972). "Latency and gain of the rabbit's optokinetic reactions to small movements." Brain Res 36(1): 59-70.

Douglas, R. M., N. M. Alam, et al. (2005). "Independent visual threshold measurements in the two eyes of freely moving rats and mice using a virtual-reality optokinetic system." Vis Neurosci 22(5): 677-684.

Gianfranceschi, L., A. Fiorentini, et al. (1999). "Behavioural visual acuity of wild type and bcl2 transgenic mouse." Vision Res 39(3): 569-574.

Guarente, L. and C. Kenyon (2000). "Genetic pathways that regulate ageing in model organisms." Nature 408(6809): 255-262.

Jellali, A., M. Hamid, et al. (2005). "The optomotor response: a robust first-line visual screening method for mice." Vision Res 45(11): 1439-1446.

Johnson, T. E. (1990). "Increased life-span of age-1 mutants in Caenorhabditis elegans and lower Gompertz rate of aging." Science 249(4971): 908-912.

Joshi, A. C., D. E. Riley, et al. (2010). "Selective defects of visual tracking in progressive supranuclear palsy (PSP): implications for mechanisms of motion vision." Vision Res 50(8): 761-771.

Joshi, A. C., M. J. Thurtell, et al. (2009). "Effect of vergence on human ocular following response (OFR)." J Neurophysiol 102(1): 513-522.

Klein, S. A. (2001). "Measuring, estimating, and understanding the psychometric function: a commentary." Percept Psychophys 63(8): 1421-1455.

Li, C., M. Cheng, et al. (2001). "Age-related changes in the mouse outer retina." Optom Vis Sci 78(6): 425-430.

Partridge, L., M. D. Piper, et al. (2005). "Dietary restriction in Drosophila." Mech Ageing Dev 126(9): 938-950.

Prusky, G. T., R. M. Douglas, et al. (2004). "Visual memory task for rats reveals an essential role for hippocampus and perirhinal cortex." Proc Natl Acad Sci U S A 101(14): 5064-5068.
Prusky, G. T., P. W. West, et al. (2000). "Behavioral assessment of visual acuity in mice and rats." Vision Res 40(16): 2201-2209.
Schmucker, C., M. Seeliger, et al. (2005). "Grating acuity at different luminances in wild-type mice and in mice lacking rod or cone function." Invest Ophthalmol Vis Sci 46(1): 398-407.
Trachimowicz, R. A., L. J. Fisher, et al. (1981). "Preservation of retinal structure in aged pigmented mice." Neurobiol Aging 2(2): 133-141.
Umino, Y., E. Solessio, et al. (2008). "Speed, spatial, and temporal tuning of rod and cone vision in mouse." J Neurosci 28(1): 189-198.
van Nes, F. L., J. J. Koenderink, et al. (1967). "Spatiotemporal modulation transfer in the human eye." J Opt Soc Am 57(9): 1082-1088.
Williams, G. A. and G. H. Jacobs (2007). "Cone-based vision in the aging mouse." Vision Res 47(15): 2037-2046.
Wong, A. A. and R. E. Brown (2006). "Visual detection, pattern discrimination and visual acuity in 14 strains of mice." Genes Brain Behav 5(5): 389-403.
Wong, A. A. and R. E. Brown (2007). "Age-related changes in visual acuity, learning and memory in C57BL/6J and DBA/2J mice." Neurobiol Aging 28(10): 1577-1593.

Appendix A: How to use eye tracking to measure contrast sensitivity in mice

Abstract

Mice are a central research subject in neuroscience, especially due to the availability of mutants. Many tests have been developed to quantify the way a mutation affects brain function and behavior. Vision plays an important role in many tests. Should a mouse with a low visual acuity participate, its sub-optimal behavior can be misinterpreted as a learning- or motor-problem. Until recently a good quantitative test for vision in mice was lacking.

We use eye tracking in head-fixed mice to record how the gain of the optokinetic reflex (OKR, a gaze stabilization reflex) decreases as moving sine grating stimuli become harder to see [1]. We can objectively estimate the visual performance of the mouse as a function of spatial frequency and stimulus contrast. This two-hour procedure is useful in characterizing animal models where vision is affected as a result of mutations, aging, retinal degeneration or neurological impairment of the visual system.

Introduction

The contrast sensitivity function (CSF) shows which contrasts can be seen at a range of spatial frequencies (the number of sine gratings in one degree of visual angle). Behavioral tests like maze tests and optomotor tests are most commonly used to test the CSF of mice. In maze tests, a mouse is trained to distinguish sine gratings from a uniform gray field to obtain a food reward [2] or find a submerged platform in a two armed water maze [3-5]. In optomotor tests a mouse is surrounded by a panoramic sine grating. As the stimulus rotates about the animal, it evokes an optomotor response (optokinetic nystagmus [6] or full body rotations [7-10]) when the mouse distinguishes the stimulus pattern from a homogeneous background.

However, there are drawbacks to both methods. In maze tests, the animal moves freely through a maze and the distance from animal to stimulus

varies in this test, making it hard or even impossible to define the perceived spatial frequency exactly.

The optomotor response scales with how well the stimulus is perceived; becoming less vigorous as stimuli are harder to perceive [7]. This makes it hard for observers to see which stimuli evoke responses close to threshold. The behavior in both types of tests is not quantified; the experimenter observes the animal and tries to judge which stimuli evoke a response. Also, the measurements are dichotome. When an animal responds, by choosing the correct arm in a maze or by rotating along with the stimulus, it is inferred that the animal sees the stimulus.

Mice are not considered to be 'visual animals'. The mouse eye is relatively simple, with photoreceptors distributed evenly over their retina; they have no fovea [11]. This means that mice don't look around but only move their eyes reflexively to compensate for large disturbances in the visual field. Part of this gaze stabilization is evoked by the movement of the visual image over the retina, resulting in the so-called optokinetic reflex (OKR), a slow reflexive eye movement that follows the moving image, thus reducing retinal slip. The gain of the OKR (i.e. the ration between eye and stimulus velocity) depends on the stimulus velocity (optimally < 10deg/s), and on the viability of the stimulus [12-15].

Using eye tracking to measure how the gain of the OKR decreases as stimuli become harder to perceive (chapter 2, figure 2) is a powerful tool to study contrast sensitivity and more sensitive than the methods currently available. Behavior in response to visual stimuli is no longer recorded as an all-or-nothing response but quantified as a graded response. A drawback of this method is that it is not suitable to use for very young (< 3 weeks) animals, or for valuable mutants, since a head fixation has to be implanted operatively. In those cases optomotor tests with freely moving animal are better suited. Additionally, this new and sensitive method is useful in characterizing animal models where vision is affected as a result of mutations, aging, retinal degeneration or neurological impairment of the visual system.

Materials

Equipment

- Restrainer: The animal is placed in a plastic tube and its head is attached to a metal bar that runs over the tube. The tube is attached to a set of linear stages (Newport, Orlando, Fl, USA) that allow for translations in three dimensions as well as rotation about the naso-occipital axis
- Anesthesia setup
- Eye tracking system: we use an Iscan ETL-200 (Iscan Inc, Woburn, MA, USA)
- Stimulus setup: We use a projection system built from a modified Electrohome Marquee 9000 CRT projector (Christie Digital Systems, Cypress CA, USA).
- Scalpel blade (no. 10, curved)
- Betadine antiseptic solution (10% povidone-iodine)
- M4 nuts and screws
- Translux Energy: Tungsten-halogen curing unit (Heraues Kulzer GmbH, Hanau, Germany)

Reagents

- Gel etchant (item no. 31297, KerrHawe S.A., Bioggio, Switzerland)
- Primer (Optibond FL prime, item no. 25881, KerrHawe S.A., Bioggio, Switzerland)
- Adhesive (Optibond FL adhesive, item no. 25882 KerrHawe S.A., Bioggio, Switzerland)
- Charisma (Heraues Kulzer GmbH, Hanau, Germany)
- Isofluoran 1–1.5% (Rhodia Organique Fine Ltd, Bristol, UK)
- Duratears (S.A. Alcon-Couvreur N.V. Puurs, Belgium)

Equipment setup

Optokinetic stimuli were created using a modified Electrohome Marquee 9000 CRT projector (Christie Digital Systems, Cypress CA, USA). The red and blue CRT tubes were replaced by green ones. The three tubes were mounted on the ceiling at a 120° angle from each other. The CRT tubes

projected their images via mirrors onto three transparent anthracite screens (156*125 cm) which were placed in a triangular formation around the recording setup (Fig 3). This created a monochrome panoramic stimulus fully surrounding the animal. The stimuli were programmed in C++ and rendered in openGL. A 360 degrees stimulus consisted of a virtual vertically oriented cylinder with a vertically oriented sine grating on its wall. The spatial resolution of the setup was 1600*1200 pixels per screen, and hence a pixel subtended 4.5 arc minutes. Luminance of the bright (I max) and dark stripes (I min) were measured using a LS-100 luminance meter (Minolta camera co. LTD, Osaka, Japan), after which contrasts were calculated using the Michelson formula:

$$C = \frac{I_{\max} - I_{\min}}{I_{\max} + I_{\min}}$$

Average luminance was 17.5 cd/m^2 in all stimulus conditions. The minimal luminance of the stimulus was 0.05 cd/m^2, the maximum luminance was 35 cd/m^2).

Eye movements were recorded with an infrared video system (Iscan ETL-200).The system resembled the one described by Stahl [11] with some modifications. Images of the eye were captured at 120 Hz with an infrared sensitive CCD camera. From this image, X and Y positions of the center of the pupil and the corneal reflection (1st Purkinje image) were recorded in pixel positions, giving their location on the 512*256 pixel grid, with a resolution of 1/3 pixel horizontally and 1/10 pixel vertically. These positions were low pass filtered with a cut off frequency of 300Hz (Axon Cyberamp 380), sampled at 1 kHz and stored for offline analysis.

Our choice in equipment is in no way critical and allows for a lot of variation, according to available space and budget. There are many ways to generate visual stimuli and record eye movements. A stimulus setup can be built from four monitors [4] and an eye tracker can be built using a consumer grade webcam and a frame grabber card [16].

Reagent setup

For all reagents, follow the instructions of the manufacturer.

Procedure

Prepare a mouse for head restraint by attaching two nuts to the skull

1) Induce anesthesia using with a mixture of Isofluoran (Isofluoran 1–1.5%; Rhodia Organique Fine Ltd, Bristol, UK) and oxygen.
2) Cover the eyes with Duratears
3) Shave the top of the head
4) Swab the head with gauze soaked in Betadine to sterilize and remove any loose hairs from the skin
5) Make a sagittal incision across the scalp, exposing lambda and Bregma
6) Reveal the skull by reflecting the skin
7) CRITICAL: Moisten the periosteum with a cotton swab and scrape it off with a round 10 blade scalpel
8) Dry the skull
9) Etch the skull for 15 seconds, using Kerr etchant gel, a gel containing phosphoric acid
10) Remove the gel completely using water and a wet cotton swab
11) Apply a drop of primer (Optibond Prime, Kerr USA, Orange CA) to the etched part of the skull
12) Dry the primer by softly blowing air over it
13) Apply a layer of adhesive (Kerr USA, Orange CA) and light cure until it forms a hard opaque layer
14) Add a layer of composite and light cure for 1 minute
15) Add a second layer of composite but don't light cure yet
16) Solder two M4 metal nuts together
17) Place two M4 metal nuts that are soldered together on the second layer
18) Light cure for 1 minute
19) Add a ring of composite around the two M4 nuts and light cure for 1 minute
20) Close the incision using a suture

PAUSE POINT: a mouse needs at least 5-7 days to fully recover from the procedure. In an adult animal, the head restraint will stay in place for at least several months.

Place the mouse in the setup

21) Induce anaesthesia using with a mixture of Isofluoran (Isofluoran 1–1.5%; Rhodia Organique Fine Ltd, Bristol, UK) and oxygen.

22) Trim any whiskers that are in front of the eye that is going to be tracked

23) Place the mouse in the restrainer and fixate the head using two M4 screws

24) Use the linear stages on the restrainer to move the mouse until its eye is in front of the camera, above the center of the table

Calibrate

25) Use the calibration method developed by John Stahl [17]: place a reference LED on the camera, aligned with its optical axis. This produces a corneal reflection (CR). By continuously oscillating the camera and moving the mouse along the Y-axis until the CR motion is minimal the center of the corneal curvature is placed at the rotation axis of the camera arm (and hence the center of the stimulus setup). Then the camera is placed multiple times in its two most extreme positions, at -13º and +13º. At each position the location of the CR and the pupil is recorded (CR1 and 2, P1 and 2). Rp is then calculated using the following formula:

$$Rp = (d1 - d2) * 26 * pi / 180$$

$$d1 = CR1 - P1$$
$$d2 = CR2 - P2$$

Run the experiment

26) Each stimulus consists of a sine grating made up of a combination of one of seven spatial frequencies (0.03, 0.05, 0.08, 0.17, 0.25, 0.33, or 0.42 cycles per degree) and one of six contrast value (100%, 75%, 50%,

25%, 10%, 1%). The 42 stimulus combinations are presented in random order and rotate about the earth vertical axis at a constant velocity of 6 º/s. It moves clockwise for two seconds, than it changes direction and moves counter clockwise for two seconds. This is repeated five times, yielding 10 changes in direction. When the mouse is able to distinguish the sine grating from a homogeneous background a horizontal eye movement can be observed.

27) Record pupil position and corneal reflection position

28) These positions are low pass filtered with a cut off frequency of 300Hz (Axon Cyberamp 380), sampled at 1 kHz and stored for offline analysis.

PAUSE POINT

Analyze data offline

29) Differentiate to get eye and CR velocity

30) Remove fast phases using a velocity threshold of twice the stimulus velocity (i.e.,12 º/s). The first 200 ms after stimulus onset and before and after each change in direction are removed as well

31) Subtract CR velocity from pupil velocity

32) Calculate gains, the ratio between eye velocity and stimulus velocity

33) Plot the gains against different stimulus conditions. For example see fig 2

CAUTION: All experiments should be done in accordance with all the relevant guidelines. For example: with approval of the local ethics committee and in accordance with the European Communities Council Directive (86/609/EEC)

Timing

- Preparing the animal for head restraint requires ~ 20 minutes per animal and should be done 5-7 days before the experiment.
- Placing the animal in the setup requires 1-2 minutes
- The calibration procedure requires 10-15 minutes
- The experiment takes ~1 hour

Troubleshooting

Step nr	Problem	Possible cause	Solution
24-27	The composite construct breaks from the skull	The periosteum was not removed properly, after which the primer and adhesive did not connect fully with the skull	Make sure the periosteum is fully removed. Moisten it for easier removal
24-27	The nuts break off from the composite construct	The nuts don't have enough grip on the composite	Drill small holes in the edges of the nuts
25-27	The pupil is too large to track	The setup is too dark	Increase lumination

Anticipated results

By measuring how the gain of the optokinetic reflex (OKR) varies with different contrasts and spatial frequencies the contrast sensitivity function can be inferred.
OKR gains decrease as slow moving stimuli become harder to distinguish from a homogeneous background (Chapter 2, figure 2). Throughout a stimulus presentation, the mice respond with a highly regular OKR-movement. The response does not diminish only close to a perceptual threshold but over a much larger range of stimuli (Chapter 2, figure 3) which means that subtle differences between groups can be detected.

References

1) van Alphen, B., Winkelman, B., Frens, M.A. Age- and sex-related differences in contrast sensitivity in C57Bl/6 mice. Invest. Ophthalmol. Vis. Sci. (2008) [Epub ahead of print]
2) Gianfranceschi, L., Fiorentini, A., Maffei, L. Behavioural visual acuity of wild type and bcl2 transgenic mouse. *Vision Res.*;**39(3)**, 569-74 (1999)
3) Prusky, G.T. & Douglas, R.M. Characterization of mouse cortical spatial vision. *Vision Res.* **44(28)**, 3411–3418 (2004)
4) Douglas, RM et al. Independent visual threshold measurements in the two eyes of freely moving rats and mice using a virtual-reality optokinetic system. *Vis. Neurosci* **22(5)**, 677-684 (2005)
5) Wong, AA & Brown, R.E. Age-related changes in visual acuity, learning and memory in C57BL/6J and DBA/2J mice. *Neurobiol. Aging* **28(10)**, 577-1593 (2006)
6) Sinex, D.G., Burdette, L.J., Pearlman, A.L.A psychophysical investigation of spatial vision in the normal and reeler mutant mouse. *Vision Res.***19(8)**, 853-7 (1979)
7) Prusky, G.T., Alam, N.M., Beckmanand, S., Douglas, R.M. Rapid quantification of adult and developing mouse spatial vision using a virtual optomotor system. *Invest. Ophthalmol. Vis. Sci.* **45(12)**, 4611-4616 (2004)
8) Jellali, A et al. The optomotor response: A robust first-line visual screening method for mice. *Vision Res.* **45(11)**, 1439-1446 (2005)
9) Schmucker, C. Seeliger, M., Humphries, P., Biel, M., Schaeffel, F. Grating acuity at different luminances in wild-type mice and in mice lacking rod or cone function. *Invest. Ophthalmol. Vis. Sci.* **46(1)**, 398-407 (2005)
10) Umino, Y., Solessio, E., Barlow, R.B. Speed, Spatial and temporal tuning of rod and cone vision in mouse. *J. Neurosci.* **28(1)**, 189-198 (2008)
11) Jeon, C.J., Strettoi, E., Masland, R.H . The major cell populations of the mouse retina. *J. Neurosci* **18**, 8936 (1998)
12) Collewijn, H. Optokinetic eyemovements in the rabbit: input-output relations. *Vision Res.* **9,** 117-132 (1969)

13) Nagao, S. Role of cerebellar flocculus in adaptive interaction between optokinetic eye movement response and vestibulo-ocular reflex in pigmented rabbits. *Exp. Brain Res*. **53**, 36-46 (1989)
14) Katoh, A., Kitazawa, H., Itohara, S., Nagao, S. Dynamic characteristics and adaptability of mouse vestibulo-ocular and optokinetic response eye movements and the role of the flocculo-olivary system revealed by chemical lesions. *Proc. Natl. Acad. Sci. USA* **95**, 7705–7710 (1998)
15) van Alphen, A.M., Stahl, J.S., De Zeeuw, D.I. The dynamic characteristics of the mouse horizontal vestibulo-ocular and optokinetic response. *Brain Res.* **890(2)**, 296-305 (2001)
16) Migliaccio, A.A., MacDougall, H.G., Minor, L.B., Della Santina, C.C. Inexpensive system for real-time 3-dimensional video-oculography using a fluorescent marker array *J. Neurosci. Meth.* **143**, 141–150 (2005)
17) Stahl, J.S., van Alphen, A.M., de Zeeuw, C.I. A comparison of video and magnetic search coil recordings of mouse eye movements. *J. Neurosci. Meth.***99(1-2)**, 101–110 (2000)

Appendix B: How to measure 3D eye movements in mice using video oculography

Bart van Alphen, Beerend Winkelman, Maarten Frens

Introduction

Compensatory eye movements are popular model system for connecting neurophysiology and behavior as well as studying the neural correlates of behavioral plasticity. It is a system where the sensory input, consisting of visual and vestibular stimuli can be fully defined. The output, reflexive compensatory eye movements and electrophysiological activity, can be recorded and correlated with the sensory input. Additionally, by manipulating those reflexive eye movements by using different combinations of sensory input, motor learning can be studied in a well-controlled environment. Fast and accurate recording of eye movements is essential when studying relations between visual or vestibular stimuli and oculomotor behavior or when investigating disorders of the visual pathways, inner ear, and cerebellum (Stahl 2004).

Mice have become an increasingly important model in neuroscience. Their small size and fast reproduction rates in combination with the availability of many techniques to generate mutants make them attractive to gain more insight in the function of the brain as well as study motor behaviour and motor learning

Over the last few years video based systems became an increasingly popular alternative. Most of these systems track the pupil and use center of mass calculations or an ellipse fitting procedure to record the eye position. These systems work well when recording horizontal and vertical (two-dimensional) eye movements. However, recording the third component, torsion, is more complicated, especially in small rodents like mice. Most systems either track two or more landmarks on the eye or they track striations of the iris. These are not applicable in animals without obvious ocular landmarks or a well-defined iris, such as rabbits and mice, limiting the options for three-dimensional video oculography in those animals.

Here we describe a protocol to place temporary artificial markers on the mouse eye and use these markers to record eye movements in 3D.

Materials

Equipment

- Restrainer:
- Anesthesia setup
- Eye tracking system: we use an Iscan ETL-200 but any system that can track makers will do. They are comercially available (Chronos Vision, Eye link, Iscan) or can be built from customer available webcams (Migliaccio, 2005)
- Stimulus setup: This can be an optokinetic drum, a projection system or a turntable for vestibular stimuli or a combination of those.

Reagents

- Minims Oxybuprocaine Hydrochloride 0.4 % (Bausch & Lomb House, Kingston-upon-Thames, UK). These are eye drops to numb the cornea.
- Titanium dioxide pigment (art. Nr 650, Custom Tattoo Supplies Europe, Enkhuizen, the Netherlands)
- Isofloran 1–1.5% (Rhodia Organique Fine Ltd, Bristol, UK)

Equipment setup

See Appendix A

Reagent setup

Titanium dioxide pigment: stir the bottle of pigment using a vortex. Then pour a few drops in a small dish. CRITICAL: as the pigment solution comes into contact with air, wait a few minutes as the liquid thickens. It is important to make sure that the pigment solution is thick enough so that it doesn't run over the whole eye but liquid enough to be painted on the cornea.

For the other reagents, follow the instructions of the manufacturer.

Procedure

34) Prepare a mouse for head restraint by attaching two nuts to the skull, using a construct of microglass composite. Do this 5-7 days before the experiment. This procedure is fully described in Appendix A. PAUSE POINT: an animal needs at least 5-7 days to fully recover from the procedure. In an adult animal, the head restraint will stay in place for at least several months.

35) Place markers on the eye. Do this right before the experiment

- **a.** Anesthetize the mouse using Isofluran and anesthetized with a mixture of Isofluoran and oxygen. After general anaesthesia induction the mouse is placed on its side.
- **b.** Locally anesthetize the eye using a single drop of Oxybuprocaine hydrochloride 0.4 %
- **c.** Wait two minutes for the Oxybuprocaine to work.
- **d.** In the meantime, pour a drop of titanium dioxide pigment in a dish
- **e.** Use a papertip to remove the Oxybuprocaine and dry a 0.5*0.5 mm area on the cornea
- **f.** Use a blunt dissection needle to apply three dots of titanium dioxide pigment (art. Nr 650, Custom Tattoo Supplies Europe) on the dried surface. These markers are temporary, staying on the eye for 4 to 12 hours after which they disappear without leaving a trace.
- **g.** Wait 3 minutes until the pigment is dry
- **h.** Place the mouse in the restrainer

36) Once the mouse is placed in the setup, two calibration steps have to be taken. In order to reconstruct the three dimensional position of each marker we need to define the sphere on which they move. To define a sphere we need to determine the position of its center and its radius.

a. Procedure for locating the center of rotation: Four IR LEDs were placed in a square formation around the lens of the camera, equidistant from the optic axis of the camera. When the camera's optic axis is perfectly orthogonal with the center of curvature of a reflective, spherical object (such as a mouse eye), the four LEDs are equidistant from the center pixel of the image. This gives the x- and y-coordinates of the center of the sphere over which the markers move. This method was previously described by Miglicaccio *et al* (2005).

b. Determine the radius: A reference LED is placed on the camera, aligned with its optical axis. This produces a corneal reflection (CR). By continuously oscillating the camera and moving the mouse along the Y-axis until the CR motion is minimal the center of the corneal curvature is placed at the rotation axis of the camera arm (and hence the center of the stimulus setup). Then the camera is placed multiple times in its two most extreme positions, at -13º and +13º. At each position the location of the CR and the marker closest to the center of the pupil is recorded (CR1 and 2, P1 and 2). The radius of rotation of the marker is then calculated using the following formula:

$$Rm = (d1 - d2) * 26 * pi / 180$$

$$d1 = CR1 - P1$$
$$d2 = CR2 - P2$$

This method was previously described by Stahl *et al* (2000), who used it to determine Rp, the radius of rotation of the pupil

37) Record eye movements. Once the radius of the eye is known and the camera is aligned with the center of rotation of the eye, the 3D rotation of the eye can straightforwardly be determined from the position of the markers, as their recorded position on the camera is now a projection of a sphere of radius Rm on a flat surface.

At the center pixel of the image acquisition software, the following is known:
x0 = 0, y0 = 0, z0 = Rm

For each marker (x1,y1,z1) the azimuth and elevation can be calculated using:

Az = asin((x1-x0)/r) * 180/pi
El = asin((y1-y0)/r) * 180/pi

Torsion can be calculated as follows:
The three markers form a triangle with points (x1, y1), (x2, y2), (x3, y3). The slope of each of the three sides of the triangle can be calculated using the Four-quadrant inverse tangent or atan2.

slope12 = atan2((y2-y1),(x2-x1));
slope13 = atan2((y3-y1),(x3-x1));
slope23 = atan2((y3-y2),(x3-x2));

Timing

- Preparing the animal for head restraint requires ~ 20 minutes per animal and should be done 5-7 days before the experiment.
- Placing the markers requires ~ 5 minutes per animal and should be done right before the animal is placed in the setup
- The calibration procedure requires 10-15 minutes

Troubleshooting

Step nr	Problem	Possible cause	Solution
2e	The anesthetized mouse closes its eye as the cornea is touched	The Oxybuprocaine is not working yet.	Add an extra drop and wait another minute
2f	The pigment is thick and sticks to the needle instead of the cornea	The pigment solution is too thick.	Take a new dish, add a drop of pigment and wait till it has the right viscosity
2f	The pigment runs over the cornea	The pigment solution is not thick enough	Place the animal back in its cage and try again the next day. The pigment will be gone
2e or f	After the mouse is placed on its side the eye moves to such an eccentric position that the markers cannot be placed	This eye movement is invoked by otholith activation as the head was tilted to expose the eye	Put the mouse upright again, wait for the eye to return to its normal position and then rotate it very slowly on its side
4	One of the markers disappears under the eye lid as the eye moves	That marker was placed in a too eccentric position	Remember to place the markers closer to the pupil next time

Anticipated results

To test whether the merging of those two video-oculography techniques produces reliable estimates of eye position based on marker postion we placed a small reflective metal sphere with three markers on it in a Helmholtz gimbal. It was aligned using the method described above so the

optical axis of the camera was orthogonal with the center of curvature of the sphere. The radius of the sphere was also determined. The gimbal was placed in different positions with azimuth and elevation ranging from -15º to +15º in steps of 5º. Some positions could not be recorded because the reflection of the IR LED overlapped with a marker position which made it impossible to see where it exactly was. Marker positions were recorded and transformed from Cartesian coordinates to azimuth- and elevation angles using custom made Matlab software.

Additional benefits:
When measuring only horizontal eye movements (rotation about the earth vertical axis) a single marker will suffice. Calibration is the same as described by Stahl 2001, where Rm replaces Rp and describes the distance of the center of the eye to the marker instead of the distance from the center of the eye to the pupil. This has two benefits:

- Rm does not vary while Rp varies as the pupil changes size. Using a marker requires less calibration during the experiment.
- When using a marker there is no need to artificially reduce pupil size using miotic drugs like Pilocarpine.

References

Migliaccio, A. A., H. G. Macdougall, et al. (2005). "Inexpensive system for real-time 3-dimensional video-oculography using a fluorescent marker array." J Neurosci Methods 143(2): 141-150.
Stahl, J. S. (2004). "Using eye movements to assess brain function in mice." Vision Res 44(28): 3401-3410.
Stahl, J. S., A. M. van Alphen, et al. (2000). "A comparison of video and magnetic search coil recordings of mouse eye movements." J Neurosci Methods 99(1-2): 101-110.

Summary

Gaze stabilization reflexes are a popular model system in neuroscience for connecting neurophysiology and behavior as well as studying the neural correlates of behavioral plasticity. These compensatory eye movements are one of the simplest motor behaviors, consisting of a more or less spherical object that rotates with three degrees of freedom, without significantly changing the load during a movement trajectory. Additionally, it is a model system where the sensory input, consisting of visual and/or vestibular stimulation, can be fully controlled. The output, reflexive compensatory eye movements and electrophysiological activity, can be recorded and correlated with the sensory input. Motor learning can be studied in a well-controlled environment by manipulating those reflexive eye movements by using different combinations of sensory input.

In this thesis, we describe another application of gaze stabilization reflexes: using them to study visual perception in mice. Because the mouse retina lacks a fovea, mice don't look around to observe the world. They don't make goal directed eye movements like saccades or smooth pursuit to aim a patch of high density photoreceptors at a target. Instead, mice only move their eyes reflexively, to stabilize vision. Where man uses five systems to guide vision, mice only use two: the VOR and OKR. This complete lack of voluntary, exploratory eye movements makes mice highly suitable to study motor control of gaze stabilization reflexes as they will only move their eyes in response to visual and vestibular stimulation to compensate for blurring, without any top down control of eye movements.

This reflexive behavior can be used to measure visual function in mice. By showing a mouse moving grating patterns of varying size and contrast, a mouse will track the moving grating with its eyes, as long as it can distinguish it from a homogeonous background. This is not an all-or-nothing behavior, instead the magnitude of the response decreases as stimuli become harder to see. This is a very useful property that we use in chapter two to describe subtle differences in contrast sensitivity between male and female mice, and between younger and older mice.

We applied this technique to measure how the visual function deteriorates in Ercc d/- mouse mutants that age rapidly because they cannot fully repair damage to their DNA. These mice go almost fully blind by the time they are 14 weeks old. This decrease in visual function can be used as a probe to measure overall degeneration of the nervous system in these mice, which can be useful for follow up studies that aim to study aging, and possibly prevent accumulating DNA damage.

Inferring visual function from gaze stabilization performance can also be done in man. Such a quantifiable measure has two benefits. First, it is completely objective and not subject to user reported bias, which often occurs in perception tasks where the stimulus is close to the perceptual threshold. Also, the response is not binomial but graded. This makes the method ideally suited to screen for small changes in visual function caused either by degenerative diseases or new by treatment methods that aim to improve visual function in low vision patients.

Besides studying vision in mice and man, we also studied three dimensional eye movements in mice. Unlike rabbits, optokinetic eye movements in mice are equally well developed in all directions, which means that the mouse can track movements in any direction equally well.

In summary, this thesis outlined several approaches to study vision and eye movements, both in mice and men, that are useful when studying patients of mouse models where vision is affected as a result of disease, mutations, aging, retinal degeneration or neurological impairment of the visual system. Also, these approaches will be valuable when evaluating treatments that aim to improve or restore visual function in low vision patients. Likewise, the method outlined in chapter 5 will be useful to study eye movements generated by three dimensional vestibular stimulation, and will provide more insight in how the brain integrates visual and vestibular information to generate accurate three dimensional compensatory eye movements.

Samenvatting

Blik stabilisatie-reflexen zijn een populair model systeem in de neurowetenschappen om motorisch leren te bestuderen en om gedrag te verbinden met de onderliggende neurofysiologie. Deze compenserende oogbewegingen zijn een van de eenvoudigste voorbeelden van motoriek, bestaande uit een min of meer bolvormig voorwerp dat draait met drie vrijheidsgraden, zonder dat de krachten die op het systeem werken veranderen tijdens de beweging, zoals dat bijvoorbeeld wel gebeurt bij arm bewegingen. Het is een model systeem waarin zintuiglijke input, bestaande uit visuele en / of vestibulaire stimulatie, volledig kan worden gecontroleerd. De output, reflexieve compenserende oogbewegingen en elektrofysiologische activiteit, kunnen worden gemeten en gecorreleerd met de zintuiglijke input. Motorisch leren kan worden bestudeerd in een goed gecontroleerde omgeving door deze reflexmatige oogbewegingen te manipuleren met behulp van verschillende combinaties van zintuiglijke input.

In dit proefschrift beschrijven we een nieuwe toepassing van blik stabilisatie reflexen: we gebruiken ze om visuele waarneming in muizen te bestuderen. Het muizenoog is eenvoudiger dan dat van de mens. De fovea, het deel van het netvlies met waarmee je de meeste details ziet, ontbreekt in muizen. Daardoor kijken muizen niet rond om de wereld te zien. Ze maken geen doelgerichte oogbewegingen. Muizen bewegen hun ogen alleen reflexmatig om hun blikveld te stabiliseren.

Waar de mens maakt gebruik van vijf systemen om oogbewegingen aan te sturen gebruiken muizen er slechts twee. De eerste is de vestibulo oculaire reflex (VOR), waarbij informatie over hoofdbewegingen wordt verkregen uit de evenwichtsorganen. Als je je hoofd beweegt terwijl je deze samenvatting leest blijven je ogen automatisch op de juiste plek doordat ze in tegengestelde richting van het hoofd draaien. De tweede reflex is de optokinetiche reflex (OKR). Deze reflex zorgt voor blik stablisatie als objecten in de wereld bewegen. Als je bijvoorbeeld dit boekje heen en weer beweegt tijdens het lezen dan zorgt de OKR ervoor dat je toch kan blijven lezen, mits je niet te snel beweegt. In tegenstelling tot de VOR kan de OKR

niet goed compenseren voor snelle bewegingen. Samen zorgen deze twee reflexen ervoor dat je scherp kan blijven zien in een dynamische omgeving.

Het gebrek aan vrijwillige, verkennende oogbewegingen maakt muizen zeer geschikt om de motorische controle van blik stabilisatie reflexen, omdat zij alleen hun ogen bewegen in reactie op visuele en vestibulaire stimulatie. Dit reflexmatig gedrag kan worden gebruikt om het gezichtsvermogen van muizen te meten.

Door een muis bewegende visuele stimuli aan te bieden die bestaan uit rasterpatronen met verschillende breedtes en contrasten en vervolgens te meten in welke mate het muizenoog deze stimuli volgt kan afgeleidt worden hoe goed de muis die stimulus kan zien. De volgbewegingen zijn geen alles-of-niets gedrag; de grootte van de respons neemt geleidelijk af als stimuli moeilijker te zien worden.

Dit is een zeer nuttige eigenschap die we gebruiken in hoofdstuk twee om subtiele verschillen in contrast gevoeligheid tussen mannelijke en vrouwelijke muizen, en tussen jongere en oudere muizen, te beschrijven. In hoofdstuk drie pasten we deze techniek om te meten hoe de visuele functie verslechtert in ERCC d / - muis mutanten die snel verouderen, omdat ze schade aan hun DNA niet volledig kunnen herstellen. Deze muizen worden bijna volledig blind tegen de tijd dat ze 14 weken oud zijn. Deze afname van contrastgevoeligheid kan worden gebruikt als een maatstaf voor de algehele degeneratie van het zenuwstelsel in deze muizenwat nuttig kan zijn voor vervolgstudies die gericht zijn op het voorkomen of herstellen van DNA schade ten gevolge van veroudering.

Ook in de mens kan het gezichtsvermogen bepaald worden door te meten hoe goed blik stablisatie reflexen werken bij verschillende visuele stimuli. Die aanpak heeft twee voordelen. Ten eerste is deze aanpak subjectief en dus niet afhankelijk van de gebruiker die rapporteert of stimuli waargenomen worden. De respons is gradueel en niet bionominaal. Dit maakt de methode bij uitstek geschikt voor het screenen op kleine veranderingen in de visuele functie die veroorzaakt zijn door degeneratieve ziekten of nieuwe methoden door de behandeling die gericht zijn op het verbeteren van de visuele functie

in low vision patiënten.

Naast het bestuderen van het gezichtsvermogen in muizen en mensen hebben we ook onderzoek gedaan naar drie dimensionale oogbewegingen in muizen. Dit onderzoek is beschreven in hoofdstuk vijf. Mensen en konijnen zijn goed in staat om horizontale of vertikale bewegingen te volgen met hun ogen. Stimuli die roteren om de optische as (kijkrichting) kunnen veel minder goed gevolgd worden. Muizen kunnen dergelijke torsie bewegingen zonder problemen maken.

Samengevat, dit proefschrift beschrijft verschillende benaderingen om oogbewegingen en gezichtsvermogens te meten, zowel in muizen en mensen. Deze nieuwe aanpakken zijn nuttig bij het bestuderen van patiënten of muismodellen waar het gezichtsvermogen aangetast is als gevolg van ziekte, mutaties, ouderdom, retinale degeneratie of neurologische aantasting van de het visuele systeem. Ook zullen deze benaderingen waardevol zijn bij de evaluatie van behandelingen die gericht zijn op verbetering of visuele functie te herstellen in low vision patiënten.
De methode zoals die beschreven is in hoofdstuk vijf kan gebruikt worden driedimensionale oogbewegingen in muizen te meten die opgewekt wordne met driedimensionale vestibulaire stimulatie. Dergelijke experimenten zullen meer inzicht geven in hoe het brein visuele en vestibulaire informatie integreert en omzet in neurale commado's die oogbewegingen aansturen.

Dankwoord

De ervaring leert dat de meeste mensen achteraan bij het proefschrift beginnen. Dus nu het officele deel van mijn proefschrift eindelijk af is, is het tijd voor het laatste, meestgelezen deel. Dit boekje is het resultaat van de geweldige tijd die ik gehad heb tijdens mijn promotie traject in het Erasmus MC. Ik heb er ontzettend veel geleerd en er zijn veel mensen die ik wil bedanken.

Allereerst mijn promotor Maarten Frens, met wie het allemaal begonnen is!

Beste Maarten, toen ik net afgestudeerd was hoorde ik van Ignace Hooge dat jij op zoek was naar een aio. Niet veel later zat kreeg ik een rondleiding door het Erasmus MC, toen nog op de 15e verdieping. Ik voelde me vanaf het begin thuis. De relaxte sfeer en de grote mate van vrijheid die je me bood hebben daar zeker aan bijgedragen. Ook de jaarlijkse barbecue in je enorme tuin in Utrecht was altijd erg leuk.

Naast Maarten zijn er een aantal andere leden van groep Frens die ontzettend belangrijk zijn geweest bij mijn projecten.

Beste Beerend, ik ben ontzettend blij dat je mijn directe collega was! Ik heb heel erg veel van je geleerd, over het programmeren van Matlab en Spike, en over alle technische zaken die komen kijken bij het opzetten van een lab. Ik ben nog steeds erg trots op het lab dat we samen ontworpen en gebouwd hebben. Als Rotterdammer kende je ook alle leuke plekken in het centrum waar het goed toeven was, en ik heb me altijd prima vermaakt tijdens onze lunches, eerst bij Coenen, en later bij de Warung Mini. Het was geweldig om samen te werken met iemand die zo'n brede interesse had, en onze gesprekken over atheisme, religie klimaatwetenschap of obscure details van de Amerikaanse politiek waren altijd erg boeiend. Ik hoop dat je een goede tijd hebt in Amsterdam!

Beste Jos, als Matlab wizard wist je me altijd te helpen als ik vastgelopen was, en in de afgelopen jaren heb ik veel van je geleerd. En het was ook altijd gezellig om samen even te gaan roken en koffie te gaan drinken.

Beste Marcella, ik was erg blij toen je ons team kwam versterken. Je hulp bij alle experimenten was onmisbaar, en je onverstoorbaarheid en humor maakten de samenwerking alleen maar beter. Veel succes met de laatste loodjes!

Beste Stefan, het was goed om je, na wat omzwervingen, weer als collega in Rotterdam te hebben. Hoewel ik het soms helemaal niet met je eens was waren onze discussies altijd erg leuk en leerzaam. Ook het langeafstands darten was erg leuk, al moeten we daar de volgende keer wat minder bier bij drinken.

Ha Marc, het was geweldig toen je als postdoc groep Frens kwam versterken. Hoe je de motor aan de praat gekregen heb weet ik nog steeds niet, maar het werkt allemaal als een zonnetje (meestal dan). Gelukkig is Nijmegen niet ver. Ik kom je snel weer opzoeken in Havana aan de Waal. Goldstrike drinken en praten over dierproeven is pas echt leuk als je het doet in een cafe vol krakers.
Beste Flip, je bent de enige pro bono aio die ik ken. Nadat je voor de zoveelste keer uitgeloot was voor geneeskunde was je bij Maarten binnengelopen om dan maar vast met onderzoek te beginnen. Gelukkig ben je uiteindelijk toch toegelaten tot geneeskunde, want ik weet zeker dat je een geweldige arts gaat worden! Het was onzettend leuk om je als collega te hebben, ik heb altijd erg genoten van alle mooie verhalen die je vertelde.

Beste Jory, het was altijd leuk om thee met je te drinken, ook nadat je al lang bij groep Frens vertrokken was. Ik heb veel bewondering voor je ambitie. Promoveren is een full time baan en geneeskunde is een full time studie. Toch weet je het allebei tegelijk te doen, zonder al te gestressed te raken. En dat met een een achtergrond als psycholoog ;-) Veel succes met de studie en de promotie. Ik kijk uit naar je proefschrift!

Beste Harm, ik weet nog steeds niet hoe je het voor elkaar gekregen hebt om geavanceerde monitor software te installeren op zoveel computers in het Erasmus MC, maar de data die dat opleverde was erg interessant. Jammer dat je op de 14e zat en ik je veel te weinig zag. Dat geldt ook voor Janneke, Albertine, Inger en alle andere leden van groep Frens op de 14e.

Beste Chris, ik heb de afgelopen jaren met veel bewondering gezien hoe je groep functioneerde, en hoe je je inzet om ervoor te zorgen dat al je studenten en promovendi goed terecht komen. Je enthousiasme en gedrevenheid zijn een bron van inspiratie.

Beste Gerard, ik vond het erg leuk en leerzaam om als assistent mee te werken aan de de computerpractica over epilepsie ion kanalen, als kon de combinatie van paranoide softwarebeveiliging en recalcitrante IT helpdesk soms wat stress veroorzaken. Ook heel erg bedankt voor de hilarische onofficiele biografie van L Ron Hubbard, die ik veel te lang van je geleend heb.

Beste Ype, de meeste wetenschappers die met proefdieren werken lopen met een grote boog om dierenrechten activisten heen. Jij bent een uitzondering die de dicussie over het gebruik van proefdieren niet ontwijkt en regelmatig in het hol van de leeuw uitlegt waarom proefdieren essentieel zijn in de wetenschap. Ik heb daar veel bewondering voor.

Beste Marcel, als expert op het gebied van het meten van oogbewegingen bij muizen heb ik heel veel aan je kennis en tips gehad.

Beste Freek en Martijn, jullie waren al aio toen ik bij Neurowetenschappen begon, en het was altijd erg leuk dat ik bij jullie binnen kon vallen, voor vragen of een praatje. Ik heb ook met veel bewondering naar jullie nek-aan-nek race met top publicaties gekeken. En nu jullie allebei postdocs zijn zijn mijn verwachtingen alleen maar toegenomen. Veel succes!

Beste Jeannette, het was erg leuk om je na onze biologie studie in Utrecht in Rotterdam tegen te komen! Ook goed dat je nu weer in Utrecht woont, want onze plannen om neurowetenschap nieuwe leven in te blazen in Utrecht moeten wel doorgaan!

Beste Nils, het was altijd erg gezellig om je tegen te komen op een van de vele vrijdag middagen. Het was ook erg prettig om met je samen te werken aan een paper. Veel succes met promoveren!

Beste John, heel erg bedankt dat je op mijn kat wilde passen toen ik naar Australie vertrok. Ook heel erg bedankt voor je geduld, toen mijn plannen om snel terug te komen steeds uitgesteld werden. Ik sta bij je in het krijt.

Beste Sara, het was erg leuk om je een paar jaar als collega te hebben, en ik heb altijd erg genoten van je, soms hilarische, verhalen over Iran.

Een promotie in onmogelijk zonder de steun van veel mensen achter de schermen.

Beste Elize, als kloppend hart van alle sociale activiteiten heb je een onmisbare rol vervuld. Ik ben ook nog steeds geconditioneerd door alle borrels. Elke vrijdagmiddag rond een uur of vijf krijg ik dorst.
Aleksandra, Alexander, Bjorn, Geeske, Titiana en alle andere mensen van de vrijdagmiddag borrel: heel erg bedankt voor alle leuke gesprekken.

Beste Hans, als onuitputtelijke bron van technische hulp, tips en politiek incorrecte grappen heb je een onvervangbare rol gespeeld bij al mijn projecten.

Beste Cees, ik ben de tel kwijt geraakt hoe vaak ik bij je binnen kwam vallen als er weer iets mis was met de opstelling. Gelukkig wist je me altijd te helpen.

Beste Suzan, hartelijk bedankt voor alle steun bij het regelen van mijn promotie!

Beste Loes en Edith, ik kwam een paar keer bij week bij jullie langs, soms voor de post maar meestal om even in de snoeppot te graaien. En na wat snoep en een gezellig praatje kon ik weer verder. Heel erg bedankt voor alle ondersteuning!

Beste Joop en Alex, jullie waren onmisbaar tijdens de opstart fase van mijn onderzoek (de eerste drie jaar!). Jullie kennis en vaardigheden waren essentieel bij het bouwen van het lab.

Een promotie verloopt niet altijd even vlot, en er is een zekere koppigheid voor nodig om het tot een goed einde te brengen. De welbekende aio-dip, waarbij de promovendus twijfelt over de zin/haalbaarheid van het project, kreeg ik in 2007 toen ik muurvast zat met mijn experimenten. Om mijn horizon te verbreden ging in deeltijd journalistiek studeren in Utrecht. Hoewel journalistiek niet zo spannend is als wetenschap (een journalist is altijd aan het reconstrueren wat er gebeurd is, in plaats van nieuwe dingen te ontdekken) was het erg leerzaam en leuk. Ik wil iedereen dan ook van harte bedanken voor het geweldige intermezzo. Met name Joost! De trein trip terug naar Rotterdam was altijd erg leuk, net als alle biertjes in Utrecht en Rotterdam.

Lieve Lena, zonder jou liefde en steun was ik nooit zover gekomen. Je wist me altijd op te vrolijken en af te leiden als ik dat nodig had, en je liefde en humor zorgden ervoor dat alle tegenslagen in mijn onderzoek gerelativeerd werden. Na alle omzwervingen door Europa zijn we nu eindelijk samen in Australie terecht gekomen voor een nieuwe fase in ons leven. Ik ben zo ontzettend blij dat je die sprong in het diepe samen met mij genomen hebt. Bedankt voor alles!

CURRICULUM VITAE

2009-

Postdoc
Queensland Brain Institute
Brisbane, Australia

2003 – 2009:

AIO
Erasmus MC, Department of Neuroscience
Rotterdam, the Netherlands

2008:

Journalistiek voor academici
Hogeschool Utrecht
Utrecht, the Netherlands

1995-2003:

Biologie
Universiteit Utrecht
Utrecht, the Netherlands

1989-1995:

VWO
Raamsdonksveer, the Netherlands

Publications

Age- and sex-related differences in contrast sensitivity in C57BL/6 mice.
van Alphen, B., Winkelman, B.H.J., Frens, M.A. (2009).
Investigative Ophthalmology and Visual Science 50(5): 2451-2458.

Three-dimensional optokinetic eye movements in the C57BL/6J mouse.
van Alphen, B., Winkelman, B.H.J., Frens, M.A. (2010)
Investigative Ophthalmology and Visual Science 51(1):623-30.

Age-related loss of hearing and vision in the DNA-repair deficient *Ercc1*$^{\delta/-}$ mouse
Nils Z. Borgesius, Marcella Spoor, Bart van Alphen, Andries P. Nagtegaal, Yanto Ridwan, Ingrid van der Pluijm, Jan H. J. Hoeijmakers, Maarten A. Frens, Gerard Borst, Ype Elgersma
In preparation

Using the ocular following response to measure contrast sensitivity
Behdokht Hosseini, Bart van Alphen, Marcella Spoor, Jos van der Geest, Maarten Frens
In preparation